



From responsiveness in biological matter to functional materials: Analogies and inspiration towards the systematic design and synthesis of new smart materials and systems

Mattia Pancrazio Cosma, Roberto Brighenti *

Dept. of Eng. and Architecture, Univ. of Parma, Viale delle Scienze 181/A, 43124 Parma, Italy

ARTICLE INFO

Keywords:

Responsiveness in living matter
Functional materials
Morphing
Smart polymers
Programmable mechanical response

ABSTRACT

Living organisms and, in general, bio-materials respond to external stimuli exhibiting specific functionalities (such as shape-morphing, color change, tissue growth and remodeling, programmed mechanical responses, adaptation of material properties, etc.) required for different needs (camouflage, locomotion, defense, food supply, biological processes, etc.). Functionalities in nature come from bio-chemo-physical-mechanical responsiveness of the complex architectures in which natural structures are organized across the nano-, micro- and meso-scales. Often inspired by natural structures and bio-functionalities, in recent years the development of synthetic responsive materials has attracted a huge interest, and increasingly still attracts the efforts of scientists to synthesize new smart materials and devices.

The paper illustrates the most compelling morphing and functional responses observable in nature – displayed by biological matter, living individuals or by the collective behavior of large groups of organisms – developed for different functional purposes, and discusses the related underlying mechanisms. In parallel, the most relevant functional materials being developed in the last decades are presented with the related mathematical models, and their underlying driving mechanisms are compared with those observable in nature. The study is aimed at providing a broad overview and to explain the strategies used in nature to obtain functionalities; the analogies with those shown by artificial functional materials, with a particular emphasis on polymer-based or polymer-like materials, are investigated. Some multi-physics models, describing the response and enabling the systematic design, optimization and synthesis of functional materials suitable to the development of new advanced applications, are also illustrated. The knowledge of natural cunning can push forward the research in the field, offers new possibilities worth of investigation by materials scientists, physicists and engineers, and opens unexplored scenarios not yet fully considered in the existing literature.

1. Introduction

Nature has shaped living organisms, such as animals, insects, fishes, plants, and in general any biological structure, to be capable of responding to external stimuli by showing specific functionalities, such as self-protection, locomotion, feeding, etc. useful to perform specific tasks or simply to enhance the survival probability.

The above-mentioned functional behavior stems from an intrinsic programming coded within the natural structure. Shape-morphing (allowing for instance a plant to close its leaves for capturing insects), color change (for camouflage purposes), the optimum design of shelters or hunting structures (nests, spider-silk net, etc.), bone tissue growth

and remodeling, to mention a few, are all relevant examples. These natural structures display intricate bio-encoded architectures, organized across the nano-, micro- and meso- scales, whose capabilities reflect in an impressive range of functional or multifunctional properties.

On the other hand, a new class of synthetic materials, namely stimuli-responsive materials also known as functional materials, active materials, etc., emerged in the last decades. Similarly to what happens in biological matter, these materials are able to respond to external stimuli, displaying shape-change, variations of their mechanical and/or physical-chemical properties, etc.

As visionarily discussed in [1], an emerging research paradigm stemming from a precious and intriguing statement of Bhattacharya and

* Corresponding author.

E-mail address: brigh@unipr.it (R. Brighenti).

James, “the material is the machine” [2], well describes the realm of the synthesis and design of stimuli-responsive materials enabling new robotic matter and machines made of smart components. Accordingly, a material-based machine can functionally respond to external inputs by displaying functionalities similar to those shown by everyday machines (grafting, lifting, locomotion, etc.), but without the need of any externally driven engine, hydraulic/electric systems, sensors etc.

Autonomous responsiveness is a typical feature of biological systems (matters and/or structures) which are naturally programmed, according to the required functionality, to respond to a specific stimulus in a precise and well-determined way.

For instance, muscles of natural livings represent an example of bio-actuators [3]: they can contract and elongate thanks to complex yet natural mechanisms occurring at the molecular level. The cooperation of actins and myosins, principal proteins of the muscle structure, is responsible for the locomotion and movement of vertebrates [4]. The relative motion between myosins and actins, triggered by chemical/mechanical stimuli, reflects in a contraction/elongation of the muscle fibers, leading to movements at the macroscopic level [3]. Another example of natural programmed matter is the bone tissue which displays stimuli-induced self-remodeling enabling adaptation [5].

Other intriguing examples can be found in the realm of superorganisms, i.e. in groups of cooperating living individuals – such as insect colonies [6] – whose smart responsiveness stems from the collecting and organized behavior of the single units. Among this family of active organisms, fire ants are incredible cooperators that can organize themselves into fascinating smart structures whose shape can morph in a programmed way according to the required functionality [7,8]. Bee swarms represent another relevant example of collective behavior: they can arrange themselves by creating structures whose shape and size are optimized to efficiently face the fluctuating thermal and/or mechanical stimuli of the surrounding environment [9].

However, cooperation among individuals, cells, insects, or other living units, is not the only way to obtain functionality. Microstructure-related functionality is also often harnessed in nature; spider-silk is a clear example on how the nanostructure of a natural material can be tuned to get different macroscopic properties, whose features depend on the purpose the silk is produced for (reproduction, locomotion, to capture preys, etc.) [10]. Along this line, bees’ honeycombs are structures optimized in terms of physical and mechanical properties related to the desired functionality: the biological process of honeycomb building is programmed to ensure proper characteristics in terms of tensile strength, breaking strain, stiffness, toughness, etc. [6,11]. Exotic functional responses can be found also in the realm of plants and vegetables [12].

Moving to the realm of artificial functional materials where polymers have a privileged place, the most known materials in this area are shape memory polymers (SMPs), hydrogels, liquid crystal elastomers (LCEs), electroactive polymers (EAPs), etc., to mention a few. By exploiting different physical/chemical mechanisms promoting the functionality of these materials to appear, intriguing smart behaviors have been obtained so far. A relevant example in this context is represented by the swelling-deswelling mechanism of hydrogels; the ability to swell or shrink in presence of a certain solvent, has been exploited for different functional purposes (drug delivery, activation of embedded smart molecules, plant bionics, etc.) [1,13,14]. Further, EAPs can change their shape or properties thanks to electrostatic forces or ions mobility induced by an electric field, enabling their use as actuators, sensors, etc. [15–17]. In LCEs an external stimulus (typically the temperature variation) can be used to change the arrangement of the microstructure of the polymer chains (nematic-isotropic transition), whose counterpart at the macroscale appears as a shape change suitable to be exploited for various functionalities, such as actuation, locomotion, to create haptic surfaces, etc. [18–22].

Numerous questions and unclear aspects in the smart materials field are still source of intense research activities aimed at exploring other

opportunities offered by this family of materials; among the unsolved issues, the following ones can be recalled: can the response of a synthetic material be precisely programmed similarly to what occurs in biological matter? Is there a way to systematically relate the synthesis of a functional material (production process), to its meso- and/or microstructure, to obtain a desired, tailored response? These are some of the most important marking points which will be discussed in the present review.

The literature in this field is really broad and sometimes dispersive. Before moving to the core of the review, it is worth citing some previous relevant review studies dealing with this topic. In [3], an inspiring review on natural and synthetic responsive matter, with particular emphasis on *shape-changing* materials, is outlined. In [6], a fascinating review on insects and living organisms has been illustrated. Mc Cracken [1] presented a comprehensive review on stimuli-responsive materials (polymers and others materials), focusing on their implementation as machines. In [23], a survey on responsive polymers suitable for advanced applications, presented by following a mechanics-related perspective, has been considered, while in [24] a review on stimuli-responsive polymers for fabricating active microscale machines has been illustrated. The study published in [25], focused on responsive materials, with a particular emphasis on soft matter enabled by bio-inspired design and additive manufacturing (AM) technology. Similarly, in [26] a review on bio-inspired materials obtained through AM technologies for producing shape-changing materials, electric devices, hydrodynamic structures, etc., has been presented.

As a matter of fact, bio-materials have been the source of inspiration for chemists, physicists, engineers, material scientists, etc., to develop new materials possessing uncommon properties, despite the realm of nature still outperforms the capabilities offered by today’s synthetic stimuli-responsive materials [3].

The picture outlined above is the starting point of the present work in which we would provide some insights in the outstanding capabilities of biological matter, and use them as sources for inspiring, promoting, and innovating the field of functional materials.

In particular, this review focuses on the most disparate morphing capabilities and programmable responses of (a) biological matter and (b) synthetic functional polymers and polymer-like materials, and tries to outline and identify common features displayed by these two realms. The future developments and the achievements of new frontiers in materials science can certainly benefit from understanding and mimicking the strategies adopted in nature. The present paper is aimed at providing a broad overview elucidating the strategies and mechanisms adopted in nature by materials and structures to achieve specific functionalities. Similarities existing between synthetic functional materials and natural bio-encoded matter together with their fascinating underlying mechanisms, can help improving functional materials as well as to enable the design and synthesis of new advanced materials possessing unprecedented capabilities. In the above-outlined context, we provide also a concise overview on synthetic functional materials developed during the last decade; a new interpretation of the underlying mechanisms providing their functional response is also considered. Accordingly, the most important aspects concerning the mathematical modeling of the functional response, suitable to be exploited for materials design purposes, are discussed. Moreover, the effective application of the mathematical description of the process-microstructure-responsiveness relationship relying on multi-physics based models, which can be exploited for encoding a desired responsiveness into a functional material, is finally illustrated.

The paper is organized as follows. Sect. 2 presents an original review on morphing and programmable response of biological matters and synthetic functional polymeric materials, and a parallelism between the underlying features and mechanisms is outlined. Sect. 3 presents an overview of functional polymers by following a novel classification based on the mechanism inducing the functional response they are based on. Sect. 4 introduces the concept of the *process-microstructure-*

responsiveness relationship, useful for the systematic design and programming of functional materials obtainable by tailoring their microstructure; in this context, some relevant examples are presented and discussed. Finally, sect. 5 closes the paper with some final remarks, future perspectives and important inspiring considerations in the field.

2. Bio-encoded matters and functional synthetic polymers: an intriguing parallelism

The development of new active materials and devices can greatly benefit from studying the strategies adopted by the natural world. In this section, we consider some relevant insights into the smart behavior of bio-encoded materials and structures, and – whenever possible – we try to outline a parallelism between natural matters and synthetic functional materials.

Before presenting the specific sections of the paper, it is worth clarifying the meaning of morphing and programmable response adopted throughout this work. Morphing is a generic term which assumes a variety of meanings: it indicates any change of a system or a material induced by some specific causes, taking place starting from an initial reference state, aimed at providing a specific response to the change of the surrounding environment. The response can involve the variation of physical, chemical, mechanical, or geometrical properties, such as shape/color/texture change, stiffness/strength variation, etc. While morphing is generally related to a change of some property induced by an applied stimulus and can be framed within the programmable response concept (a material can be programmed to morph in a certain way when stimulated), a programmable response not always involves morphing. In fact a programmable response does not necessarily imply changing the properties of a material or a structure: as an example, a material can be programmed to provide a mechanical response characterized by a pre-defined target stress-strain response. The extremely different mechanical responses shown by spider-silk, whose properties depend on the specific chemical composition and nanostructure, is an example of programmable response of a natural matter.

Sources of inspiration from nature can be found by considering different perspectives focusing on various aspects, such as mechanism adopted for obtaining functionalities, specific functional response, etc. Because of the vastness of the topic and the diversity of the functionalities involved, a systematic classification is non trivial. Since this section is aimed at providing inspiration for future developments in the field, it has been intentionally organized by following a classification based on *sources of inspiration* which can be found in nature while, in parallel, we discuss some features of synthetic functional matters. In more detail, Sect. 2.1 is inspired by the collective synergy of living organisms enabling functionality, while Sect. 2.2 takes inspiration from camouflage strategies in nature. Sect. 2.3 considers the locomotion mechanisms of living organisms. Sect. 2.4 discusses the defense strategies, Sect. 2.5 takes inspiration from the realm of plants and vegetables, while Sect. 2.6 considers bio-encoded matters synthesized by insects.

2.1. Collective actions enabling functionality

Collective efforts and synergies are commonly adopted by natural systems to obtain efficient solutions. The collective response comes from the reciprocal interaction of individual units (organisms, cells, etc.), leading to an overall response of the cluster they form (super-organism, colony, swarm, etc.). The behavior of a single unit interacting with many others is usually quite different from that it would be when the same individual is left alone [27]. In the cluster, the behavior of individual units is influenced by the neighboring units, and the reciprocal well-organized cooperation allows achieving a common and effective overall response corresponding to a particular desired functionality.

In nature, examples of collective responses can be found in many contexts and at different scales [7,27]; relevant examples are provided by organisms used to living in groups, such as bees [9], ants [28], birds

[29], fishes [30], bacteria [31,32], etc. Even animals not used to living in groups gain specific functionalities when grouped; as an example, it has been shown that a single rat employs a longer time compared to a group of rats to find a reward in a confined environment [33], indicating that the exchange of information among individuals provides enhanced capabilities. Scaling down to the microscale, cells can exploit collective action to promote functionality [27,34–40]. A relevant example is provided by living cells possessing mechanosensing capability, a crucial task for their physiological and pathological processes [38]: when mechanically stressed, they are able to detect and translate such a stimulus into a wide range of biological functional responses (cells migration, morphing, etc.). This smart capability has been shown to be amplified when cells respond collectively rather than when a single cell is concerned [41]. Collective response of cells takes place for instance in locomotion and actuation (such as in muscle tissues, see Sect. 1), in embryogenesis, wound healing, etc. It is worth mentioning that collective actions of living cells in some circumstances lead to undesired consequences, such as the body invasion of tumor cells [27].

Insects are often used to living in colonies and so they are capable of a collective behavior; the aggregate they form displays quite different characteristics according to the type of interactions existing among the single units. The emerging living matter is characterized by a response which can range from that of a solid to that of a fluid [42]; from a mechanical viewpoint, a very dense aggregate of living organisms can be considered as a viscoelastic material, whose variable rheological properties can correspond to that of an elastic-plastic solid or of a viscous liquid [42].

In the insect kingdom, fire ants work synergistically, Fig. 1(a-c): by exploiting a collective action, they can arrange themselves to form a variety of structures – displaying a solid-like rather than a liquid-like behavior – possessing advanced functionalities emerging in response to environmental stimuli [43]. As a matter of fact, they can create a giant buoyant raft for surviving during floods [44], Fig. 1(b,c), build optimally-shaped living bridges [45] or ladders suitable for food supply, etc. [7,8], Fig. 1(a). From a mechanical viewpoint, these aggregates are among the most effective example of self-healing and self-assembling material [46]. The mechanical behavior of fire ant aggregates has been investigated and, despite the difficulty to interpret their multifunctional capabilities, some quantitative results have been obtained based on the mechanics of their reciprocal interaction: in response to the applied stress, ants can dynamically re-arrange their conformation and are capable of storing elastic energy, displaying a mechanical behavior which resembles that of viscoelastic solids rather than of purely viscous fluids [43]. However, the capability of fire ants to change their arrangement in space is not unlimited; a maximum stress level (estimated to be around 250 Pa) cannot be overcome by the cluster, and above this limit ants start separating apart [43]. From rheological tests, it has been shown that in some particular conditions, namely for low stress values, a liquid-like behavior can be recognized [43,47]. The mechanical properties of fire ant aggregates depend also on ants' activity/inactivity level (quantifiable by a non-dimensional speed parameter) [48]; in other words, fire ants can regulate the level of their activity to program the mechanical response of the cluster they form in a very surprising smart way.

Honeybee swarms are others examples of solid-like aggregates possessing advanced functionalities emerging when triggered by physical (thermal or mechanical) stimuli, Fig. 1(d,e). They are very efficient in the thermal regulation of the swarm, ensuring a noticeable energy economy [49,50]. In fact, honeybees can arrange the swarm's density and area-volume ratio for maintaining a near constant core temperature upon large fluctuations of the environmental temperature conditions [9]. A honeybee swarm is able to form a stable solid-like structure in presence of mechanical actions, Fig. 1(e); their collective behavior allows the colony to withstand mechanical loads (static gravity and dynamic shaking loading, such as that induced by wind), showing a surprising morphological response providing mechanical stability to the

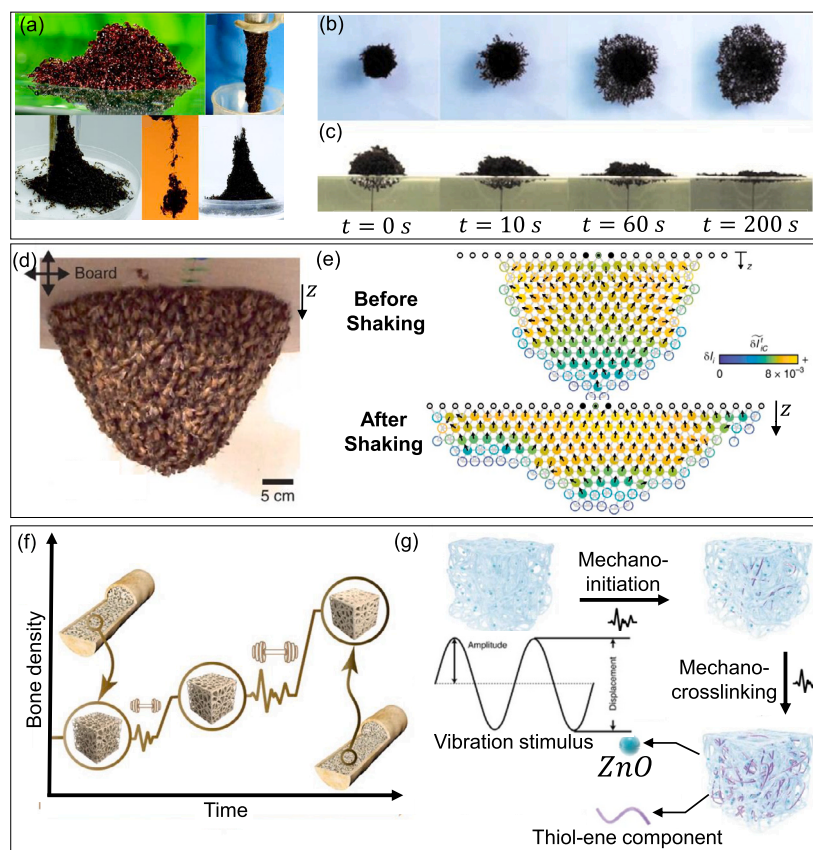


Fig. 1. Some examples of collective actions inducing functionality. Collective behavior of fire ants (a-c): cluster of fire ants whose overall shapes can change over time for functional purposes (float, food supply, etc.) (a), reproduced from [28] with the permission from The Company of Biologists Ltd, Copyright 2014; time-dependent organization of several fire ants into a single buoyant raft (b,c), adapted from [44] with the permission from PNAS, Copyright 2011. Collective action of honeybee swarms (d-e), adapted from [9] with the permission from Springer Nature, Copyright 2018; a cluster of honeybees attached on a moving plate (d) displays shape-morphing when shaken (e): according to a self-detected local strain of the overall cluster (see the blue-yellow color field, (e)) honeybees rearrange their position to avoid cluster breaking. Collective action of bone cells leading to a time-dependent bone density increase (f) and similar functional behavior encoded into a synthetic responsive polymer leading to a stiffness increase under mechanical action (vibration) obtained by exploiting a mechanically-driven polymerization reaction (g), adapted from [54] with the permission from Springer Nature, Copyright 2021.

cluster [9]. This surprising behavior depends on the relative bees position, which seems to drive the shape adaption of the honeybee swarm; by assuming the swarm to be an ideal continuum material, the relative bees' displacement induces a self-equilibrated stress state. This mechanical behavior has been shown to be naturally-programmed: when a certain strain threshold is achieved, bees move from regions characterized by low strain values (i.e. low relative displacements among bees) to highly strained regions, in order to functionally ensure stability to the overall cluster [9], Fig. 1(e).

Other studies have tried to determine the mechanical properties of flying insect swarms which, despite quantitative results (such as the stress-strain law) are still far from being clearly established, can be considered solid-like materials. An insect swarm has been quasi-statically separated into smaller swarms, suggesting the existence of emergent mechanical properties such as the Young's modulus and the tensile strength, while the viscous flow response, typical of fluids, appears to be not clearly existent in these aggregations [51,52]. Since the mechanical properties depend on the insects reciprocal interaction mechanisms (which encodes the internal structure of the swarm), a functionally programmable and adaptable mechanical response can be recognized [53].

A great effort has been made by the scientific community to develop active colloidal materials displaying a behavior which resembles that of biological aggregations [7], such as microbubbles [55], Janus particles [56], vesicles [57–59], etc. Microbubbles are constituted by a fluid core (liquid or gas) encapsulated within a polymer-like shell [60] with tailorable and programmable mechanical properties [61,62]. To some

extent, they can be considered as hydrogel-like materials whose functional properties typically stem from a pressure stimulus (for instance induced by exposure to ultrasounds), capable of inducing movement and/or morphing (shape-change, growth, controlled-breaking, properties variation, etc.) of the bubbles. They have been used in different applications in the biomedical sector [55], such as for creating sites of mechanical stimulation of tissue in ultrasound-based therapies [63,64], for drugs and gene delivery [65,66], as functional agents to drive the dissolution of blood clots [67], as contrast agents in clinical diagnostic [61,62], etc.

A collective-like behavior can be also found in Janus particles whose functional features stem from their particular structure composed by two or more parts having quite different (or even opposite) chemical-physical properties [56,68–70]. Typically, a Janus particle has a spheroidal shape and is constituted by one hydrophilic hemisphere and one hydrophobic one. These particles have been developed also in other shapes (cylindrical, disc-shaped, etc.) and can be made of different materials, such as polymers, inorganic or polymeric-inorganic matters [56] often characterized by opposite behaviors. Polymeric Janus particles have attracted a great attention because of the soft-nature of their polymer backbone, and because of the feasibility to program and tailor their asymmetric properties arrangement [56,71,72]. Janus particles can be programmed to show simultaneously or alternatively the features of different materials, enabling their use in drug delivery systems [73–75], fluid separation [76], as emulsion stabilizing agents [77,78], in bio-sensing and bio-catalysis [79], bio-imaging [80], etc.

It is worth highlighting the use of Janus particles for creating controllable holes in membranes under mechanical actions [73]; similarly to the behavior shown by some cells, these particles can act as a zip agent by self-assembling to close an hole present in a sufficiently highly stressed membrane. Beyond a threshold stress, the cluster formed by these particles disappears, thus providing re-opening of the hole [73]. This mechanism, which can be triggered by different stimuli (such as pH, temperature, etc.), and depending on the particular feature required to the membrane, represents a prominent inspiration for the design of smart membrane containing open or closed holes “on demand”, to be used for example in drug delivery systems and fluid separation applications.

Even if the literature on this topic is quite broad, a direct connection between active colloidal synthetic materials and biological aggregations is still lacking, despite it would be prominent for future advancements in the field [7]. Within this context, the published researches are mainly focused on methods of preparation and applications of these materials, whereas theoretical and numerical models describing their functional and mechanical behavior need to be developed beyond the present knowledge.

A further example of adaptable and programmable response based on collective actions can be found in the bone tissue, Fig. 1(f): by exploiting the synergic collective behavior of bone cells (osteoblasts and osteoclasts), the shape, structure, mass and mechanical behavior of the bone change continuously to adapt to external forces. According to the detected load level, osteoblasts add bone tissue at highly stressed regions, whereas osteoclasts remove bone tissue from sites with low stress levels [5]. Similarly, a polymeric material displaying a continuous increase of stiffness as a function of the mechanical actions has been developed [54], Fig. 1(g). This behavior can be obtained by harnessing the so-called mechanically driven polymerization reaction: a chemical specie (ZnO) embedded in the polymer matrix acts as mechanochemical transducer, detecting a mechanical stimulus and promoting the polymerization reaction, Fig. 1(g). Accordingly, the cross-link density continuously changes, providing a material characterized by a shear modulus distribution which depends on the applied stress [54]. In [54], the monotonic stiffness variation of the material in function of the mechanical stress level has been demonstrated: the controlled polymerization reaction leads to a shear modulus increase, while decreasing is not possible. The development of a material which, under mechanical stimuli, can either increase or decrease its elastic properties through controllable cross-linking and de-crosslinking reactions, remains still a challenge [54]. Another tunable mechanical properties response can be found in [81], where the interaction of a hydrogel with clusters of minerals (polymer-cluster interaction) has been exploited to create a thermal-stiffening material displaying a dramatic stiffness increase (around 13000 times the initial value) upon heating.

Moving back to natural systems, a further relevant example of collective behavior is provided by the well-known baker's or brewer's yeast (*Saccharomyces cerevisiae*), a living material which proliferates when exposed to air. Inspired by yeast, a polyacrylamide hydrogel with embedded *Saccharomyces cerevisiae* has been developed [82]. This composite material proliferates when triggered by environmental stimuli by displaying shape and volume-change. Both the tunability of the mechanical properties of the hydrogel network, as well as the level of activity of the living cells, can be exploited to program the desired shape-change. When the stiffness of the hydrogel increases, the volume change provided by the cell proliferation decreases; this response has been argued to be justified by the limitation of the expanding colonies by increasing the hydrogel's elastic resistance limit. In this way, the elastic modulus distribution can be encoded in the material by performing a controlled photopolymerization in which the exposure time and/or light intensity are properly tuned [20,83–87]), promoting a desired shape-morphing. Alternatively, the level of activity of the living cells can be hindered by the exposure to UV-light, as done in [82],

where the light has been used to kill living cells in specific regions, thus providing a programmed proliferation leading to shape change.

In some cases, the collective action of living organisms is aimed at transforming a destructive input (such as a mechanical action) into a constructive action, sometimes referred to as constructive adaptation [88]; an example is represented by muscles transformation induced by training: repeated loads induce the formation of new mass and increase in mechanical strength. On the other hand, traditional synthetic engineering matters usually fail or weaken when loaded, and so they do not display any constructive adaptation [88]. Research studies aimed at encoding a constructive adaptation in functional synthetic polymers to infer them new properties, have been recently published [89–91]. A relevant example is provided by the swelling phenomenon taking place in gels; it is well-known that when water migrates into the polymer matrix, the network swells until an equilibrium condition is achieved. Failure can also occur when the osmotic pressure attains the elastic strength of the polymer [14,92]; moreover, it has been shown that the material's stiffness and mechanical strength decrease during swelling [93,94]. In contrast to this well-known behavior and inspired by the constructive adaptation of living organisms, a polymer capable of increasing its stiffness and strength under swelling by harnessing a water-assisted cross-linking reaction, has been recently proposed [88], see Fig. 2.

The systematic programming of the mechanical response of materials, obtained for instance through a controlled synthesis [95], is an ongoing challenge increasingly adopted in materials science. In advanced applications, it could be necessary to design a material having precise mechanical properties (shear modulus, tensile strength, etc.) according to the level of the applied load. To pursue this feature, a quantitative relationship between the synthesis, the microstructure, and the related parameters (process-microstructure-response relationship, see Sect. 4), is required to program the material response in a precise way. Within this context, understanding and investigating the behavior of living organisms is often beneficial for developing functional bio-inspired materials; inspired to the collective action of living organisms, among the most interesting functionalities required in applications involving smart materials, it is worth mentioning self-healing, self-assembling, self-strengthening, drug delivery, self-diagnostic (bio-imaging), ultrasound-therapy, etc.

2.2. Camouflage strategies

Morphing inducing camouflage of living organisms – aimed at eluding visual detection or recognition, or to launch signals – is quite common in nature: it represents the ability of an organism to morph its appearance (skin's color, shape, etc.) and/or behavior when exposed to specific surrounding stimuli [96–100]. Camouflage in nature is a strategy frequently adopted by both animals and plants [100].

In nature, morphing for obtaining camouflage is achieved through different strategies: the most common one is the ability of living organisms to morph the color/pattern (optical camouflage) or roughness (haptic camouflage) of their skin, scales, etc.; other mechanisms, such as postural-camouflage inducing shape-change, are also used. Living organisms detect signals coming from the environment and, through a complex neural elaboration, activate a quick response to get camouflage (bio-encoded functionality) [101]. Based on this fascinating capability, the synthesis and design of functional materials capable of detecting and responding to environmental stimuli, for launching signals, to reveal the presence of chemical species, to measure quantities, etc., is one of the main challenges of materials science. Some considerations concerning this aspect are discussed in the rest of this section.

By assuming the skin of a living organism to be a body-environment bio-material interface, the optical or haptic camouflage can be thought as the change of the characteristics of such an interface as the result of various physical-chemical mechanisms triggered by external stimuli. For instance, chameleons can blend into the background by tuning the arrangement of guanine nanocrystals present in the skin cells to change

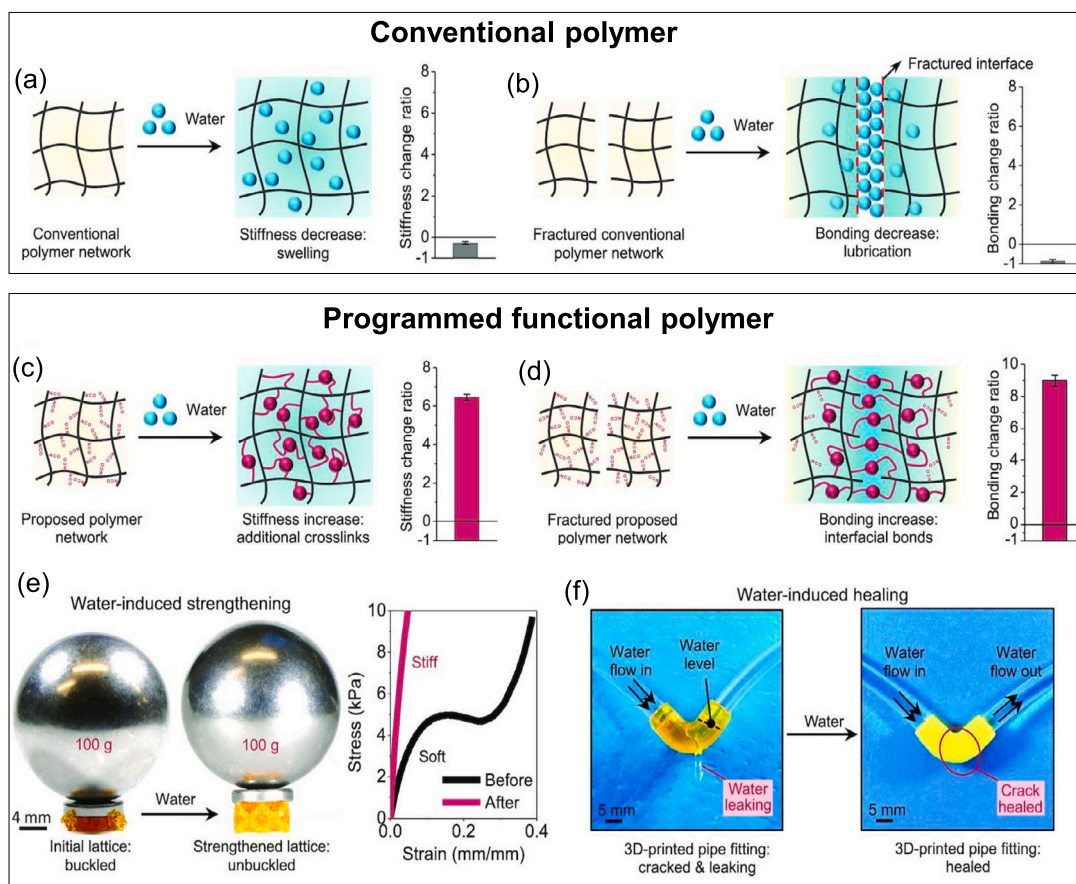


Fig. 2. Programmed mechanism of constructive adaptation of a functional synthetic polymer in water (a-f), adapted from [88] under a Creative Commons CC BY license from Oxford University Press, Copyright 2022. Schematic of the swelling-induced stiffness decrease of a conventional polymer network (a): water molecules migrate in the network, providing a volume expansion corresponding to a decrease of the cross-link density; the corresponding stiffnesses ratio, defined as $(E_d - E_s)/E_s$, being E_d and E_s the Young's modulus of the initial dry and of the swollen (after immersion in water for 24h) specimen, respectively, is also shown. Schematic of the swelling-induced bonding decrease of a fractured conventional polymer network, and plot of the bonding change ratio (b). Schematic of the mechanism of the swelling-induced stiffness increase of a programmable functional polymer obtained by exploiting a water-induced additional polymerization reaction and plot of the corresponding stiffness change ratio (c). Schematic of the swelling-induced self-healing of a functional polymer (d). Examples of applications exploiting 3D-printed structures made of the programmed functional material (e,f): Water-induced strengthening of a structure loaded with a metal ball, and corresponding compressive stress-strain curves of the structure before and after immersion in water for 24h (e). Water-induced self-healing of a 3D-printed pipe (f): a crack in the broken pipe can be healed after immersion in water allowing the fluid flow restoration.

the wavelength of the reflected light [102]; this smart responsiveness can occur either for mimicking (e.g. not to be detected by predators) but also for launching signals, resembling the function of a smart sensor. Moreover, it has been observed that the skin of a male chameleon can reversibly change color when it encounters a female chameleon [102], Fig. 3(a). Some aquatic living organisms, such as jellyfish, octopus, and cuttlefish can change their skin's colors or patterns in order to adapt to the most disparate environments they detect [101,103,104], thanks to bio-encoded responsiveness which involves complex visually-neurally-controlled actions [101].

Similarly to organisms capable of changing color or to emit bioluminescence triggered by external stimuli, functional self-diagnostic polymers have been developed; such polymers are capable of changing color or to emit fluorescence passing from a stress-free state (undeformed configuration) to a stressed one (deformed configuration), thus enabling to visually quantify their stretched state. By exploiting a mechanically-induced chemical transformation or reaction, these materials behave like a sensor, not tethered to any external electric systems, capable of transforming a mechanical stimulus into a specific detectable signal (color, luminescence, etc.), Fig. 3(b) [105–107,110], enabling strain measurements or damages detection [105,108–120]. As a matter of fact, optical camouflage can be thought as the natural counterpart

of self-diagnostic materials where a change of appearance is related to some external input.

Functional polymers capable of displaying camouflage have been recently developed to obtain synthetic bio-inspired soft robots [121,122]. For instance, in [121] a bio-inspired robot capable of color-shifting by exploiting the thermal-regulated swelling of Poly(N-isopropylacrylamide) (PNIPAM) has been proposed; when immersed in water at room temperature, the material is transparent because it is almost entirely (90%) made of water, while when the material's temperature increases above a threshold value, the reversible temperature-controlled swelling-driven mechanical response [123] induces shrinking (see Sect. 3.2) responsible for color change [121]. Upon cooling, water molecules can enter again in the material leading to swelling and so inducing a further color change [121] until the initial transparency is recovered. Similarly, it is worth mentioning the development of smart hydrogels containing photochromic microcapsules possessing the capability of quickly changing color and electrical conductivity under thermal or UV stimuli: as a result, they can be used to timely sense and visualize human physiological activities, as well as in applications requiring an adaptive camouflage [124].

The need of synthetic materials possessing effective camouflage capabilities, has promoted a huge research effort, especially in the military field: among the various sought possibilities, the so-called thermal cam-

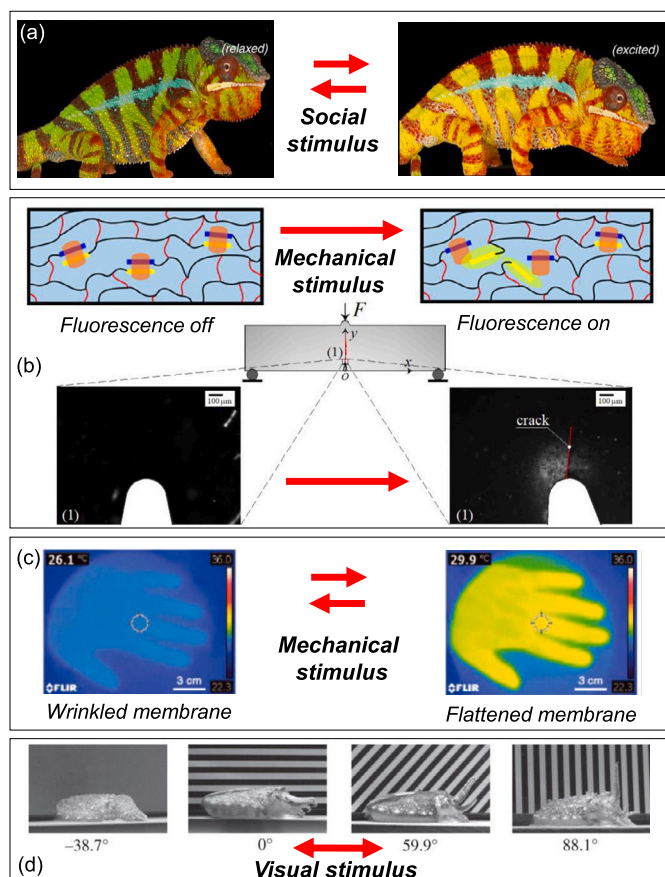


Fig. 3. Examples of camouflage in nature and in synthetic responsive polymers. Skin of a male chameleon can reversibly change color (from a relaxed to an excited state) due to a social stimulus, (a), adapted from [102] under a Creative Commons CC BY license from Springer Nature, Copyright 2015. Fluorescence emission of a synthetic self-diagnostic polymer induced by a molecule conformation change arising when passing from a stress-free state (undeformed configuration, no bending) to a stressed one (deformed configuration of the specimen under bending) upon application of a mechanical action F (b), adapted with permission from [110], Copyright 2017 American Chemical Society. Camouflage of a synthetic polymeric membrane provided by a mechanical-induced roughness change of its surface; a target (warm hand) can be hidden when observed by a NIR camera (c), adapted from [125] with the permission from John Wiley and Sons, Copyright 2020. Postural camouflage of cuttlefish provided by the bending response of their arms resulting in different bending angles according to different visually-detected backgrounds (d), adapted from [126] with the permission from The Royal Society (U.K.), Copyright 2012.

ouflage or thermal cloaking (indicating the capability of a material to hide itself or a target when observed through an infrared (IR) camera) is a recent topic which has opened new scenarios in the field of security services [127]. The IR device transforms the detected radiative energy emitted by an object into an electrical signal, enabling the reconstruction of its temperature field [127]. However, by properly tuning the material's properties, this capability can be functionally controlled, achieving the so-called thermal camouflage [127].

Strategies allowing to code into a material an uncommon thermal behavior, aimed at obtaining thermal invisibility at a fixed background temperature (static thermal camouflage), belong to the so-called design of the material's emissivity [127]. However, in real applications the surrounding environment could change, and the thermal camouflage can be hindered. A material characterized by an adaptable thermal camouflage, provided for instance by an adaptive emissivity under different environmental variations (electric field, light intensity, temperature, mechanical stress, etc.), would be the most desirable in future applications [127].

The possibility to get a dynamic thermal camouflage in a soft polymeric membrane via mechanical stimuli (a tri-layer structure made of an acrylate elastomer sandwiched between two sulfonated pentablock copolymer membranes) suitable to hide a target object, has been shown in [125]. The adopted membrane is characterized by a wrinkled surface (roughness equal to about 564 nm) in the undeformed configuration, whereas it becomes flat (surface roughness 15 nm) under the application of a certain tensile stretch [125,127], Fig. 3(c). The IR image of the membrane can be modified by tuning its surface roughness and thickness via mechanical stimuli [127]. When no mechanical actions are applied, the detected temperature of the wrinkled membrane T resembles that of the background T_B (i.e., $T \approx T_B \approx 26^\circ\text{C}$), whereas when the membrane is stretched to get a flat surface ($T \approx 30^\circ\text{C}$), the hidden warm object appears ($T \neq T_B$) [125], Fig. 3(c). If the temperature of the background changes (achieving $T_B \approx 30^\circ\text{C}$), the flat configuration becomes the optimal one for getting camouflage. The reversibility of the wrinkling mechanism as well as the integrity of the membrane play a fundamental role: according to [125], the material is stable and fully reversible even after applying hundreds of strain cycles. Beyond mechanical stress, other approaches to promote dynamic wrinkling, such as those based on the electro-mechanical transition in dielectric elastomers, have been proposed [128–130] (see Sect. 3.3) [125].

Similarly, it is worth mentioning the use of Liquid Crystal Elastomers (LCEs, see Sect. 3.1) which are suitable to obtain surface morphing thanks to their capability of creating wrinkled patterns under temperature changes [130,131]. LCE-based devices can be designed to self-reconfigure their wrinkled surface by simply responding to a temperature change of the environment, enabling their application for thermal camouflage purposes.

A systematic design of materials aimed at encoding precise and reversible surface wrinkling (obtained by controlling the wrinkle wavelength, amplitude, direction, etc.) at different length scales, should be implemented in order to enable adaptable camouflage. To this aim, theoretical and computational approaches based on a mechanical engineering treatment of the wrinkling phenomenon [132–135] represent promising tools to promote innovation in this field. A comprehensive review on recent advancements in the mechanics of tension-induced film wrinkling and re-stabilization, can be found in [136].

The membrane designed in [125] can be considered to some extent as a synthetic skin characterized by two different camouflage mechanisms: a passive haptic-like camouflage (change of surface roughness induced by a mechanical stimulus), and an active haptic-like camouflage (color change occurring in the IR light domain). A membrane capable of morphing from a 2D into a 3D shape under a pressure stimulus for getting synthetic camouflage has been proposed in [137]; the membrane is constituted by a composite structure with a soft elastomeric bulk material reinforced with a patterned fiber mesh acting as an internal constraint. By exploiting the patterned reinforcement, several 3D target shapes have been obtained [137]. Based on the concept of creating materials whose spatially-dependent stiffness enables inhomogeneous deformations leading to 2D-3D shape-change, several other studies have been performed [138–144]. It is worth recalling that a rigorous classification of the above-described materials is not trivial; when the mechanism enabling the desired functionality is mainly based on the topological arrangement of its constituents, the material falls within the so-called metamaterial family, namely topological-functional-based polymers or architected materials, see Sect. 3.6.

The haptic camouflage of living organisms whose morphing features (tunable shape, temperature, etc.) are triggered by external stimuli, represents a source of inspiration to design synthetic haptic surfaces [25] [145–149]. Haptic surfaces find applications in the most disparate fields, such as in robotics [150], in virtual and augmented reality [149], healthcare [151], in smart electronics applications [152], etc. Among the various possibilities offered by synthetic functional polymers, electroactive polymers [145,153,154], LCEs [155,156], etc.,

enable unprecedented and multi-modal human-machine physical interactions [145,146].

In nature, camouflage is not limited to variations of color, texture, roughness, etc. but can also involve complex movements or shape-change of the entire structure (postural-camouflage) [126,157]. Living organisms can morph to achieve anti-predator goals [158] (preys eluding visual detection), or to facilitate predation [99] (predators avoiding to be visually detected to capture preys). For instance, salamanders are known to use their head, tail and legs in multiple postures with anti-predator functions [157]. In the marine environment many examples of postural-camouflage can be observed; cuttlefishes and squids can bend their arms according to the environment they detect, enabling camouflage in the most disparate conditions. A surprising experimental study [126] has investigated how a visually detected environment affects the arms posture of cuttlefish; by changing the background pattern (characterized by a uniform grey color, rather than by various patterns made of grey and white alternate strips with different orientation angles), cuttlefishes morphed their arms position accordingly, Fig. 3(d).

It is worth mentioning that, while shape-change in cuttlefishes is limited to bending of their arms, other living organisms (such as octopus) without any rigid internal structures, can exhibit very complex 3D shape-morphing aimed at obtaining camouflage [126].

The postural camouflage of living organisms has inspired the development of soft robots [159]; to date, 2D and 3D shape-morphing structures made of functional polymers have been obtained. Synthetic functional polymers have been employed to develop mechanical actuators capable of promoting grafting, releasing, lifting, etc. [160,161]. An example of artificial material mimicking the octopus tentacles, is represented by the temperature-dependent shrinking/swelling response of PNIPAM/PAM-AA bilayer hydrogels (see Sect. 3.2); their reversible bending/unbending mechanical response has been exploited to develop soft actuators with gripper capabilities [122].

Despite recent findings, it is still difficult to exactly replicate the postural-camouflage of living organisms; a tentative to solve this issue has been done by using a bi-layer LCE cantilever beam to obtain morphing upon heating/cooling [162,163]; simple bending as well as wavy-like complex shapes, whose aspect can be tuned according to the microstructure of the synthesized material (see Sect. 3.1 and Sect. 4), can be obtained. However, to date responsiveness induced by visual detection of the environment is far from being obtainable through functional artificial materials.

So far, many studies have focused on materials characterized by a single camouflage capability triggered by an external stimulus; however, the next frontier in this field is the design of materials characterized by multi-stimuli camouflage capabilities, i.e. materials displaying a variety of responses according to a single or multiple stimuli [121,164,165]. An hydrogel capable of simultaneously morphing its shape, surface roughness, and color when the temperature changes, rather than when it is exposed to a pH variation, represents an example of multi-stimuli responsive material. Programming and encoding multiple responsiveness in materials, still represents an outstanding achievement in materials science.

2.3. Locomotion mechanisms

Living organisms are naturally programmed to functionally morph their body for performing locomotion in the most disparate environmental conditions [166].

In terrestrial environment, the morphing enabling locomotion (such as walking, running, crawling, jumping, climbing, etc.), which typically involves contact with a solid substrate, is influenced by the features of the substrate itself, such as roughness, texture, geometry, friction, stiffness, mechanical properties, etc., [167–171]. A relevant example is provided by the roughness of sand surfaces that affects the locomotion of fire ants; these insects are capable to move faster and with more sinusoidal trajectories on fine sand rather than on coarse sand [168]. Further,

snakes harness bending of their body and the asymmetric friction of their scales to move sideways [172,173]. Living organisms possessing multiple legs (such as caterpillars, spiders, geckos, etc.) perform locomotion by exploiting the legs' muscle deformation, whereas limbless animals (such as snakes, snails, earthworms, etc.) have bio-encoded body deformation capabilities allowing self-locomotion without needing any leg [174]. Thanks to bio-encoded outstanding physical properties, some animals are capable of very awkward self-locomotion mechanisms, such as climbing without needing any external support or structure; in this context, the climbing ability of gecko is mainly attributed to its adhesive toe pads interacting with the solid substrate which, together with the capability of arranging toes in different configurations (shape-morphing), allows self-attachment/detachment enabling locomotion [175].

In the aquatic environment, the swimming performance of living organisms is influenced by hydrodynamic mechanisms, such as vortices or other hydrodynamic stimuli. Fishes gain energy from aquatic vortices, thus reducing the muscle activity enable to improve and optimize their swimming performance [176]; they are usually attracted by turbulent three-dimensional water flows, such as those taking place in streams, while too highly turbulent flow can hinder and overwhelm their motility [167,177] or can induce animal to look for flow-proof refuges [167,178]. Several swimming modes can be observed in aquatic locomotion [179]; however, swimming is not the only way to move in a fluid. Some living organisms have evolved different underwater locomotion strategies, such as crawling, walking and jumping on the seabed; this class of strategies is adopted for instance by sea slugs and snails benthic invertebrates which are capable of crawling underwater [180]. These locomotion strategies are similar to those observed in terrestrial motion, despite beyond the features of the substrate (the seabed in the case of locomotion underwater), seawater properties play also an important role. Beyond locomotion strategies in water, the fascinating world of locomotion on water also exists; thanks to the light weight, extreme hydrophobic legs, as well as the ability of their legs of acting as driving paddles, some living organisms such as water striders, can easily move on the water surface [181–184].

Body morphing enabling locomotion is common also in air where living organisms are adaptable to flight in extremely different conditions; for instance, insects are able to fly both in presence of rest air as well as in turbulent air. From this perspective, the air movement can be considered as an external stimulus (it can be static, unsteady, or fully turbulent), requiring the flight mechanism to be tailored to the specific condition the organism faces [167]. The functional response enabling flight, relies on complex passive and active kinematics morphing mechanisms of wings and body, leading to a stabilized body motion even in presence of aerial perturbations, [185]. Passive morphing of wing is typically related to the deformations of their elastic structure, inertial effects and aerodynamic forces (aeroelastic behavior) interplay [186]. On the other hand, active morphing in air is related to the shape-change of animal body-parts induced by the sensomotor system, triggered by muscle activation [187].

Morphing enabling locomotion of living organisms has inspired researchers and engineers in developing functional materials for locomotion purposes; different actuation technologies, physical mechanisms, as well as distinct locomotion modes which, to some extent, mimic natural living structures, have been proposed [174,188,189]. In applications requiring autonomous locomotion, untethered materials are particularly relevant. In this field, a growing interest in synthesizing untethered soft robotic matter, characterized by autonomous shape-morphing capabilities in response to external stimuli, has recently emerged [19]. The adopted strategies typically leverage shape-morphing to obtain a directional spatial displacement of the center of mass of the structure. By considering functional polymers capable of locomotion and propulsions, self-adaptive locomotion mechanisms triggered by changes of the surrounding environment have been explored. In the following, we recall and compare the locomotion of living organisms in different

environments (water, ground, and air), with examples of bio-inspired locomotion obtained by using functional polymers.

Inspired by locomotion of organisms in aquatic environment, several works have been recently proposed [180,182,188,190–198]. Light-driven LCE swimming robots have been developed [190,191]; in these materials, the self deformation comes from the nematic-isotropic transition of LC mesogens (see Sect. 3.1) inducing shape-morphing of the polymer backbone which, if properly exploited, enables motion to occur. For instance, in [191] a periodic and reversible light-driven transformation of trans/cis isomeric azobenzene LC mesogens [199,200] induces bending responsible for a fish-like swimming motion. The locomotion can be controlled by different light sources: periodic and synchronized ON-OFF light intensity cycles make the robot backbone capable of exhibiting an alternate bending mechanism whose curvature enables swimming. Sea slugs and snails are capable of multiple locomotion modes in aquatic environment; similarly, a soft-bodied-LC-based robot capable of multiple light-driven locomotion modes has been designed [180]. Inspired by water striders, see Fig. 4(a), functional polymer-based robots capable of walking on water have been developed and potential applications have been proposed, despite the advancements in this field are still in their early stage [182,193]. A functional LC-based material containing three different types of embedded photothermal particles characterized by different photothermal properties, has been developed [182] for obtaining a tri-legged robot, Fig. 4(b), capable of multi-directional locomotion, Fig. 4(c). The mechanism allowing locomotion is determined by the nematic-isotropic transition occurring selectively in each leg of the robot; thanks to the selective heating of the photothermal particles lighted by a NIR light radiation of different wavelengths, a sequence of leg deformations inducing directional movement has been obtained [182]. Inspired by jellyfishes, a magnetic composite elastomer-based robot capable of swimming when exposed to a magnetic field has been developed [198]. Dielectric elastomers have been also used to obtain locomotion in water, even if they are far from providing autonomous, feasible, and untethered locomotion modes because of the drawback of requiring a voltage application to induce actuation. An attempt to overcome this limitation by embedding a small electric circuit and a battery to obtain a wireless swimming control, has been made to obtain a jellyfish-like dielectric-elastomer-based robot [201]. In [192], light-driven swimming locomotion of a polymer-based material has been obtained by exploiting the so-called Gibbs-Marangoni effect: a polymeric material (polydimethylsiloxane, PDMS), doped with photothermal particles characterized by different absorption properties, has been used to fabricate two different modular selective wavelength photothermal elements assembled into a polypropylene substrate to obtain a swimming actuator [192]. Upon light radiation with a laser of specific wavelength, the photothermal elements were heated giving rise to an asymmetric thermal distribution. As a result of temperature increase, the water surface tension arising around the actuator decreases, leading to a partial surface tension gradient responsible for the driving-force inducing directional propulsion [192,202]. The locomotion direction of the obtained device is simply controllable by modulating the light wavelength rather than controlling the position of the light source; this solution presents several advantages, especially in microsize components where controlling precisely the laser position might be difficult [192].

Terrestrial locomotion in nature has inspired and promoted the development of functional polymers aimed at creating autonomous devices moving on solid surfaces. Some examples are provided in the following. Similarly to living organisms whose locomotion capabilities are obtained by exploiting legs movements (such as spiders Fig. 4(d)), a two-legged polymer-based robot capable of moving forward due to the environment humidity change, has been developed by exploiting non-homogeneous swelling phenomenon in hydrogels [203], see Figs. 4(e,f). The main structure of the robot is made of a bi-layer composed by an active hygroscopic layer and an inactive hygroscopic one, each one connected to two polymer-based legs, Fig. 4(e). When exposed

to humidity, non-homogeneous swelling induces the bending mechanism which is responsible for the shape-morphing of the legs leading to locomotion, Fig. 4(f). The research has outlined that the legs movement is not purely driven by the bending mechanism of the functional bi-layer, but is influenced and governed also by the type of contact with the substrate. In fact, in order to make the directional motion to occur, the two legs-substrate contact must be characterized by different static friction coefficients: this can be achieved by synthesizing the legs with different materials or, as done in [203], by creating different leg-substrate contacts, see Fig. 4(e), [203]. It is worth outlining that obtaining locomotion by the systematic programming of the environment humidity- and leg-substrate-contact -driven bending mechanism, represents a very complex challenge. Inspired by caterpillars, whose motility is due to their multiple legs, Fig. 4(g), a LCE-based robot without active legs has been designed [204], see Fig. 4(h). The bio-inspired material synthesized in [204] is constituted by a LCE film with alternate nematic director alignments (patterned configuration), which - triggered by a spatially modulated moving light - displays a synchronized, time-dependent shape-morphing response enabling a directional advancement motion. As recalled above, limbless animals can simply self-propel thanks to body deformation; a relevant example is represented by the peristaltic-based locomotion typical of earthworm, whose unidirectional movement is achieved by alternate contractions and elongations of their body along its main axis [172,174,205]. In performing such a movement, the animal body displays elongation-contraction waves localized close to the body-surface contact region; a mechanical interpretation of the peristaltic locomotion can be found in [205]. Within the realm of limbless animals locomotion, it is worth mentioning the serpentine periodic S-curve movement (body undulation typical of snakes), where elongation-contraction waves can propagate in different directions; this strategy has been adopted to develop a snake-like LCE actuator [206]. Inspired by the peristaltic gaits of living organisms, functional matters capable of a peristaltic motion have been developed by using hydrogels or other functional materials [207,208]. Rolling-based locomotion mechanism has been adopted by some living organisms (such as scaly anteaters, caterpillars, etc.) to obtain motion on a solid surface. This strategy has inspired the development of rolling self-propelled devices made of functional polymeric materials [19,174], Fig. 4(i); by organizing the structure into two outer rigid polymeric rails linked together by LCE-based controllable hinges, the nematic-isotropic transition induced by an hot surface, induces the structure to morph from an initial flat shape into a cylindrical one enabling rolling to occur. The actuation of secondary LCE hinges provides a torque angular momentum responsible for the advancement through rolling; the self-propelling capabilities of the developed robotic matter mainly depend on the material characteristics and on the geometrical features of the structure [19].

The development of functional polymers capable of flight locomotion modes is, to the best of our knowledge, still a mirage. Some strategies suitable to be exploited within this context are briefly discussed in the following. Taking inspiration from insects, a lightweight polymer backbone with passive polymer wings driven by active polymer parts could theoretically represents a solution to this challenge. Nowadays, novel AM techniques and other advanced synthesis processes have been used to obtain artificial wings with tunable features [209,210]. Inspired by the functional morphology and mechanics of insect wings [211–214], lightweight passive polymeric wings characterized by a tailored-process-related mechanical properties (comparable to those of insects wings) have been obtained [209,210]. The mechanical properties of artificial wings can be tailored by tuning their shape and the internal venation structure [209,210]. The development of active synthetic wings capable of self-shape-morphing enabling flight locomotion, represents an awkward challenge; on this line, it is worth mentioning the development of origami-based structures which can be exploited to get locomotion in the air environment [215]. Light-actuated or other functional polymers discussed above, which are nowadays capable of

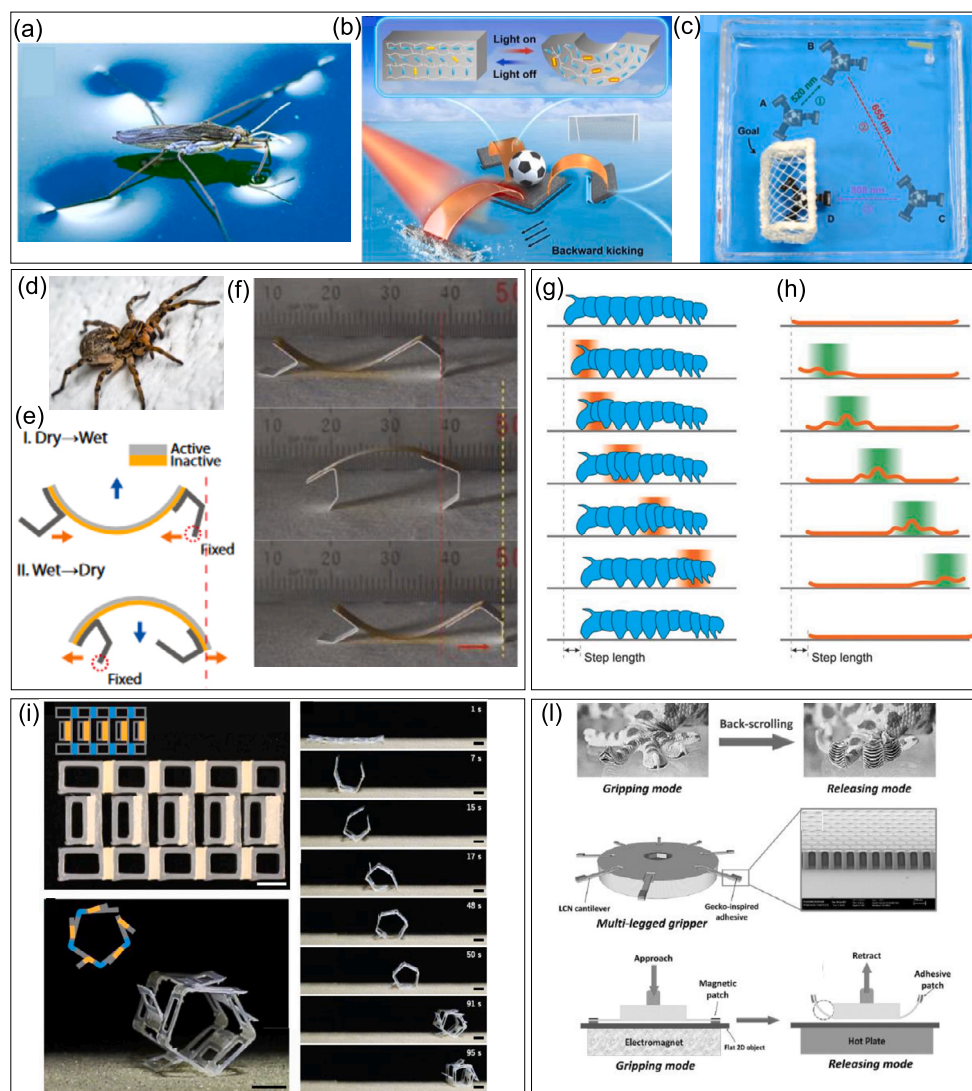


Fig. 4. Examples of locomotion mechanisms in nature and in synthetic functional polymers. A water strider can walk on the water surface by exploiting its light weight and smart hydrophobic legs (a); bio-inspired LCE-based robot capable of a multi-directional movement on water which, under a programmed radiation with NIR light, can reach a target position (b,c), (a-c) adapted from [182] with the permission from Elsevier, Copyright 2022. Walking capability of a spider on a substrate enabled by its legs movement and by contact interaction mechanisms with the substrate (d); a bio-inspired two-legged polymer-based robot capable of moving driven by a bending response induced by environmental humidity change (non-homogeneous swelling phenomenon) and different legs-substrate contacts (e-f), reprinted from [203] with permission from AAAS, Copyright 2018. A caterpillar is capable of locomotion through the use of multiple legs (g); a similar locomotion gait triggered by a selective-moving light irradiating a bio-inspired LCE-based robot (h), reproduced from [204] with the permission from John Wiley and Sons, Copyright 2016. A LCE-based device capable of a self-propelling through a rolling mechanism on a hot surface; the nematic-isotropic transition taking place in LCE hinges (orange and blue regions) induces shape-morphing from a flat to a cylindrical shape (i), reprinted from [19] with permission from AAAS, Copyright 2019. An hybrid responsive polymer, inspired to the locomotion of geckos, used to obtain a functional multi-legged gripper used for grasping/releasing target objects (l), reproduced from [175] with the permission from John Wiley and Sons, Copyright 2016.

locomotion in terrestrial and aquatic environments, in future will be perhaps capable of flying [216]. The adoption of bio-inspired geometries and mechanisms is quite relevant to the development of small unmanned aerial vehicles [217] whose future development will certainly benefit from the use of responsive polymers.

Locomotion of living organisms represents a source of inspiration not only for the development of functional materials enabling locomotion, but also for exploring other functionalities. Inspired by the gecko locomotion strategy, a functional multi-legged gripper made of hybrid adhesive-LCE cantilevers has been developed [175], Fig. 4(i); the functional response of this structure is capable of mimicking both the attachment/grasping and detachment/releasing mode of the gecko toes during locomotion [175]. The functional multi-legged gripper has been obtained by assembling several cantilevers, made of LCE mate-

rial, having a gecko-inspired magnetic adhesive at their extremities. The developed hybrid material exploits an electromagnetic stimulus applied to the substrate to obtain the attachment to a flat object, and a thermally-driven bending of the LCE elements to get detachment (peeling of the adhesive patch), Fig. 4(i). In order to obtain an effective gripping-releasing mechanism, such an engineered material must be characterized by some minimum requirements: gripping requires the magnetic field to be sufficient to get the necessary adhesive strength between the adhesive patch and the flat object, while releasing requires a suitable bending deformation to trigger crack-like detachment mechanism to occur.

Thanks to the outstanding opportunities offered by materials capable of autonomous (i.e. untethered) controlled locomotion, the interest in developing new advanced functional materials has increased in-

cent years. To date, the light stimulus has been proven to be an effective and versatile stimulus to drive and control materials designed for locomotion purposes; simple and feasible spatial-temporal control, as well as the possibility of controlling intensity, wavelength and polarization, make light-driven actuation a very attractive solution [192]. The directional motion of autonomous robot for transporting objects through complicated paths is a major challenge to be overcome in the future [192]. The majority of the existing studies have considered the development of functional materials capable of locomotion in a specific environment (in water, on water, on a solid substrate, etc.): the development of bio-inspired matters capable of locomotion on demand in different environmental conditions, represent a complex challenge for future researches. Similarly, the development of functional materials showing adaptive locomotion strategies in response to environmental changes typically found in living organisms, is another relevant challenge to be faced in the forthcoming years. In fact, despite the recent progresses in synthesizing functional polymers capable of multimodal locomotion is still an open issue. Recently, an attempt to build a bio-inspired soft robot made of dielectric elastomers capable of crawling and climbing, has been proposed [218]. Future developments and new scenarios in synthesizing new materials to be employed in advanced applications, can certainly benefit from the observation and interpretation of locomotion of living organisms [175].

2.4. Defense strategies

Living organisms can exhibit programmed functional responses to protect themselves against external dangers and threats [219], through defensive strategies. Many defensive strategies exist in nature, some of which have been already recalled in the previous sections. Self-protection of living organisms is often obtained by collective actions, such as that shown by a cluster of bees which adapts its shape to get protected against mechanical actions (e.g. wind, shaking, etc.), see Sect. 2.1. Protection can be also obtained through hiding strategies (e.g. camouflage, Sect. 2.2) or by escape (locomotion mechanisms, Sect. 2.3). However, other bio-encoded functional responses enable self-protection in nature, such as mechanical and chemical defense, death feigning, etc. [220], exist. Autotomy (or self-amputation), despite appearing an unsatisfactory strategy, represents instead a surprising example of smart response in nature: some body target regions are intentionally “self-broken” and then lost, by exploiting different mechanisms, to elude a grasp, to distract predators, etc. [221]. Despite tail dropping in lizards is the most iconic example of autotomy, this functional response is also displayed by several other living organisms, like octopuses (which can release their arms), crabs (dropping their claws), insects (which voluntarily amputate their legs), etc. [220,221]. It is worth noticing that some living organisms can restore their original body parts (self-healing mechanisms); lizards provide a surprising example in this context thanks to remarkable regenerative capabilities [222]. The self-breaking capability and successive growth characterize bio-encoded matter capable of self-breaking and self-healing on demand.

On the other hand, completely different strategies exploit defense mechanisms based on the release of chemical substances; as an example, insects can produce an impressive arsenal of chemical agents to enable protection; when released, the chemical agents can either harm attackers or simply repel predators [6,220].

Inspired by defensive strategies in nature, an overview on synthetic functional polymers suitable to obtain protection mechanisms or possessing functionalities relevant to this purpose is provided in the following.

A relevant bio-inspired example of functional polymers with self-protection capabilities is offered by materials possessing multiple unusual and tunable physical/chemical properties. Within this context, mechanisms aimed at separating oil from oily wastewater are particularly important [223,224]; materials having unusual physical/chemical properties, such as materials being both super-hydrophilic and

super-oleophobic, used as functional membrane for oil/water separation, have been developed [224]. Further, functional polymers have been also exploited to develop surfaces with a stimuli-controllable wettability, i.e. suitable to be used for controlling oil/water separation processes [224,225]. In oil/water separation process, a relevant “secondary threats” may arise: as an example, membrane often displays a dramatic fouling due to adhesion of oil droplets to the membrane surface [223]; by integrating hydrophilic polymer brushes and hydrogel layer on oil/water separation membranes, a double-defence-material capable of ensuring both oil/water separation and super-anti-fouling mechanisms, has been recently proposed [226].

Similar to what has been discussed above, it is worth mentioning the bio-fouling phenomenon, consisting in the accumulation of microorganisms, plants, algae, insects, etc., on structures and components, leading to material degradation, especially in the marine environment. Analogously to the release of chemical agents shown by some insects, some studies have developed antifouling coatings based on the continuous release of toxic metal ions to repel or to kill organisms approaching the surface [227]. However, such an approach has been shown to be harmful to non-target organisms and to the environment. The development of environmental-friendly alternative is an urgent need, and strategies based on functional polymers, typically relying on the use of polymers with embedded anti-foulants, have been recently proposed [227]. Stimuli-responsive polymers are excellent candidates for the development of smart coatings possessing a programmable wettability, self-renewability, capabilities of releasing eco-friendly antifouling agents, etc. One of the main approaches in this direction is the so-called material fouling-release technology; it is based on the idea that microorganisms adhere poorly to substrates with low surface free energy and can therefore be easily removed; this implies that using mechanical forces of low intensity, such as the shear stresses arising at the ship hull-fluid interface during sailing, or in cleaning procedures [227], microorganisms detachment from the substrate can be easily achieved. The possibility of tuning the mechanical properties of the coating material plays a fundamental role in regulating its anti-fouling performances, and allows opening new scenario in the context of interface bonding mechanisms [227–229], driven by an ad hoc programmed behavior of the coating material. Surface roughness is also relevant to fouling-release which is usually enhanced by nano- or microscale roughness [227]. Finally, it is worth recalling the use of membranes showing wrinkling on demand [230] to prevent bio-fouling (see Sect. 2.2 devoted to camouflage obtained through responsive materials).

In the context of functional materials with self-protection capabilities, the realm of the healthcare sector is particularly relevant. Responsive polymers used for drug release purposes have been developed [231]. Similarly to an insect programmed to release chemical agents to get self-protection, responsive polymers can be programmed to release into the human body in a controlled way a therapeutic substance against virus, diseases, etc. [232]. A quantitative understanding of the drug release capabilities, especially at the molecular scale, is a key aspect to design materials suitable for such an activity [23]. Functional polymers have been also exploited for the development of medical adhesives aimed at protecting skin or to promote wound healing [233,234]. Wound healing is a complex and dynamic bio-mechanical growth process that restores the function of a biological tissue [233]. Human skin is perhaps the most excellent material possessing bio-encoded self-protection mechanisms which, in presence of severe damage, has to be complemented by external actions (sutures, medical adhesives, etc.). Properly functionalized medical adhesives are able not only to bind strongly the failed tissue, but also to promote wound repair [233].

The defense strategies adopted by living organisms in nature can also inspire the development of responsive polymers characterized by other functionalities, not necessarily devoted just to protection purposes. A brief discussion on this aspect is presented below.

Fishes have evolved unique locomotion and lubrication mechanisms based on the highly hydrated surface mucus and enhanced by muscles

with an adaptable stiffness; both features are also exploited for the defense purpose, Fig. 5(a). Some fishes possess a tunable skin-external object friction coefficient depending on their skin muscle-driven elastic modulus whose variation is triggered by external stimuli [235], Fig. 5(a). The adaptable skin elastic modulus can lead to decreasing the contact area, and the mechanical deformation can further minimize the surface friction force enabling the fish to easily escape. Inspired by this behavior, a functional polymer suitable to be used for the development of artificially regulated lubrication systems, has been recently proposed [235], Fig. 5(b-d). It consists of a top mucus-like hydrophilic lubricating layer and a bottom muscle-like hydrogel, Fig. 5(b), which can stiffen via thermal-triggered phase separation, Fig. 5(c,d), inducing a tunable lubrication mechanism [235].

Pillbugs (*Armadillidium vulgare*) represent another relevant example in this context: they are capable of morphing their body shape by rolling and closing (conglobation mechanism) when triggered by strong vibrations or pressure typically produced by predators [219]. A similar mechanism has been obtained in silicon-based shell structures patterned with a regular array of circular voids and mechanically deformed by controlling the difference between internal and external pressure [236]; below a critical pressure, the ligaments placed between voids exhibit buckling, leading to the closure of the structures (encapsulation, a mechanism similar to the conglobation exhibited by the *Armadillidium vulgare*, [236]). From a mechanical perspective, the conglobation mechanism can be considered an unstable-like response; studies aimed at harnessing the instability mechanisms (buckling) to develop smart materials and structures are currently under an intense investigation [141,236–241]. Despite instability is typically considered a negative phenomenon in structures and materials, buckling is nowadays used to get a precise mechanical response enabling interesting functionalities. Elastic buckling typically takes place as a sudden switch from an initial shape into a buckled one with a significant amount of energy release, appearing as a load drop in the response curve [237]. This feature makes buckling an interesting mechanism suitable to be exploited to program the material/structure response, such as in designing energy dissipation systems and stabilizers [237] and in obtaining soft reconfigurable auxetic materials [141,242,243].

2.5. Taking inspiration from plants

The realm of plants and vegetables represents a precious source of inspiration in the field of morphing and programmable response of advanced materials. Despite being less evident compared with other living organisms, also plants are characterized by complex and intriguing programmed mechanical behaviors inducing shape-morphing, movement, color variation, etc., for achieving the most disparate functional responses (growing, nutrition, defense, reproduction, camouflage, etc.), Fig. 5(e,f).

Shape-morphing is quite common in plants and is typically responsible for plants movements which is generally classified in nastic and tropic, [244]. A nastic movement is not stimulus-direction-dependent, i.e. it is induced by a bio-encoded response which does not depend on the stimulus direction. For instance, the ability of some plants to close their leaves in response to a contact mechanical stimulus for capturing insects, Fig. 5(e), is an example of nastic movement; upon contact, the leaves close in a pre-defined way, irrespectively of the contact stimulus (lateral, from above, etc.). The so-called “sleep movement” shown by some plants moving their leaves during night, is another example of nastic movement, [245]. In other words, a nastic movement takes place with a single bio-encoded kinematical “pattern”. On the other hand, tropic movements depend on the stimulus direction (such as the gravitropism, i.e. the tendency of plants to grow following the direction of gravity, see Fig. 5(f)). Another example can be found from the underground activity of roots which growth and spread toward regions rich of water (stimulus).

Plants can exhibit movements in a wide range of speeds: slow, fast and sudden [244,246,247]. The majority of these movements are very slow, often imperceptible, and requires the expert eye of naturalists to be revealed [247]. Despite plants do not possess any muscle, some movements are very fast, similarly to those observed in the animal kingdom [247–249]. The turgor pressure (an internal hydrostatic stress) inside plant’s cells is the main responsible for most of the plant movements [247]. The amount of pressure is affected by complex physical-chemical interactions with the surrounding environment (atmosphere condition, soil features, water content, etc.); in particular, the water exchange between plant cells and the surrounding environment taking place by osmosis or evaporation, plays a crucial role in tuning the arising responsiveness. Similarly to what occurs in hydrogels (see Sect. 3.2), water flow in plants is driven by a gradient of water potential [247] which vanishes at equilibrium, giving rise to an internal hydrostatic stress. Plant cells are able to sustain a large range of pressure values thanks to their stiff cell’s wall [247,250,251]. To balance the internal pressure induced by absorbed water, mechanical stresses make the cell’s wall to deform; the interplay among water flow, stress-state, and cell-wall deformation, are the basis of water-driven movements in plants [247]. From a mechanical perspective, this mechanism is typically called expansive growth. A comprehensive understanding of this mechanism is relevant for the development of plants-inspired design of advanced materials. It requires bridging the gap between molecular mechanics and macroscopic behaviors; as a matter of fact, the literature on molecular biology and biochemistry in plant and fungi growth is quite huge; however, the macroscopic behavior – described by the governing equations which can be linked to the underlying molecular physics – needs to be considered for the engineering assessment and design of plants-inspired advanced materials [252].

In the field of functional materials inspired by plants, modern polymer-based materials, obtained by exploiting new AM technologies, have been developed for reproducing the complex structure of plants. According to [253], the main research directions in this field are the following: (1) development of water-driven materials for simulating the morphological changes of plants and vegetables, and (2) development of light-driven or heat-driven materials for simulating the blooming process of flowers. Inspired by plants displaying water-driven changes in their morphology, hydrogels with encoded localized swelling anisotropy responsible for shape-morphing has been developed [13]. The anisotropic stiffness induced by rigid fibrils contained in plant cell’s walls, has inspired hydrogel made of a composite ink with stiff cellulose fibrils embedded in a soft acrylamide matrix [13]. The possibility to easily align fibrils as well as to realize complex architectures by using AM technologies, make possible to program the shape-morphing of these materials in the most disparate ways.

The natural phenomena taking place in plants have also opened new scenarios in the robotic field; recent progress in the development of hydrogel-based soft robots, characterized by plant-inspired designs and actuation mechanisms, can be found in [244].

Some carnivorous plants, such as the Venus flytrap (*Dionaea muscipula*) or the aquatic *Utricularia*, are capable of capturing preys by exploiting elastic instabilities mechanisms triggered by external stimuli; upon touching their sensor cells, leaves close suddenly by exploiting a buckling mechanism accompanied by release of stored elastic energy [12,247,249,254,255]. Similarly to what has been considered in Sect. 2.4 dealing with defense strategies in nature, this natural mechanism represents a source of inspiration for the development of smart materials and structures with buckling mechanisms [12,141,237,254,256,257]. The flytrap response can be also replicated without the use of elastic instability; the bending deformation of a LCE with integrated optical fibres has been used to obtain self-closing under a light stimulus on demand [258], Fig. 5(g). Thanks to the self-recognition capabilities offered by the embedded optical fibre, smart grippers suitable to selectively grasp objects can be obtained.

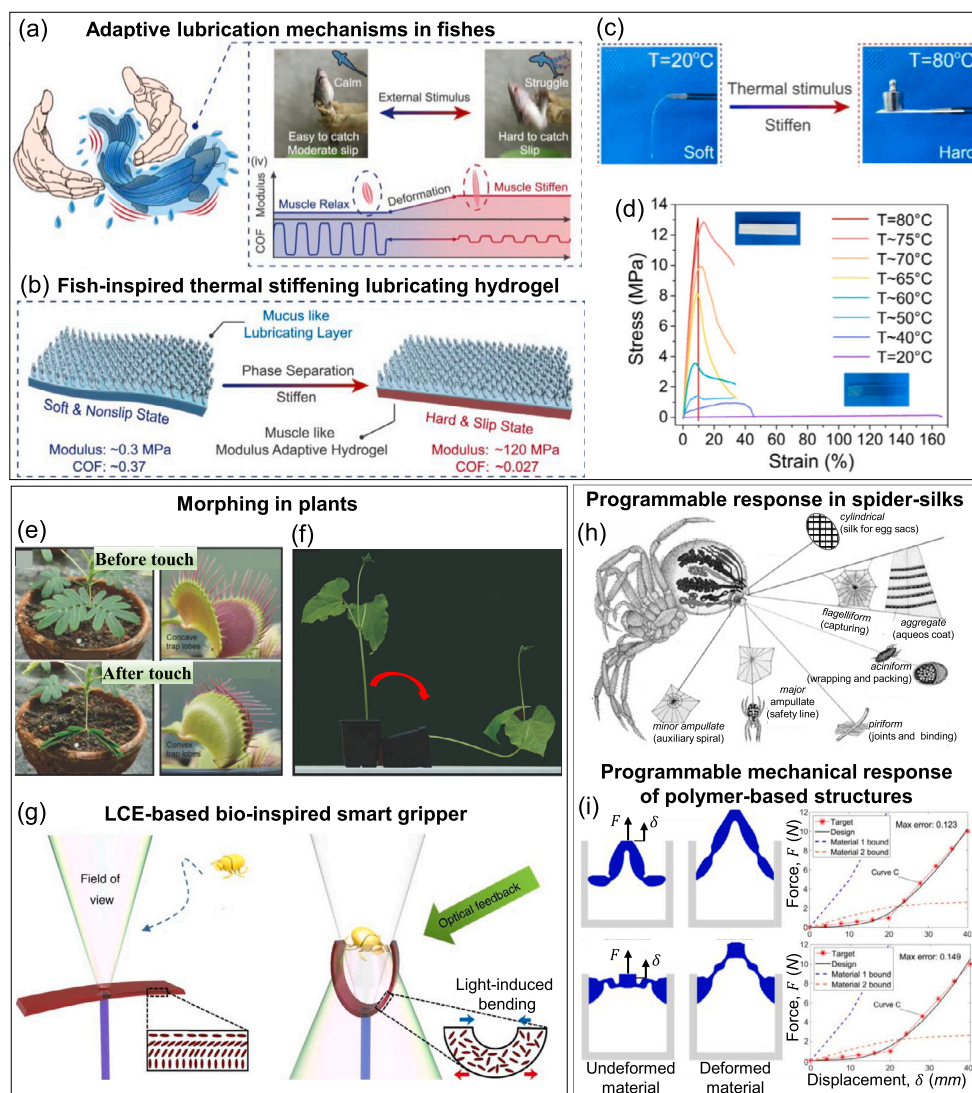


Fig. 5. Defensive strategies in nature (a-d), functional responses in plants (e-g) and bio-encoded matter synthesized by insects (h,i). A lubrication mechanism based on the highly-hydrated surface mucus and further promoted by a muscle-induced adaptable stiffness, allows fishes escaping from dangerous situations (a). A fish-inspired polymer-based material, made of a top mucus-like lubricating layer and a bottom muscle-like thermal stiffening hydrogel, constitute an artificially-regulated lubricating surface (b); the mechanical behavior of the hydrogel can be strongly affected by thermal stimuli (c,d); its mechanical response ranges from that typical of a soft material ($T \approx 20^\circ\text{C}$) to that of a rigid one ($T \approx 80^\circ\text{C}$) (c); different tensile stress-strain curves obtained from tests at different temperature values (d). (a-d) adapted from [235] under a Creative Commons CC BY license from Springer Nature, Copyright 2022. Nastic morphing of a flytrap plant which closes its leaves upon a mechanical stimulus (e); the tendency of plants to grow upward (gravitropism, a typical example of tropistic morphing) against counteracting mechanical stimuli (f). (e,f) adapted from [12] with the permission from John Wiley and Sons, Copyright 2017. A LCE-based smart gripper inspired by a flytrap plant capable of recognizing target objects and to close under a light-stimulus enabling gripping on demand (g), adapted from [258] under a Creative Commons CC BY license from Springer Nature, Copyright 2017. Different types of spider-silks possessing bio-encoded physical-chemical-mechanical responses enabling a functional response (h), adapted from [265] with the permission from Elsevier, Copyright 2000. Programmable mechanical response of polymer-based structures: through an advanced multi-material topology optimization, a wide range of programmed force-displacement responses can be obtained (i), adapted from [266] with the permission from Elsevier, Copyright 2021.

Plants, vegetables, and fungi have been recently used for developing new bio-compatible and bio-degradable programmable materials [259–264]. In [260] a new category of self-growing, fibrous, natural composite materials with controlled physical properties, has been proposed. In [259], natural matters coming from plants and vegetables (such as tomato sauce, agro-waste, etc.) encoding unusual and enhanced physical-mechanical properties, have been used to develop new bio-compatible and bio-degradable polymer-based materials for the packaging sector. Despite the literature thoroughly covers the methods of preparation and the experimental investigation of these materials, effective multi-physics models suitable for a proper engineering design are still under development.

2.6. Materials development inspired by bio-encoded matter synthesized by insects

Insects are master synthesizers of functional materials. They exploit specialized glands to emit an extreme variety of secretions characterized by extreme properties, used for the most disparate functional purposes (as chemical adhesives, coating, etc.) [6].

Framed within this context, it is worth highlighting the capability of some insects to build optimized refuges and nests structures characterized by complex design. These natural structures are typically made of materials with unusual physical-chemical-mechanical properties, and have precise and extremely complex shapes, geometries, and intricate microstructures responsible for their advanced smart response.

In materials science, the challenge of developing materials characterized by desired properties, and understanding how these properties can be obtained and tuned by controlling the material's microstructure is the key aspect to be solved [267,268]. For instance, the study of the spider silk is an useful example covering all the above-recalled aspects. Spider silk is naturally programmed at the microscale level to properly meet some functional needs, Fig. 5(h); it can be viewed as one of the most excellent functional matter in nature having a programmed response. In fact, spiders can synthesize up to seven different types of silks, each one used for a precise functional behavior (reproduction, locomotion, prey capture, etc.) [10], Fig. 5(h). Depending on the functionality of interest, spider silk has different and precise bio-encoded chemical-physical-mechanical-geometrical properties linked to the desired feature; they exhibit a diversity of mechanical properties which are naturally-programmed and optimized for the required functionality [265,268–270]. For instance, the dragline thread (or major ampullate, MA thread), used for escaping from predators (safety line), is characterized by a combination of strength and extensibility providing an incredible toughness, greater to that shown by modern industrial materials such as Kevlar. The dragline silk is made of a semicrystalline like-polymer characterized by a remarkable strain-hardening behavior attributed to an unfolding mechanism taking place at the molecular level; it enables the dragline filaments to become gradually hardened during mechanical stretch, allowing efficient energy buffering when escaping is required [271]. This feature enables a quick energy absorption and hinders the structure oscillations which might occur upon an impact. Mimicking this functional response allows designing new synthetic functional materials useful for kinetic energy buffering and absorption [271]. On the other hand, the flagelliform silk constitutes the core thread of the spiral in spider web: its tensile strength is lower than the MA thread, but it is much more extensible, thus displaying a high toughness level [10]. Together with the aciniform silk, it is used for wrapping preys. The minor ampullate silk has instead mechanical properties suitable for stabilizing the platform during web construction. Spider silk can also display an intrinsic sensitivity to the external signals, such as humidity, optical, thermal and electric stimuli; this can inspire innovative, smart materials and devices [10] having shape memory property similar to that shown by spider web: it absorbs water from the capturing-devoted silk for recovering the daytime-distorted shape during night through water-sensitive shape memory effects [272].

Structures, such as nests built by bees, consist of large arrays of regular elements (typically hexagons). Despite their relative small sizes, Bees' honeycombs are capable of supporting large masses; each kilogram of beeswax is capable of supporting about 22 kg of honey [6]. Honeycomb cells are geometrically arranged in a precise way to achieve functionality: regular hexagons have the smallest perimeter within polygon family that fills a plane without gaps, making them the most efficient geometry for packing honey, pollen, and brood. Bees can make their wax less strong, more susceptible to fracture and more deformable at high temperature to facilitate its use as a building material. Nests made entirely of pure wax should completely collapse around 45 °C [6]; however, this does not happen since the honeycomb structure is actually made of a composite material with pure wax and other biological components organized according to a complex bio-encoded synthesis process [6]. For this reason, even at high temperatures the structural integrity of honeycomb nests noticeably surpasses that of pure wax at room temperature [11,273]. Even though pure beeswax has poor mechanical properties, the naturally-programmed architecture and building process are optimized to provide a structure with outstanding mechanical properties and functionalities.

The development of synthetic materials and structural systems characterized by programmable responses, can benefit from the extreme functionality of natural refuges or matter synthesized by insects [6]. Recent advances in the development of functional spider silk-inspired materials can be found in [269,274]. The unique properties of honeycomb structures which, depending on their structures, size scale, and material

properties, have found applications in a diversity of fields, ranging from architecture to biomedicine [275]. In parallel to the complex design of natural nests, it is also worth highlighting a recent research direction based on coupling and/or arranging different materials and/or structures, to get advanced materials characterized by unusual properties and new functionalities (see metamaterials and topological-functional-based polymers, Sect. 3.6) [266,276,277]. In [266], composite structures obtained through a two-material topology optimization method have been designed to achieve a vast range of programmed force-displacement responses under finite deformations. Structures developed in [266] have been functionally designed to respond in a specific tailored way to external actions (programmable response): they deform in a pre-designed way or show a specific target force-displacement curve when stimulated, Fig. 5(i). According to [266], the proper spatial-arrangement of two materials leads to a force-displacement response which is physically unattainable with either of the two materials alone. Further studies could be carried out for discovering unusual behavior by adopting a multi-material topology optimization (e.g. by using more than two different materials), or by engineering new materials with a specific response-related design. Other approaches, based on material topology, have been used for obtaining programmable response such as in auxetic materials [278,279], energy-absorbing materials [280], materials with tunable elastic properties [281], and tunable deformation [282]. Alternatively, the development of new materials possessing uncommon mechanical properties obtained by harnessing microscale feature rather than topological ones, still represents an open challenge. Recent AM technologies have been demonstrated to have a relevant role in producing novel materials with micro- and meso-structures whose functional behavior is similar or, ambitiously, beyond the capability of natural structures [283]. Biological matters produced by insects (such as beeswax), have been also exploited to develop new bio-compatible polymer-based materials with enhanced properties, successfully used for example in the food packaging sector [259].

The main aspects discussed in this section are summarized in Table 1.

3. Functional polymers: mechanisms and models of the functional response

Functional polymers are materials capable of providing a proper detectable functional response when specific external stimuli are applied [284–286]. They are typically characterized by a molecular scale response, which usually involves nanoscale changes (molecular bond rearrangement/cleavage, molecular motion, morphology change, etc.), whose activation provides detectable changes at the meso- and macro-scale. The detectable response displayed by a functional material could be related to changes in its chemical-physical-mechanical properties, color and/or shape changes, tailored mechanical responses, etc.; all of them are suitable to be exploited to get the desired functionality. Since the macroscopic responsiveness typically comes from the molecular architecture of the material, its responsiveness can be designed and tuned to obtain stimulus-specific responses in terms of chemical, physical, or mechanical changes [23]. Understanding the nano- or micro-scale mechanism inducing the functionality (consisting, for instance, in shape-morphing, tailored mechanical response, controlled fluid release, etc.), is fundamental for the systematic modeling and design of functional polymers (Sect. 4) suitable to be exploited in the most disparate functional-based applications requiring locomotion, actuation, drug delivery, etc.

In this section we provide an overview on functional polymers; a novel classification based on the mechanisms providing the functional response is followed. The considered responsive materials are organized as follows. Sect. 3.1 discusses Liquid crystal elastomers whose morphing functionality is determined by a reversible order-disorder arrangement transition of liquid crystal mesogens. Sect. 3.2 deals with functional polymers whose responsiveness stems from swelling/deswelling

Table 1

Summary of the main functionalities, strategies and mechanisms adopted in biological matters and analogy with synthetic functional polymers.

Sect.	Main functionalities	Main strategies and/or mechanisms	Analogy with synthetic materials	Main References
2.1	Morphing of various types, optimal shape and organization at different scale for mechanical, thermal and biological purposes	Collective behavior	Active colloidal synthetic materials, Janus nanoparticles, composite functional hydrogels	[7], [9], [27,28], [54]
2.2	Camouflage, adaptation to the environment	Shape morphing, color change, controlled surface roughness	Shape morphing polymers (LCE, SMP, Gels), mechanophores, selfdiagnostic polymers, cloaking in metamaterial	[101,102], [108–110], [121], [127]
2.3	Locomotion, actuation, adhesion	Shape morphing, material-environment interactions	Shape morphing polymers (LCE, SMP, Gels, EAPs), functional polymer-based adhesives	[19], [166–175], [182], [203],
2.4	Defense	Shape morphing, chemical release, autotomy (selfbreaking) and selfhealing	Shape morphing materials, wrinkling driven polymers, gels, super-hydrophilic/super-oleophobic materials, buckling-dependent response, self-healing materials, drug release-driven materials	[6], [220–222], [226–233]
2.5	Motion, actuation, shaping, feeding, accretion	Shape morphing, instability, expansive growth	Water-driven shape-morphing materials, active fibre composite materials, buckling-dependent response, bio-degradable materials with tunable properties	[244], [246,247], [251], [253], [258,259]
2.6	Feeding, structural stability, adhesion, building refuges	Tailored chemical-physical-mechanical properties, architected microstructure	Metamaterials, mechanophores, composite graded materials, buckling-dependent response	[6], [266–271], [274]

mechanism governed by the solid-fluid interplay. Sect. 3.3 illustrates electroactive polymers (EAPs) whose functional response mechanism is governed by Coulomb forces arising in the material and/or by the diffusion of mobile ions driven by electrical stimuli. Sect. 3.4 considers shape memory polymers whose functional responses is provided by a phase transition between a glassy and a rubbery state. Sect. 3.6 presents functional polymers whose functionalities come from the topological arrangement of the material at different scales. For each functional material, we also provide the most important aspects related to their mathematical modeling; suitable quantitative models (see for instance Sect. 4 and 5) are fundamental for a systematic design of functional materials capable of displaying precise and tailored responses in the most disparate situations (see Sect. 3.7).

Being usually entropic-dominated solids, polymers are suitably described by considering the statistical arrangement of their microstructure, namely the underlying chain network. This is typically done by providing the statistics of the chain end-to-end vector \mathbf{r} through the so-called chain distribution function [287]:

$$\rho_0(\mathbf{r}) = c_{a0} \varphi_0(\mathbf{r}) \quad (1)$$

where c_{a0} is the cross-link density and φ_0 is the dimensionless chain distribution which, for common polymers, is well described by the 3D Gaussian function, $\varphi_0(|\mathbf{r}|) = \left(\frac{3}{2\pi Nb^2}\right)^{3/2} \exp\left(-\frac{3|\mathbf{r}|^2}{2Nb^2}\right)$, having mean value $\mathbf{r} = \mathbf{0}$ and standard deviation $b\sqrt{N/3}$ [288]. It is worth mentioning that ρ_0 represents the distribution of the polymer chains in the chain configuration space. It can be recalled that the integral of ρ_0 over the chain configuration space Ω (i.e. spanning all the lengths and orientations) provides $\langle \rho_0(\mathbf{r}) \rangle = c_{a0}$, being $\langle \mathbf{r} \rangle = \int_{\Omega} \mathbf{r} d\Omega =$

$\int_0^{2\pi} \int_0^\pi \left(\int_0^{Nb} \mathbf{r}^2 dr \right) \sin\theta d\theta d\omega$, i.e. the integral of the quantity \mathbf{r} in the spherical coordinate system of the chain configuration space, [287,289]. According to this simple model, each chain is assumed to be made of N rigid (undeformable) segments of equal length b randomly organized in space; accordingly, the maximum chain extension (contour length) becomes Nb , [290].

In polymer physics, the shear modulus μ of the material is expressed by the simple relationship $\mu = c_{a0} k_B T$, where k_B and T are the Boltzmann constant and the absolute temperature, respectively [288].

Any mechanical deformation applied to the network reflects into a variation of the chain distribution function $\rho(\mathbf{r}, t)$, while its integral over the 3D space – if chain rupture and self-healing mechanisms are neglected, and the material is incompressible – keep maintaining the initial value, $\langle \rho(\mathbf{r}, t) \rangle = c_{a0}$; it is worth recalling that for a compressible material it is $c_a = J^{-1} c_{a0}$, being $J = \det \mathbf{F}$, with $\mathbf{F} = \partial \mathbf{x} / \partial \mathbf{X}$ the deformation gradient tensor and \mathbf{x}, \mathbf{X} the position vectors in the deformed and in the undeformed state, respectively. For an incompressible polymer, as always assumed hereafter, it happens to be $c_a = c_{a0}$. It is worth also introducing the material velocity gradient $\mathbf{L} = \dot{\mathbf{F}}\mathbf{F}^{-1}$, which will be used in the following. The current value of the chain distribution function is the main quantity which can be used for linking the network arrangement at the molecular scale to the mechanical response arising at the continuum level. As recalled above, it is worth mentioning that this distribution can be modified by an applied macroscopic mechanical deformation, and by other phenomena taking place at the molecular level, such as the nematic-isotropic changes arising in LCEs (see Sect. 3.1), chain detachment-reattachment and sliding mechanisms, presence of mechanophores, etc. [287,289].

A quantity related to the mechanism inducing the functional response of the material suitable to quantify the mechanical state of the network (see Sect. 4), is provided by the chain distribution tensor [287]:

$$\boldsymbol{\mu}(t) = \int_{\Omega} \varphi(\mathbf{r}, t) \mathbf{r} \otimes \mathbf{r} d\Omega = \langle \varphi(\mathbf{r}, t) \mathbf{r} \otimes \mathbf{r} \rangle \quad (2)$$

The tensor $\boldsymbol{\mu}$ assumes the simple diagonal form $\boldsymbol{\mu}_p = \text{diag}(\mu_1, \mu_2, \mu_3)$ in the principal directions frame of reference, being μ_1, μ_2, μ_3 its eigenvalues. The above-mentioned diagonal terms have the physical meaning of providing the standard deviation of the end-to-end distance component $\langle r_i^2 \rangle$ in the i -th principal direction; in the stress-free state it is $\mu_{0i} = \langle r_i^2 \rangle = Nb^2/3$.

The energy density of the material is expressed as:

$$\begin{aligned} \Delta\Psi(t) &= \Psi - \Psi_0 = \int_{\Omega} \varphi(\mathbf{r}, t) \psi(\mathbf{r}) d\Omega - \int_{\Omega} \varphi_0(\mathbf{r}) \psi(\mathbf{r}) d\Omega \\ &= c_a \langle [\varphi(\mathbf{r}, t) - \varphi_0(\mathbf{r})] \psi \rangle + \pi [J - 1] \end{aligned} \quad (3)$$

being $\psi(\mathbf{r})$ the deformation energy of a single chain which, according to the Gaussian statistics valid for not too highly stretched chains, depends on the square of the end-to-end distance $\psi(\mathbf{r}) = \frac{3k_B T}{2Nb^2} |\mathbf{r}|^2$, and π is the hydrostatic stress fulfilling the isochoric constraints usually adopted in polymer mechanics. More general expressions for $\psi(\mathbf{r})$ exist, such as that based on the Langevin statistics which is applicable in a wide range of chain deformation values. The energy density can be also evaluated as $\Delta\Psi = \frac{3c_a k_B T}{2Nb^2} \text{tr}(\boldsymbol{\mu} - \boldsymbol{\mu}_0) + \pi(J - 1)$, being $\boldsymbol{\mu}_0 = \frac{Nb^2}{3} \mathbf{1}$ the deformation tensor in the stress-free state [21].

The stress state of the material can be easily related to the actual chain distribution tensor through the expression [287]:

$$\boldsymbol{\sigma}(t) = J^{-1} \mathbf{P} \mathbf{F}^T = \frac{\partial \Delta\Psi}{\partial \mathbf{F}} \mathbf{F}^T = \frac{3c_a k_B T}{Nb^2} [\boldsymbol{\mu}(t) - \boldsymbol{\mu}_0] + \pi(t) \mathbf{1} \quad (4)$$

being \mathbf{P} the first Piola stress tensor, where the incompressibility constraint $J = 1$ has been assumed. In Eq. (4), $\boldsymbol{\mu}(t)$ is the actual chain distribution tensor depending on all the stimuli-triggered effects responsible for the polymer network change at the microscale. The actual chain distribution tensor can be easily determined by integrating the chain distribution tensor rate over the time domain, i.e. $\boldsymbol{\mu}(t) = \boldsymbol{\mu}_0 + \int_0^t \blacksquare(\boldsymbol{\mu}) d\tau$; in the previous equation, \blacksquare represents the time derivative of the chain distribution tensor quantifying the evolution of the network conformation provided by the various actions involved, here schematically indicated with \blacksquare (pure mechanical deformation, nematic-isotropic transition, attachment/detachment of polymer chains, etc.), see Sect. 4.

3.1. Liquid crystal polymer networks

LCEs are synthesized by cross-linking liquid crystal mesogens units possessing a preferential orientational order, to an highly deformable isotropic polymer chain network, Fig. 6(a). The orientational order inferred to the nematic mesogens can be reversibly destroyed by different stimuli (thermal, magnetic, mechanical, etc.). The high deformability of the entropic energy-dominated network microstructure, and the reversible phase transformation (nematic-isotropic transition) shown by nematic mesogens, make LCEs capable of displaying shape morphing at will when a proper mesogens ordering pattern is inferred to the material in the stress-free state. [163,291–294]. The reversible order-disorder transition of LC mesogens occurring at the molecular level, correspondingly induces a polymer chain conformation re-arrangement, and in turn promotes a macroscale deformation responsible for the mechanism enabling their actuation, Fig. 6(a). Various building approaches have recently been developed to create LCE-based devices possessing a controlled mesoscale architecture suitable to produce the desired actuation [295,296]. The most promising production approaches are those based on 3D printing technologies, such as the Direct Ink Writing (DIW), enabling to precisely control the director alignment to create 2D/3D

patterns in the LCE domain [19,297,298]. Other recently proposed technologies are based on assembling several materials units with distinct nematic directors [299]; these strategies have shown the possibility to encode an arbitrary three-dimensional nematic director distribution (not necessarily related to the printing path), to get complex 3D shape-morphing.

Typically, the microstructure of LCEs in the nematic state is characterized by the director field describing the spatial organization of the mesogen molecules in a preferential direction. The description of the microscale physical phenomena and the related mechanical behavior of LCEs have been provided through a statistical description of the network chains by accounting for the non-isotropic chains arrangement in the 3D space [291]. At the time of cross-linking, the statistics of the chains length and orientation is provided by a non-isotropic Gaussian distribution function [291]:

$$\varphi_{0n}(\mathbf{r}) = \frac{1}{\sqrt{\det \boldsymbol{\ell}_0}} \sqrt{\left(\frac{3}{2\pi Nb}\right)^3} \exp\left[-\frac{3 \mathbf{r} \cdot \boldsymbol{\ell}_0^{-1} \mathbf{r}}{2Nb}\right] \quad (5)$$

where $\boldsymbol{\ell}_0 = \ell_{0\perp} \mathbf{1} + (\ell_{0\parallel} - \ell_{0\perp}) \mathbf{n} \otimes \mathbf{n}$ is the step-length tensor of the chain distribution quantifying the anisotropy of the chain arrangement; the initial step lengths, $\ell_{0\perp}$ and $\ell_{0\parallel}$, provide the effective lengths of the chains conformation perpendicular and parallel to the director \mathbf{n} of the mesogens, respectively [292]. The step length tensor gives information on the degree of alignment of the polymer chains and so it quantifies the anisotropy of the network at the time of cross-linking. In a highly ordered chain network it is $\ell_{0\parallel} \gg \ell_{0\perp}$: the higher the alignment degree, the higher the deformation capability obtainable upon stimulus; on the other hand, if the network does not possess any alignment (isotropic state), the mean square end-to-end chain distance is $\langle r_i^2 \rangle = \frac{Nb^2}{3}$, $i = 1, 2, 3$, $\ell_{0\parallel} \cong \ell_{0\perp}$, and the step length tensor becomes proportional to the identity tensor, $\boldsymbol{\ell}_0 = b \mathbf{1}$.

The order tensor $\mathbf{Q} = \frac{Q}{2} (3\mathbf{n} \otimes \mathbf{n} - \mathbf{1})$, also known as the de Gennes tensor [294], describes the chain arrangement in LCEs. It is related to the step length tensor through the following relationship:

$$\boldsymbol{\ell}(t) = b[2\mathbf{Q}(t) + \mathbf{1}] = b[(1 - Q(t)) \mathbf{1} + 3Q(t) \mathbf{n} \otimes \mathbf{n}] \quad (6)$$

being $Q(t) = \left\langle \frac{3}{2} \cos^2 \theta(t) - \frac{1}{2} \right\rangle$ the order parameter quantifying the degree of dispersion of the mesogen units with respect to their average alignment direction \mathbf{n} measured through the angle θ . The extreme cases $Q = 1$ and $Q = 0$ indicate perfectly aligned and isotropically distributed chains, respectively; values ranging between the two above-cited cases represent intermediate degrees of alignment characterized by a degree of dispersion which increases as $Q \rightarrow 0$.

In the above expressions, the dependence of the involved quantities at time t has been emphasized to outline that the order direction can be modified by suitable stimuli applied to the material. Usually, it happens to be $\theta(t) = \theta(T(t))$, i.e. the dispersion angle changes with the temperature: if $T < T_{NI}$ (being T_{NI} the nematic-isotropic transition temperature) the material stays in the nematic state, if $T > T_{NI}$ the network displays a phase transformation leading the material to an isotropic state [21,300].

The chain distribution tensor (Eq. (2)) can be related to the step length tensor and to the order tensor through the following relationships [301]:

$$\mathbf{Q}(t) = \frac{1}{2} \left(\frac{\boldsymbol{\ell}(t)}{b} - \mathbf{1} \right) = \frac{1}{2} \left(3 \frac{\boldsymbol{\mu}(t)}{Nb^2} - \mathbf{1} \right) \quad (7)$$

so the three tensors result to be strictly related each other. The mathematical description of the material microstructure based on the chain distribution tensor, can be conveniently adopted to characterize the process-microstructure-responsiveness relationship of LCEs (see Sect. 4), suitable for programming the material behavior.

The nematic-isotropic transition induced by heating up the material reflects into the above tensors through Eq. (7); the knowledge of the $Q - T$ relationship suffices to update the mechanical-related quantities

of the network. A simple $Q - T$ equation can be assumed in the form $Q(T) = \frac{Q_0}{1 + \exp\left(\frac{T - T_{NI}}{s}\right)}$, where the parameters Q_0 and s , quantifying the initial order parameter and the transition gradient of Q with respect to the temperature variation, respectively, can be experimentally determined.

It is worth highlighting that the intrinsic features of LCEs are, to some extent, shared with some biological matters. As an example, the anisotropic characteristics observed at the molecular level and the hierarchical self-organization inducing the functionality (shape-morphing, movement, etc.) of skeletal muscles [3,302] or of biomolecular motors, are based on a similar principle [37,303]; their response resembles that observed in the nematic-isotropic transition inducing functionality in LCEs, [302]. From this perspective, LCEs are capable of converting molecular motion into macroscopic shape-morphing, as can be observed in the above mentioned natural structures; to this aim, it is of paramount importance to precisely control the organization and synergistic effect of LC mesogens for encoding the desired detectable response possessing the suitable magnitude [303].

3.2. Swelling-driven mechanism inducing functionality in hydrogels

It is well-known that some polymers are hydrophilic, i.e. they are keen to absorb a large amount of fluid with a consequent volume increase, Fig. 6(b); when the absorbed fluid is water, the polymer is termed hydrogel. The physical properties, porosity, and high-water content in hydrogels resemble those of living tissues, and make them good candidate for bio-related applications. Functionality in hydrogels mainly stems from their swelling-deswelling behavior, corresponding to an increase-decrease of their volume; a controlled swelling mechanism can be obtained by adopting different strategies, which can be harnessed to obtain precise and tunable deformations enabling their use in a variety of application, ranging from soft-robotics, drug delivery, self-healing, self-stiffening, tissue engineering, etc. [304–308].

Hydrogels are soft and environmentally sensitive materials which can be usefully adopted for the development of morphing structures as well as for a wide range of other applications requiring a functional response. Among all the developed hydrogels, those responsive to pH and temperature are of crucial interest in applications since these stimuli are often found in bio-related applications (e.g. in biomedicine). In particular, differential swelling easily obtainable in layered elements [309,310], or temperature-driven swelling-deswelling in poly-N-isopropylacrylamide (PNIPAm) hydrogels [311] can be exploited to obtain a controlled deformation. However, it is worth mentioning that the swelling-driven mechanism of hydrogels has been also exploited to get functionalities not necessarily aimed at obtaining specific target deformations. For example, as mentioned in Sect. 2.1, a polymer capable of self-stiffening under swelling has been proposed [88]. Similarly, a mechanical adaptive hydrogel capable of self-regulating its mechanical properties by exploiting a pH sensible-swelling has been proposed in [312]. The controlled swelling mechanism in hydrogels, enabling their mechanical properties to be adapted to different environments by properly engineering their microstructure, has opened the door to the realm of drug delivery [313].

From a physical perspective, the swelling mechanism relies on the solid-fluid interaction that ultimately characterizes the functionality of hydrogels.

According to the hydrogel's chemical properties, the degree of fluid absorption can be tuned by leveraging on different stimuli, such as temperature, pH variation, presence of particular ions or molecules, enzymes, electric field, etc., making them active materials suitable for obtaining smart devices [314].

Thermo-responsive hydrogels display a phase transition by raising the temperature above a critical value, namely the so-called lower critical solution temperature (LCST); upon crossing LCST, hydrogels shrink abruptly by loosing their water content [315]. Below the LCST the polymer is hydrophilic and its network is swollen with the solvent, whereas

above the LCST dehydration occurs due to hydrophobicity increase [316].

In hydrogels the fluid enters into the gel network and its amount (quantified by the fluid concentration value, C_s) is determined by a chemo-mechanical equilibrium. Starting from the fluid conservation equation, $\frac{\partial C_s}{\partial t} + \nabla_{\mathbf{X}} \cdot \mathbf{J} = 0$ (with $\nabla_{\mathbf{X}}$ the gradient operator, and \mathbf{J} the fluid flux crossing the boundary of the gel ∂B_0 per unit time), and introducing the Fick's law to quantify the fluid flux-chemical potential μ gradient relationship [307], $\mathbf{J} = -\frac{D}{v_s k_B T} (J - 1) \mathbf{C}^{-1} \nabla_{\mathbf{X}} \mu$, the fluid balance equation reads:

$$J^{-1} \left[\frac{\partial C_s}{\partial \mu} \dot{\mu} + \frac{\partial C_s}{\partial \pi} \dot{\pi} \right] - \frac{c_s D}{k_B T} \nabla^2 \mu = 0 \quad (8)$$

where π is the osmotic pressure, D is the diffusion coefficient, $\mathbf{C} = \mathbf{F}^T \mathbf{F}$ is the right Cauchy-Green deformation tensor, while $k_B = k_B A_n$, being k_B , A_n the Boltzmann constant and the Avogadro's number, respectively.

In swollen gels, the relative volume change $J = V/V_0 = \det \mathbf{F}$ is not equal to 1 as in pure incompressible polymers. Because of the individually isochoric response of both the fluid and the polymer, the following volume constraint needs to be fulfilled at any time: $J(t) = \det \mathbf{F}(t) = 1 + C_s(t)v_s$, being v_s the molar volume of the solvent molecules. It is worth recalling that the solvent concentration in the current (c_s) and in the reference (C_s) configuration are linked through the relationship: $c_s = C_s / \det \mathbf{F}$.

Upon fluid-network mixing, the free energy density of the polymer-solvent system Ψ_{gel} can be obtained by adding up the mechanical deformation contribution and the energy of mixing [317]:

$$\Psi_{\text{gel}} = [\Psi_{\text{net}}(\mathbf{F}) + \Psi_{\text{mix}}(C_s, T)] + \pi [(1 + v_s C_s) - J] \quad (9)$$

where the last term accounts for the volume increase constraint, i.e. the hydrostatic osmotic stress π can be thought as the internal stress state enforcing the proper above-recalled volume change ratio J [14,318,319]. In the particular case where no external mechanical stresses are applied to the hydrogel, its swollen state must be in equilibrium with the fluid, and the hydrostatic stress arising from stretching the polymer chains due to the fluid-induced volume expansion, must balance the osmotic pressure [123]; in other words, at equilibrium the stress state in the polymer network is $\sigma = \pi \mathbf{1}$ (hydrostatic tension), while the fluid is under an hydrostatic compression stress π . The osmotic pressure induces the gel to swell against the elastic stress arising in the polymer network [14]. The total stress of the gel (considering both the fluid and the solid) is therefore identically zero because of the equilibrium condition; it is worth recalling that the stress in the polymer network could also lead to chains ruptures if the network strength is overcome during swelling [92]. The mixing energy is expressed as [305]:

$$\Psi_{\text{mix}} = \frac{k_B T}{v_s} \cdot \left[(J - 1) \ln \left(\frac{v_s C_s}{J} \right) + v_s C_s \frac{\chi(C_s, T)}{J} \right] \quad (10)$$

where the network energy $\Psi_{\text{net}} = \Delta \Psi(\mathbf{F})$ can be evaluated by using Eq. (3).

It is worth recalling that the chemical potential μ corresponds to the derivative of the mixing energy with respect to the solvent concentration, $\mu = \partial \Psi_{\text{mix}} / \partial C_s$ [308], while χ is the Flory-Huggins (FH) polymer-fluid interaction parameter [305]. In pNIPAm temperature sensitive hydrogels it happens to be $\chi = \chi(T)$, a dependence that can be exploited to control the fluid uptake/release through the temperature variation [123].

The free energy of the system must be stationary at equilibrium, i.e. $\delta(d\Psi_{\text{gel}}) = 0$, and the gradient of the chemical potential is zero everywhere in the gel domain, $\nabla_{\mathbf{X}} \mu = 0$, indicating that no flux of solvent molecules occurs. In the swollen state, the deformation gradient tensor induced by the fluid uptake assumes the form: $\mathbf{F}_s = \text{diag} \lambda_s$, with $\lambda_s = J^{1/3}$.

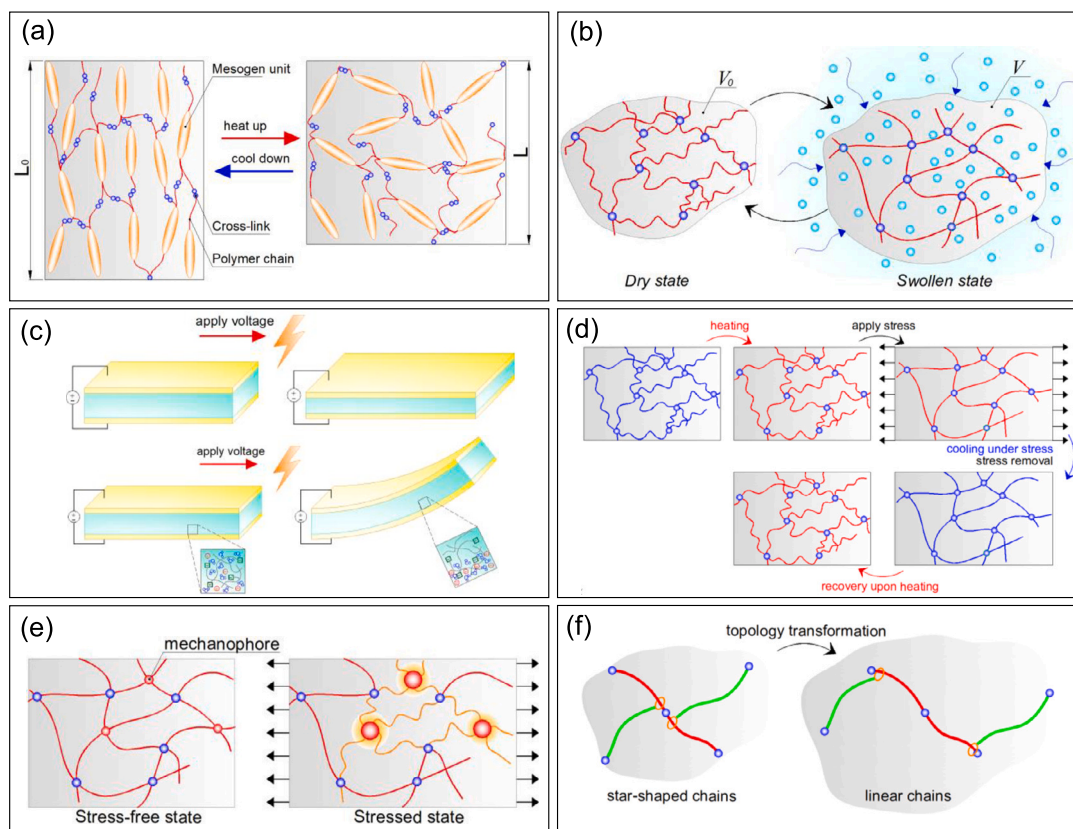


Fig. 6. Schematics of functional polymers. Liquid crystal elastomers showing self deformation upon heating/cooling (a). Swelling/shrinking of an hydrogel (b). Actuation in dielectric elastomers (upper sub-figure) and in ionic polymers (lower sub-figure) (c). Shape change and recovery in shape memory polymers (d). Activation of mechanophores linked to the polymer network upon application of stress (e). Topology change in a polymer with sliding ring cross-links (f).

Swelling is a quite common phenomenon in nature taking place in the most disparate biological matters interacting with a fluid. It can be usually recognized in various functional phenomena occurring in living matters. As an example, the brain tissue is one of the most complex, delicate and heterogeneous tissue of the human body which interacts with a fluid [320,321]. Being made of a soft polymer-like matrix filled with free to move cerebrospinal fluid, the brain tissue behaves like a sponge [320]. The swelling-driven mechanism arising in the brain tissue can be used to justify various phenomena; from a functional perspective, it has a fundamental importance for the brain function, delivering vital nutrients to the neural cells and playing a crucial role in therapies based on drug delivery [320,322]. On the other hand, the loss of cerebrospinal fluid during surgery could trigger a complex physico-mechanical undesired mechanism which is the main responsible for providing human brain deformation (brain shift) [320,323]. Swelling is also the main phenomenon responsible of the morphing response (expansive growth, shape-morphing, movements, etc.) and other functionalities in most plants and vegetables, see Sect. 2.5.

3.3. Electroactive polymers

EAPs are materials whose mechanism inducing functionality is triggered by electrical stimuli. They are typically capable of deforming upon the application of a voltage or to produce an electric potential difference when deformed, Fig. 6(c). The large compliance shown by elastomers and, in general, by soft polymers responsive to an electric stimulus, has enhanced their use as sensors or actuators by coupling them with an electrical field [324–326].

According to the chemical-physical mechanism triggering the functional response, EAPs can be subdivided into two sub-classes: (1) electric EAPs (piezoelectric polymers or dielectric elastomers), whose func-

tional response is driven by electric fields or Coulomb forces, and (2) ionic EAPs whose response is instead related to the mobility and/or diffusion of mobile ions embedded in the polymer matrix [15], Fig. 6(c).

By embedding in the polymeric matrix, which is typically a dielectric material, some conductive fillers such as graphene, carbon nanotubes, carbon black, etc., the so-called piezoelectric effect can be obtained. In polymeric structures with integrated ceramics responsible for the piezoelectric effect, the actuation is associated with tensile or compressive stress that distorts the distribution of charged atoms within the material. On the other hand, the piezoelectric response of purely polymeric materials is due to the presence of permanent molecular-scale dipoles capable to reorient, align and maintain their alignment when electrically stimulated [1]. In this context, it is worth recalling the development of highly deformable and polarizable materials, such as the polyvinylidene fluoride (PVDF) usable for both sensor or actuators enabling unprecedented applications [327,328]. On the other hand, dielectric elastomers (DEs) are elastomeric materials that are synthesized to be electrically active: this is typically obtained by creating charged surface coatings or by inserting an elastomeric film between compliant electrodes [1,17,329]. The mechanical response of dielectric elastomers is provided by the application of an electric potential triggering the attraction of the surfaces with opposite charge, resulting in an electrostatic compressive force on the elastomeric film and on a corresponding lateral expansion typically induced by the incompressibility of the material.

Differently from electric EAPs, ionic EAPs are electro-chemical materials, in which mechanics and electrochemistry are coupled; their responsiveness is related to the mobility of ionic species [330]. The behavior of ionic EAPs strongly depends on the nature of the constituent ions and on the way these species are embedded in the polymer matrix [1]. The mechanism inducing functionality in ionic EAPs is mainly

based on the spatial diffusion of the ionic species: upon application of an electric stimulus, they redistribute within the polymer matrix, providing an osmotic pressure gradient across the thickness, which is responsible for producing a differential volume change inducing bending deformation. It is worth mentioning that, since the mechanical response of ionic EAPs is based on the mobility and diffusion of the ionic species within the material (to some extent, similar to what happens in hydrogels, Sect. 3.2), the actuation speed can be slow (fraction of seconds) in comparison to electric EAPs which instead can actuate even in fraction of milliseconds. On the other hand, ionic EAPs are capable of displaying large deformation even when a low voltage is applied, while EAPs typically require high voltage to be actuated [16].

Similarly to the above-illustrated responsive polymers, multi-physics mathematical coupling is necessary to describe both electric and ionic EAPs. For sake of brevity, we provide in the following a brief overview of the mathematical framework formulated for modeling electric EAPs (in particular dielectric elastomers). On the other hand, the mathematical treatment of ionic EAPs, which involves a nonlinear interplay among electrostatics, ions and solvent transport, and mechanics, can be found in other studies [330,331].

Electro-mechanical coupling is usually quantified through the related forces, whose intensity is proportional to the square of the electric field intensity, $|\mathbf{e}|$, weighted by the electric permittivity of the free space, ϵ_0 , times the elastomer's dielectric constant ϵ_r , [332].

Typically, DE actuators are obtained by coupling two compliant parallel plate electrodes with a dielectric material placed in between; an electric potential applied to the electrodes makes these plates to attract each other due to electrostatic forces, thus inducing a mechanical stress in the polymer. If the material is polarizable, i.e. if it can form dipoles in its microstructure, a further stress arises due to the electric forces on the dipoles. Because of the high deformability of the elastomer, the electric field changes, leading to a highly non-linear coupled electro-mechanical problem.

In the current (deformed) configuration, the so-called electric displacements vector \mathbf{d} , the electric field \mathbf{e} and the polarization vector \mathbf{p} , are related each other by the well-known relationship [333]:

$$\mathbf{d} = \epsilon_0 \mathbf{e} + \mathbf{p} \quad (11)$$

When the polarization is aligned with the electric field \mathbf{e} , it holds $\mathbf{p} = \epsilon_0 \tau \mathbf{e}$, while when the polarization is zero (such as in vacuum), it is: $\mathbf{d} = \epsilon_0 \mathbf{e}$. In EAPs, the susceptibility-relative electric permittivity relationship is usually expressed as $\tau = \epsilon_r - 1$, where τ is the so-called susceptibility.

If a dielectric material is capable of developing dipoles when exposed to an electric field, it is termed polarizable. The polarizability expresses the ratio of the induced dipole moment to the applied electric field. In electrostatic problems where no free charges are involved and velocities and magnetic interactions are neglected, the electric field \mathbf{e} is irrotational, i.e. $\nabla_{\mathbf{x}}^T \times \mathbf{e} = \mathbf{0}$. Thus, the electric field in the current and in the reference configuration can be obtained by means of a scalar potential Φ as follows:

$$\mathbf{e} = -\nabla_{\mathbf{x}} \Phi, \quad \text{or} \quad \mathbf{E} = -\nabla_{\mathbf{X}} \Phi \mathbf{F} \quad (12)$$

Further, the following balance relations (Gauss' law), $\nabla_{\mathbf{x}} \cdot \mathbf{d} = 0$, $\nabla_{\mathbf{x}} \cdot \mathbf{D} = 0$ hold true; they state that the electric displacements (in both the deformed and in the reference configuration) represent a divergence-free vector field.

The electric field and the electric displacements must also satisfy the following boundary conditions on each surface of discontinuity present in the problem:

$$\llbracket \mathbf{D} \rrbracket \cdot \mathbf{N} = 0, \quad \llbracket \mathbf{E} \rrbracket \times \mathbf{N} = \mathbf{0} \quad (13)$$

where the notation $\llbracket \mathbf{■} \rrbracket$ indicates the jump of the electric displacement and of the electric field on the discontinuity surface while \mathbf{N} is the outward unit normal vector in the reference configuration.

When electromechanical interactions are present, the equilibrium problem can be stated as follows [334,335]:

$$\begin{aligned} \nabla_{\mathbf{x}} \cdot \mathbf{P} + \mathbf{B} &= \mathbf{0} && \text{in } \mathcal{B}_0 \\ \mathbf{FP}^T \frac{\mathbf{F}^{-T} \mathbf{N}}{|\mathbf{F}^{-T} \mathbf{N}|} &= \mathbf{T}_m + \mathbf{T}_{me} && \text{on } \partial \mathcal{B}_0 \end{aligned} \quad (14)$$

$$\text{with } \mathbf{P} = \mathbf{P}_m + \mathbf{P}_{me} = \mathbf{P}_m + \epsilon_0 \epsilon_r \left[\mathbf{e} \otimes \mathbf{e} - \frac{1}{2} (\mathbf{e} \cdot \mathbf{e}) \mathbf{I} \right] \mathbf{F}^{-T}$$

where \mathbf{B} is the body force vector in the reference configuration, \mathbf{P}_m is the mechanical first Piola stress tensor, \mathbf{P}_{me} is the Maxwell-Piola electromechanical stress tensor, while $\mathbf{T}_m = \mathbf{FP}_m^T \frac{\mathbf{F}^{-T} \mathbf{N}}{|\mathbf{F}^{-T} \mathbf{N}|}$, $\mathbf{T}_{me} = \mathbf{FP}_{me}^T \frac{\mathbf{F}^{-T} \mathbf{N}}{|\mathbf{F}^{-T} \mathbf{N}|}$, are the corresponding traction stresses assigned on the boundary, respectively. In all the above-reported relations, the elastomer has been assumed to be incompressible.

It is worth noticing that the above mentioned Maxwell Piola stress tensor corresponds to a further body force field \mathbf{B}_{0e} due to the electromechanical interaction, [335].

It is worth highlighting that nature has deeply inspired and open the way to the development of EAPs. The capability of providing an electric potential difference in response to a deformation (piezoelectricity), was early discovered in 1880 by Pierre and Paul Jacques Curie dealing with natural crystals [16]. They found that certain types of natural crystals (e.g. quartz, tourmaline, Rochelle salt, etc.) emit a voltage on their surface upon compression along certain axes. Later on, the observed reversible mechanism, i.e. deformation induced by applying an electric stimulus, has paved the way to new frontiers in EAPs development.

It is here worth recalling the electric-stimuli induced functionalities in living organisms: a relevant example is provided by the contraction of muscles provided by electric signals [336] already mentioned in the context of LCEs (sect. 3.1). Brain-controlled electric signals, transmitted to muscles by means of the nervous system, trigger complex rearrangements (hierarchical principles) at the molecular level, leading to muscles contraction [3]. This mechanism is also exploited in therapeutic strategies where an external electric signal evokes muscle contraction.

3.4. Shape memory polymers

Shape-memory polymers (SMPs), such as crystalline trans-polyisoprene, are polymeric smart materials having the ability to undergo transition between two different deformed states, a temporary shape and the original permanent shape; this transition can be induced by an external stimulus, such as temperature change, light, etc.

Phase transition approaches and viscoelastic models are commonly used to describe the shape memory response of SMPs. The material can be described as a mixture of a rubbery (active) phase and a glassy (inactive) phase which can transform into each other and whose volume fractions depend on the temperature. When the polymer is at low temperature, the network chains are almost frozen, and the material is in the glassy state without showing any significant viscous response; a purely elastic model can be used in this case to describe the material behavior. On the other hand, the polymer in the rubbery state shows a viscoelastic response which can be assessed by proper micromechanical models [287] or by simply using the classical spring-dashpot elements [337–342].

The mechanism inducing functionality in SMPs can be described as follows. During deformation at high temperature, SMPs are almost entirely constituted by the active phase in the rubbery state, while upon cooling down the active phase is gradually transferred to the frozen one, and the material transforms almost entirely in the glassy state, freezing the polymer chains in the deformed state because of their reduced mobility. During shape recovery obtained by heating up the material, the chains mobility increases, and the frozen phase is transferred to the active one, leading to recover the initial shape because of the stored pre-strains release [343–345], Fig. 6(d).

The mobility reduction of polymer chains at low temperature can be quantified through a phase transition law describing the mobility of molecule chains [346]; basically, two types of bonds are assumed to exist, namely “frozen” (whose volume fraction is $\phi_f = V_f/V$) and “active” ones (whose volume fraction is $\phi_a = (V - V_f)/V$) corresponding to bonds that hinder conformational motion and to those enabling a localized free conformational motion, respectively. The volume fractions of the above-mentioned phases are expressed as:

$$\phi_f = 1 - \frac{1}{1 + c_f(T_h - T)^n}, \quad \phi_a = 1 - \phi_f \quad (15)$$

where c_f and n are material parameters, while T_h is the highest temperature experienced by the polymer and T is the actual temperature. The total strain of the SMP can be expressed as:

$$\boldsymbol{\varepsilon} = \bar{\boldsymbol{\varepsilon}}_s + \boldsymbol{\varepsilon}_T + \boldsymbol{\varepsilon}_M \quad (16)$$

where $\boldsymbol{\varepsilon}_s, \boldsymbol{\varepsilon}_T, \boldsymbol{\varepsilon}_M$ are the storage, the thermal and the mechanical strain tensors, respectively. In particular, the average frozen (stored) entropic strain is expressed as: $\bar{\boldsymbol{\varepsilon}}_s = 1/V_f \int_{V_f} \boldsymbol{\varepsilon}_s(\mathbf{x}) d\phi$, being $d\phi = dV/V$. The temperature-dependent stiffness of the material is provided by:

$$\mathbf{C} = [\phi_f \mathbf{S}_f + (1 - \phi_f) \mathbf{S}_e]^{-1} \quad (17)$$

being $\mathbf{S}_f, \mathbf{S}_e$ fourth-rank elastic compliance tensors related to the internal deformation (frozen phase) and entropic deformation (active phase), respectively, while the stress tensor is given by:

$$\boldsymbol{\sigma} = \mathbf{C} : (\boldsymbol{\varepsilon} - \bar{\boldsymbol{\varepsilon}}_s - \boldsymbol{\varepsilon}_T) = \mathbf{C} : \boldsymbol{\varepsilon}_M \quad (18)$$

This simple model allows obtaining a relation between the frozen/active phase and the temperature history of the material.

To date, it is not trivial to recognize a shape-memory-like behavior in keratin-based natural materials (feathers and hair) in aqueous environment, has been recently reported [347–349]. According to [348], bird feathers are characterized by a remarkable shape-memory behavior. The intriguing experimental study of Liu et al. [348] has demonstrated that after applying a severe deformation to the natural shape of a bird feather, it successively recovers the initial conformation upon immersion in water and subsequent drying [348]. According to [348], this smart response is strictly associated with the viscoelastic behavior of dry and wet feathers; accordingly, the shape-memory recovery kinetics of feathers has been attributed to complex mechanisms involving motion of macromolecular polymer-like chains, taking place upon the transition of an activation energy, promoted by lubricating effects, swelling and structural changes induced by water.

3.5. Polymers with embedded responsive molecules

In recent years, the introduction into the polymer backbone of functional molecules (moieties) capable of responding to different external stimuli, has been deeply studied for the development of advanced materials [350]. By following this strategy, polymers sensitive to temperature [351], pH [352], mechanical stress [353], electric and magnetic fields [354], light [355], etc. have been reported. The mechanism inducing functionality typically relies on the stimuli-induced-changes of the embedded molecules, sometimes corresponding to a switching between two different stable states, Fig. 6(e). Molecules change is responsible for different observable effects, such as to detect the material's deformation quantified by a color change or fluorescence emission. Approaches based on the introduction of mechanochromic molecules (mechanophores), usually excimer-forming dyes capable of changing color upon mechanical stress, can be usefully adopted to quantify deformations in polymeric matrices [108,120]. Other approaches, such as those based on supramolecular mechanoluminophores (based on the host-guest technology) [115], enabling damage detection at low strain values, have been also proposed. On the other hand, some

mechanophores can change their geometrical conformation after reaching a threshold strain; this mechanism can be exploited for different functional purposes. For instance, they can act as energy absorbers capable of enhancing the toughness of the polymer network [356]. Further, the change of geometrical conformation may be potentially exploited to synthesize molecular-scale auxetic materials; deployable mechanophores with a large stored length are desirable for the development of new materials [356,357].

Within this class of polymers, mechanoresponsive materials containing mechanophore molecules have a relevant role; mechanophore show a predictable chemical modification induced by mechanical forces [14,118], Fig. 6(e). So far, the most common strategy used to induce mechano-responsiveness in mechanophores relies on the presence of weakened bonds, isomerizable bonds or strained rings keen to react once a sufficiently high mechanical stress is transmitted to the moieties through the polymer chains. Thanks to the advancements reached in the last years in mechanophore synthesis, a broad range of mechanically-triggered transformations has been obtained: among the multiple possibilities, it is worth mentioning color change/fluorescence emission [107,110], isomerizations [358], release of small molecules [359] and activation of latent transition metal catalysts [360]. Among the wide class of materials containing responsive molecules, pH-responsive polymers are of paramount importance for the development of a broad range of applications, such as controlled drug delivery, biological and membrane science, viscosity modifier, colloid stabilization and water remediation [352].

By considering a polymer network containing embedded responsive molecules, whose state switches from the state A (reference state Ω_1) to the state B (switched state Ω_2) upon a mechanical stimulus, the time rate of the state change is given by the following kinetic equilibrium reaction law [361]:

$$\frac{d\phi_B}{dt} = k_a \phi_A - k_d \phi_B \quad (19)$$

where ϕ_A, ϕ_B are the volume fraction of the mechanophores in the state A and B, respectively, while $\phi = \phi_A + \phi_B$ is the total volume fraction of mechanophores embedded in the polymer network, and k_a, k_d are the activation and deactivation rates, respectively. By defining the fraction of active molecules with respect to their total amount, $h = \phi_B/\phi$ (or equivalently, $\phi_A = (1 - h)\phi$), the above relation can be rewritten as:

$$\frac{dh(\mathbf{F})}{dt} = k_a - (k_a + k_d) h(\mathbf{F}) \quad (20)$$

where the dependence of h on the deformation gradient \mathbf{F} has been emphasized.

In mechanophore molecules, the activated and deactivated states are separated by an energy barrier separating the two stable states. The dependence of the above-mentioned rates on the energy barriers when no mechanical actions are applied (i.e. when no deformation is applied and correspondingly the deformation gradient tensor is $\mathbf{F} = \mathbf{I}$, being \mathbf{I} the identity tensor), is expressed through the well-known Arrhenius equation [361]:

$$k_{a0} = C_a \cdot \exp\left(-\frac{\Delta G_{A0}}{k_B T}\right), \quad k_{d0} = C_d \cdot \exp\left(-\frac{\Delta G_{D0}}{k_B T}\right) \quad (21)$$

where C_a, C_d are the so-called frequency factors, while ΔG_{A0} and ΔG_{D0} are the energies required in absence of any mechanical force for the forward ($A \rightarrow B$) and the backward ($B \rightarrow A$) transformation of one molecule, respectively. When a mechanical force is applied to the molecule, the above-mentioned barriers change in order to promote the forward and hinder the backward transformation; this reflects in the modification of the activation and deactivation rates as follows:

$$\begin{aligned} \delta G_A &= \Delta G_{A0} - \mathbf{f} \cdot \delta \mathbf{s}_m, & \delta G_D &= \Delta G_{D0} + \mathbf{f} \cdot \delta \mathbf{s}_m \\ k_a &= C_a \cdot \exp\left(-\frac{\delta G_A}{k_B T}\right), & k_d &= C_d \cdot \exp\left(-\frac{\delta G_D}{k_B T}\right) \end{aligned} \quad (22)$$

where f is the force applied to the mechanophore and s_m is the vector quantifying the molecule's conformation change, so that $f \cdot \delta s_m$ represents the work done by the force.

The functionality induced by the activation of the smart molecules is related to the amount of molecules per unit volume that switch from the inactive state A to the active state B. For this reason, the evolution law of h is relevant to be determined or programmed for design purposes; it can be obtained by solving Eq. (20), where different molecules activation mechanisms can be accounted for. In the particular case of a constant applied deformation, the solution of Eq. (20) by assuming the initial condition $h(t=0) = 0$, is:

$$h(t) = \frac{k_a}{k_a + k_d} \left[1 - e^{-(k_a + k_d)t} \right] \quad (23)$$

where k_a and k_d can be evaluated as illustrated in Eq. (22) in the case of a pure mechanical activation provided by a (constant) applied force; at the steady state, the equilibrium condition provides $h_\infty = \lim_{t \rightarrow \infty} h(t) = k_a / (k_a + k_d)$.

It is worth highlighting that the activation/deactivation mechanism can also be induced by stimuli of different nature acting together with the mechanical one; for instance, in [14], a model describing the mechanics of polymers with embedded smart molecules, whose activation is promoted by time-dependent mechano-chemical stimuli, has been proposed; the solvent entering in the polymer matrix affects the molecules' activation mechanism because of the pH change, and because of the mechanical network deformation induced by the swelling mechanism; this leads to a complex and intriguing interplay between the two stimuli.

Functional response provided by mechanochemical processes (mechanochemistry) is quite common in many biological systems. A relevant example is provided by living cells. A vast range of biological processes relies on coupling mechanical and chemical phenomena [362]; living cells typically translate mechanical stimuli useful to the most disparate biological functions into biochemical signals and/or functional responses of different types [363,364]. For example, as recalled in Sect. 2.1, cells of the bone tissue are characterized by a mechanochemical response which triggers a collective mechanism leading to adaptivity in bones [5,363]. The adaptive and superior strength and toughness of many biomaterials has been attributed to specific molecules (proteins) capable, upon an applied mechanical stretch, of absorbing a large amount of energy by breaking sacrificial bonds [363,365,366].

3.6. Metamaterials and topological-based-functional polymers

Metamaterials and topological-based-functional polymers are typically characterized by an organized structure (either concerning geometrical aspects and/or types of materials) at different scales; this properly designed structure is the main responsible for the material's functionality. According to [367], a metamaterial is characterized by properties which go beyond those of the constituting materials or, even more interestingly, are characterized by unprecedented properties not found in standard materials.

Functionality in metamaterials and topological-based polymers, typically stems from the particular arrangement of the material in a periodic (or non-periodic) representative unit cell and in the way such cells are organized in space. The topological arrangement of the material can be either at the level of the material's microstructure as well as at the level of the structural element [367]. It is worth noticing that all the previously illustrated functional materials may eventually be architected in specific patterns: beyond the functionality coming from the material itself, further functionalities can be obtained by properly arranging the material in organized patterns. This can be obtained, for instance, in LCE-based elements whose director field is set along different directions in specific sub-regions; in these cases, the responsiveness comes from both the order-disorder transition of the chain network as well as from the particular director pattern arrangement.

Although the concept of incorporating an architecture into materials is not new, recent developments in the field of AM technologies have further enabled the fabrication possibilities of metamaterials with very complex architectures at different length scales, [368,369].

Origami and kirigami-based metamaterials, whose mechanical functionality comes from a proper folding and/or cutting and assembling of planar 2D parts to form complex 3D structures, have shown functionalities, for instance through the existence of multi stable configurations activated at will, leading to programmable stiffness and deformations, negative Poisson's ratio, etc. [282,368,370].

Since the shape or topology of a polymer (at the microscale level) is one of the crucial factors in determining its properties [371], tailoring the architecture of polymer molecules represents also an effective way of controlling and encoding desired properties into the polymer matrix [372]. Within this context, novel strategies to design unprecedented polymer topologies based on synthesizing a polymer matrix characterized by chains having static or dynamic tailored geometries (linear-, cyclic-, star-, H-shaped, etc., -based-polymers), represent an on-going challenge in polymer science and technology [371–375]. Morphing in topology-based materials under external stimuli (in the so-called topology-transformable polymers, such as in slide-ring gels [23,375]), Fig. 6(f), has been also exploited to get materials characterized by adaptable microstructures and properties [23,371].

Tailoring the material microstructure has been recognized to be a proper way of obtaining responsiveness in materials; however, functionally graded materials or topological-based materials, characterized by a proper and desired non-uniform spatial arrangement of unit constituent cells, can be also harnessed to obtain functionality [162,296,376]. Topological-based functionality has been exploited to obtain a target force-displacement curve [266], while self-bending capabilities have been obtained by encoding a controlled residual stress field in photopolymerized materials obtained by using the Direct Laser Writing AM technology [377].

Beyond mathematical models describing the complex chemical-physical-mechanical behavior of such materials, theoretical or artificial intelligence-based algorithms capable to solve optimization problems, e.g. providing the optimum materials' configuration given a target functional response, are promising tools for the systematic design and programming a new generations of metamaterials.

Natural materials are, to some extent, the most iconic example of metamaterials and topological-based functional materials since their outstanding capabilities are often determined by the particular arrangement of their natural constituent elements. Bones, shells, crabs, spider silks, etc. to name a few, are characterized by properly arranged structures over multiple length scales, whose properties go beyond those shown by non properly organized architectures made of the same components [4,378–381]. Another relevant example provided by nature can be found in clusters of living organisms (bees, fire ants, etc.). Despite they might apparently appear as randomly un-organized structures, they possess a properly bio-encoded hierarchical architecture designed for performing functionalities. Similarly to the strategy consisting into the specific repetition of a material unit cell to obtain a smart response in synthetic metamaterials, the particular spatial arrangement and synergistic interactions of organisms used to living in groups are responsible for the numerous smart functionalities shown by the aggregates they form (see Sect. 2.1).

3.7. Applications

Thanks to their particular features, functional polymers have gained a remarkable attention and have opened new scenarios in a wide range of advanced applications. Some of the relevant applications involving functional polymers – with particular emphasis on those inspired by natural matters – are briefly summarized in this section.

Controlled drug delivery. Stimuli-responsive polymers are widely used in applications requiring a controlled drug delivery tailored to the

most disparate situations. The concept of drug delivery systems based on responsive polymers was first reported in the late 1970s by using thermo-sensitive liposomes for the local release of drugs via hyperthermia [382,383]. Although drug delivery is common in a wide range of applications, it is particularly relevant to the healthcare and biomedical sectors: as recalled in Sect. 2.4, similarly to insects which release chemical agents to obtain self-protection, responsive polymers can be engineered to precisely release on demand therapeutic substances against pathologies, virus, etc. [232]. In this context, several works have been proposed [23,73–75,231,382,384–386] and various kinds of materials have been employed such as active materials based on collective actions (Janus particles, see Sect. 2.1), hydrogels (see Sects 2.4 and 3.2), etc. Bio-compatible, biodegradable, and low toxicity stimuli-based responsive polymers are of crucial importance for a safe interaction with the human body [387]. Chitosan represents a multi-stimuli natural-based responsive polymer which has been exploited for drug delivery applications for cancer therapy and skin treatment [387]. Despite the literature is extremely vast in this field, the engineered design of materials showing a precisely controllable and adaptable of the stimulus-dependent amount of drug to be released is still in its infancy.

Robotics, artificial muscles and actuators. The innate capability of living organisms of exploiting natural strategies to obtain locomotion, actuation, etc., have inspired and opened new scenarios in a wide range of applications requiring smart movement capabilities; this feature would have been almost impossible to be faced by using traditional materials. The development of responsive polymer-based robots or microrobots, artificial muscles, actuators, etc. – often based on the use of soft materials – can be exploited in various applications such as for environmental control, surgery, assembly, movement and delivery of objects, on demand target capturing, gripping and releasing, etc. [19,25,122,150,244,258,388]. The responsiveness of functional polymers allows generating autonomous and self-adapting locomotion/actuation without using electronics or other classical remote controls.

Sensing, biosensing, augmented reality. Living organisms possess a vast range of biosensors capable of detecting the surrounding environment and consequently to react by performing different tasks. Responsive polymers behaving similarly to living organisms are exploited in a vast range of applications requiring sensing, biosensing, augmented reality, etc. [25,285]. Sensing and measurement of environmental indicators can be obtained by harnessing smart materials operating as translators of the detected physical, mechanical, chemical, or biological stimuli into readable and quantifiable signals [285,389]. Usually, the conversion mechanisms translate the felt stimulus into optical, thermal, electrical or electrochemical signals, which can be easily quantified by standard measurement tools. Self-diagnostic polymers (Sect. 2.2 and 3.5) used for damage detection and prevention are particularly relevant in this field, [105,110,112–115]. Responsive materials can be also used to detect and counteract mechanical vibrations with active and tunable vibration absorption mechanisms operating in a wide frequency range; this is particularly useful in obtaining high-precision movements and trajectories of machines and robots [390]. Materials like biosensors are instead capable of detecting and quantifying biological species [285]. For example, some hydrogel-based sensors can be used to reveal and prevent food contamination; thanks to their highly porous structure, good biocompatibility, shape-adaptation, and tailored stimulus-responsiveness, they represent very promising candidates to revolutionize the food safety realm. [391]. Haptic interfaces used in applications requiring human-machine interactions (relevant to medical purposes, in virtual and augmented reality, to support persons with sensory impairments, etc.), have been also developed so far [25,145,146,149,151,392].

Adhesives. A vast range of living organisms exploits different natural mechanisms for performing attachment (adhesion) to substrates, surfaces, etc. For example, gecko can climb thanks to the microstructure

of its adhesive toe pads (Sect. 2.3) whereas other organisms such as octopus, plants, etc., can emit gluing substances enabling adhesion [393]. Functional polymers have been largely employed in applications requiring adhesion to surfaces [175,393,394], especially in situations where adhesion represents a challenge. For example, two dry surfaces can instantly adhere upon contact with each other through intermolecular forces generated by hydrogen bonds, electrostatic or other interactions. On the other hand, the adhesion phenomenon is extremely challenging in applications dealing with wet surfaces (such as when body tissues are involved), because water molecules hinder the adhesion mechanism [395]. To this aim, a mechanism based on a diffusion-assisted chemical crosslinking reaction promoting binding between wet surfaces has been recently developed [394,395]. In this field, functional polymer-based materials have been also used to fabricate medical adhesives (Sect. 2.4): if properly functionalized, they can synergistically bind the failed tissue and promote wound healing [233].

Applications in the healthcare and biomedical sector. Beside the applications discussed above (such as drug delivery, medical adhesives, etc.), in the healthcare and biomedical sector responsive polymers and polymer-like materials are also exploited with other purposes. Collective actions of responsive polymer-based materials (see Sect. 2.1) have been exploited in ultrasound-based therapies, clinical diagnostic, etc. [61–64]. 3D printed bioinspired polymer-based synthetic structures, whose mechanical and functional behavior is comparable to the natural structures of the human body (blood vessels, tissues, organs, etc.), are opening new scenarios in biomedical applications [396–398]. For instance, synthetic functional vascular tubes have been fabricated [396], and their potentialities as vascular models for in vitro disease studies and as grafts for in vivo vascular surgeries have been discussed [396]. However, applications dealing with in vivo vascular reconstruction require further studies to be effective [396]. It is also worth mentioning the potentiality of functional polymers in fabricating advanced biomedical devices (such as stents) capable of effectively accomplish their task as well as to enable their remote control [399,400]. It must be emphasized that the effective and daily application of responsive polymer-based medical devices still represents an awkward challenge and requires further studies and investigations.

Smart coatings and surfaces. The body of living organisms is usually enclosed in a material interface (such as the skin of the human body, etc.) which can be considered a smart coating possessing various functionalities, such as thermal regulation, camouflage, self-healing, etc., see Sect. 2 for more details. Artificial coatings made of responsive polymers have been developed for the most disparate applications. For instance, it is worth recalling the development of smart coatings based on different strategies (see Sect. 2.4), aimed at preventing and hindering the bio-fouling phenomenon [227–230]. The textile-based transdermal therapy finds also application in this field: functionalized textiles coated with stimuli-responsive hydrogel layers can balance the skin moisture and give comfort by actively controlling the body temperature [387]. Similar approaches have been implemented to fabricate sweat-wicking clothes [401]. Smart coatings have also been used in applications devoted to preventing the corrosion phenomenon of surfaces. For example, a pH-responsive polymer has been exploited to fabricate a self-healing and anti-corrosion coating [402] capable of selectively release corrosion inhibitors as well as of self-repairing mechanical damages.

Hiding target objects. The capability of some living organisms to perform camouflage to elude visualization from predators, has inspired and opened new unprecedented scenarios in real applications. In particular, it is worth recalling the so-called thermal camouflage aimed at thermally hiding target objects [125,127] enabled by responsive polymers (see Sect. 2.2 for more details).

Microfluidics, fluid separation, synthetic lubrication systems. Applications requiring a precise control of the fluid transport at the small scale

are increasingly requested in the development of micro-devices (microfluidics) where classical hydraulic tools (valves, pumps, etc.) are hard to be implemented due to size limitations. Microfluidic applications are adopted in several fields, such as in biomedical engineering, biotechnology, biology, medicine, etc., [403]. Responsive polymers represent an effective solution to pursue remote self-control of fluid transport in microscale applications [404,405]. Responsive polymers have been also used in applications requiring fluid separation [223–226], as discussed in Sect. 2.1 and 2.4, or to fabricate controlled lubrication systems [235].

4. Programming a synthetic functional material: the process-microstructure-responsiveness relationship

An important aspect to be considered in the development of tailored synthetic functional materials is the knowledge of the so-called process-microstructure-responsiveness relationship. This concept is relevant to the engineered design of advanced responsive materials and devices characterized by tunable features, enabling the functionalities required by the application of interest.

Controlling the synthesis of a functional polymer, nowadays easily achievable through the use of AM technologies, allows encoding a proper material's microstructure leading to a wide range of tailored responses.

Within this context, several studies based on the so-called “experimental-based design of materials”, have been proposed [296,406–413]; according to this approach, several prototypes of material/component are built by varying the process parameters (or the composition of the bulk material) aimed at encoding the desired responsiveness.

On the other hand, physics-based models relying on the mathematical description of the process-microstructure-responsiveness relationship, enable a quantitative prediction and link the material's intrinsic features to the desired functional responsiveness. By following this route, the present section briefly illustrates the use of multi-physics models, developed by the authors in previous studies, suitable for the systematic simulation and programming of functional materials, with particular reference to shape-morphing of LCEs (Sect. 4.1) and to the tailorable response of photopolymerized materials (Sect. 4.2) [21,83,162,163,301,414–416].

4.1. Programmable shape-morphing of liquid crystal elastomers

LCEs materials display shape-morphing under external stimuli (see sect. 3.1). The nematic directors, the cross-link density, and the nematic-isotropic transition temperature, are the main design parameters to be exploited for quantitatively programming the material's response.

As an example, by exploiting the DIW AM technology a photosensitive LCE ink is deposited filament-by-filament on a substrate; this extrusion is done through a small diameter nozzle leading to the alignment of the LC mesogens along the printing direction. Setting the printing pattern allows obtaining different nematic director alignments within the printed domain, Fig. 7(a). Once the filament has been deposited, the material is irradiated by UV-light to induce the photopolymerization reaction to solidify and freeze the LCE microstructure in the nematic state. Both the mesogens alignment and the photopolymerization can be used singularly or synergistically for programming the shape-morphing capabilities of the material, Fig. 7. Since the nematic-isotropic transition induced by a thermal stimulus provides a macroscopic contraction along the nematic director and an expansions along the normal direction, a proper spatial arrangement of the nematic director leads to a strain field responsible for a desired macroscopic shape change, Fig. 7(b). On the other hand, the degree of contraction arising along the nematic director can be controlled and programmed via the cross-link density of the material, Fig. 7(c-e). As illustrated in Fig. 7(c), in this case the LCE specimen is assumed to be fabricated without changing the

printing direction (assumed nematic director pattern), but the material is subjected to a tailored photopolymerization process where the laser light intensity (I_m) distribution, and/or exposure time t_c are the process parameters to be tuned, Fig. 7(d). This leads to a desired cross-link density value in different regions of the domain, i.e. $c_a(I_{m1}, t_{c1}) = c_{a1}$, $c_a(I_{m2}, t_{c2}) = c_{a2}$, etc. Different cross-link density values are responsible for different degree of actuation of the LCE material triggered by a given external stimulus, Fig. 7(e).

The physical description of the LCE network can be conveniently provided by the chain distribution tensor, introduced in Sect. 3. It describes the process-dependent physical state of the network at the time of cross-linking (i.e. immediately after synthesis) and the evolution of the network conformation upon external stimulus.

At the time of cross-linking, by assuming the nematic director \mathbf{n} induced by the filament deposition direction to be coincident with the x -axis of the Cartesian frame of reference, i.e. $\mathbf{n} \equiv \mathbf{x} = (1, 0, 0)$, the chain distribution tensor can be expressed as follows:

$$\boldsymbol{\mu}_n(t=0) = \boldsymbol{\mu}_{0n} = \frac{Nb^2}{3} \begin{bmatrix} 1+2Q_0 & 0 & 0 \\ 0 & 1-Q_0 & 0 \\ 0 & 0 & 1-Q_0 \end{bmatrix} \quad (24)$$

After the synthesis of the material, the conformation change of the LCE chain network typically occurs because of (1) a pure mechanical deformation applied to the material, and (2) a spontaneous deformation induced by the nematic-isotropic transition. Correspondingly, the time derivative of the chain distribution tensor is expressed as [21]:

$$\dot{\boldsymbol{\mu}}(t) = \dot{\boldsymbol{\mu}}_F(t) + \dot{\boldsymbol{\mu}}_{NI}(t) \quad (25)$$

in which $\dot{\boldsymbol{\mu}}_F(t)$ and $\dot{\boldsymbol{\mu}}_{NI}(t)$ represent the time derivative due to the purely mechanical deformation and nematic-isotropic spontaneous deformation, respectively. These two terms can be evaluated as follows:

$$\dot{\boldsymbol{\mu}}_F(t) = \left. \frac{\partial \boldsymbol{\mu}(t)}{\partial t} \right|_{NI} = \langle \varphi_n(t) \mathbf{r} \otimes \mathbf{r} \rangle \mathbf{L}(t) = \mathbf{L}(t) \boldsymbol{\mu}(t) + [\mathbf{L}(t) \boldsymbol{\mu}(t)]^T \quad (26)$$

$$\dot{\boldsymbol{\mu}}_{NI}(t) = \left. \frac{\partial \boldsymbol{\mu}(t)}{\partial t} \right|_F = 2 \frac{Nb^2}{3} [\dot{Q}(t) - \mathbf{W}(t) \mathbf{Q}(t) + \mathbf{Q}(t) \mathbf{W}(t)] \quad (27)$$

where $\left. \boldsymbol{\mu} \right|_{NI}$, $\left. \boldsymbol{\mu} \right|_F$ indicate the evaluation of the quantity $\boldsymbol{\mu}$ at constant nematic order parameter and at constant deformation, respectively. The term \mathbf{W} in Eq. (27) is the so-called spin tensor, $\mathbf{W} = 1/2(\nabla \dot{\mathbf{u}} - \nabla \dot{\mathbf{u}}^T)$, being \mathbf{u} the displacements vector, [417], and is required to make the rate (Eq. (27)) objective (frame-indifference). In Eq. (27), $\dot{Q}(t)$ is the time derivative of the order tensor (see sect. 3.1); it can be evaluated as follows:

$$\dot{Q}(t) = \begin{bmatrix} \dot{Q}(t) & 0 & 0 \\ 0 & -\dot{Q}(t)/2 & 0 \\ 0 & 0 & -\dot{Q}(t)/2 \end{bmatrix} \quad (28)$$

where \dot{Q} is the time derivative of the order parameter, which depends on the $Q - T$ relationship (sect. 3.1); it can be computed as $\dot{Q}(t) = \frac{\partial Q}{\partial T} \frac{\partial T}{\partial t} = -\frac{\exp \frac{T-T_{NI}}{Q_0 s}}{Q_0 s} Q(T)^2 \dot{T}$. This time derivative is zero when the order parameter is constant in time; this occurs for instance when the temperature does not change ($\dot{T} = 0$) or the temperature of the material T is far from the nematic-transition one, [21]. It is worth noticing that the time derivative of the order tensor does not depend on the time derivative of the nematic director: in fact, during the nematic-isotropic transition the degree of alignment of mesogens reduces (i.e. greater scattering angle, quantified by \dot{Q} , arises), without any change of the director \mathbf{n} encoded in the material during the synthesis process [301].

By assuming that the time derivative $\dot{\boldsymbol{\mu}}_F(t)$ and $\dot{\boldsymbol{\mu}}_{NI}(t)$ are independent on each other, the chain distribution evolution can be computed as follows:

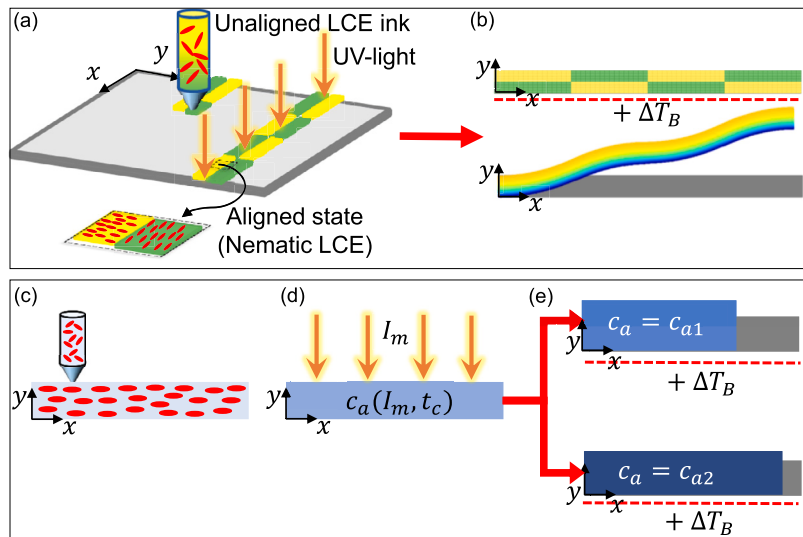


Fig. 7. Programmable shape-morphing of LCEs obtained by exploiting the synthesis-microstructure-responsiveness concept by tuning the nematic director pattern and/or the cross-link density. Schematic of the synthesis process of a LCE element through DIW process synthesized by adopting different printing paths creating different nematic director regions (a) and corresponding mechanical response of the element under a thermal stimulus (b). Synthesis of LCE with a uniform nematic director (c) photopolymerized by adopting different photopolymerization setups (different light intensities or exposure times) (d) inducing different cross-link densities responsible for different degree of actuations (e).

$$\boldsymbol{\mu}(t) = \underbrace{\boldsymbol{\mu}_n(t=0)}_{\text{process-dependent}} + \underbrace{\int_0^t [\dot{\boldsymbol{\mu}}_F(\tau) + \dot{\boldsymbol{\mu}}_{NI}(\tau)] d\tau}_{\text{process-stimulus-dependent}} \quad (29)$$

which is the sum of two terms, the first describing the network conformation after synthesis (process-dependent), while the second one is related to the evolution of the network due to the applied stimuli (process-stimulus-dependent); overall, the current chain distribution tensor $\boldsymbol{\mu}(t)$ results to be process-stimulus dependent. Once the chain distribution has been determined, the stress state in the LCE material can be computed as follows:

$$\boldsymbol{\sigma}(t) = \frac{3c_a k_B T}{N b^2} (\boldsymbol{\mu}(t) - \boldsymbol{\mu}_{0n}) + \boldsymbol{\pi}(t) \quad (30)$$

which consequently results to be process-stimulus dependent (process-microstructure-responsiveness relationship).

The cross-link density of the polymer network plays a fundamental role on the material responsiveness [162], thus it can be exploited to program the material response [20,162,418–420]. LCE synthesis inducing a non-uniform photopolymerization reaction intensity (such as, for instance, by irradiating selectively the domain), can be adopted to obtain a material characterized by complex shape-morphing capabilities [420]. In [419] a similar strategy has been adopted by properly non-uniformly de-crosslinking the LCE to create a spatial arrangement of regions where self-deformation occurs with different intensity degrees. Programmable actuations obtained by coupling LCE bi-layer domains, where the responsiveness of each layer is tuned by changing the degree of cross-link, has been experimentally shown in [20].

The cross-link density of the LCE matrix can affect the self-induced deformation capability, see Fig. 7(e), but it may also have a role in tuning the nematic-isotropic transition temperature of the material [20,162,421,422]. The above discussed physics-based model can be extended to account for this latter aspect. To this end, both constant nematic-isotropic transition temperature and fixed initial order parameter are assumed in the following discussion [162]. Since polymer chains are reciprocally connected, the order variation induced by the mesogens rotation results in a macroscopic deformation of the material, taking place if the cross-link density is low enough to allow the thermal motions of polymer chains driven by the mesogens rotation, [423]. On the other hand, when the reciprocal connection among

polymer chains is too high (such as in presence of high cross-link density values), the self-deformation capability of the material decreases because of the network constraint which hinders the motion of the polymer chains. The so-called self-deformation effectiveness (f) indicates the amount of macroscopic deformation occurring when the temperature change crosses the nematic-isotropic transition temperature. This parameter can be experimentally measured and related to the actual cross-link density of the material. From experimental evidence, it appears that there are two ideal regions that characterize the behavior of the material [162]. In the first region (region I), the actuation effectiveness increases by increasing the cross-link density from $c_a = 0$ (no actuation, being the material in the liquid state) to $c_a = \bar{c}_a$ (maximum actuation). In the second region (region II), the actuation capability decreases from the maximum value occurring for $c_a = \bar{c}_a$ up to zero for $c_a = c_t$ (no actuation because of the too strong constraints existing between the chains), [162]. A microscopic self-deformation effectiveness, suitable to describe the material behavior in the two above-mentioned regions, can be conveniently introduced:

$$\phi_I(c_a) = \frac{1}{1 + \left(\frac{\bar{c}_a - c_a}{c_a}\right)^{\alpha_I}} \quad (31)$$

$$\phi_{II}(c_a) = 1 - \left(\frac{c_a - \bar{c}_a}{c_t - \bar{c}_a}\right)^{\alpha_{II}} \quad (32)$$

where \bar{c}_a , c_t , α_I and α_{II} , are material's dependent parameters which can be experimentally determined by adopting the affine deformation hypothesis $f(c_a) = \phi(c_a)$, [162]. The microscopic self-deformation effectiveness provided by the mesogens rotation is maximum when $c_a = \bar{c}_a$; correspondingly, the LCE network is assumed to be made of a single network displaying the maximum effectiveness. On the other hand, in region I ($0 < c_a < \bar{c}_a$) and II ($\bar{c}_a < c_a < c_t$), the microscopic self-deformation effectiveness is lower than the maximum one. In these cases, the LCE network can be fictitiously assumed to be made of a double network: the first one, the effective network responsible for the actuation, has a cross-link density $c_{a1} = \bar{c}_a$; in order to take into account the influence of the actual cross-link density c_a , its microscopic effectiveness is weighted by the parameter $\phi(c_a)$. The second fictitious network, with cross-link density $c_{a2} = c_a - \bar{c}_a$, is assumed to be not able to display self-deformation. Despite this latter network is characterized by a cross-link density which formally restores the LCE actual one, it

ideally represents one of the two limits where no actuation takes place (i.e., $c_a = 0$ in region I or $c_a = c_i$ in region II), [162]. In other words, the actual network is fictitiously assumed to be made of two sub-networks: the first one produces the maximum achievable actuation, but its effectiveness is weighted by the microscopic parameter ϕ , (region I or region II). The second sub-network has no effect on the self-deformation because of the too low (region I) or too high (region II) cross-link density; both of them are responsible for no self-deformation capabilities of the material.

In this case, the time derivative of the chain distribution tensor related to the nematic-isotropic transition is evaluated as follows:

$$\dot{\mu}_{NI}(c_a, t) = \phi(c_a) \dot{\mu}_{NI1}(\bar{c}_a, t) + \dot{\mu}_{NI2}(c_{a2}, t) \quad (33)$$

in which $\dot{\mu}_{NI1}(\bar{c}_a, t)$ can be evaluated as indicated in Eq. (27) but has to be weighted with the microscopic effectiveness $\phi(c_a)$, while $\dot{\mu}_{NI2}(c_{a2}, t) = 0$ since the second fictitious sub-network does not produce any actuation. Once the time derivative of the chain distribution tensor is known, it can be adopted for performing the time integration (Eq. (29)) to assess the actual chain distribution tensor; finally, the stress state of the material is obtained as shown in Eq. (30).

In order to induce the nematic-isotropic transition in LCEs, a proper external stimulus, typically a temperature variation, has to be applied. The temperature change can be obtained by directly heating the material; in this case, the evolution of the temperature field can be assessed by adopting the standard heat conduction equation equipped with the proper boundary conditions [21]. On the other hand, a temperature variation can also be obtained by exploiting the so-called photo-thermal effect: in this case, a light-radiation induces internal heat generation through light-thermal conversion taking place in nanoparticles dispersed into the material [123,301,424,425]. The corresponding generated heat must be considered in writing the heat conduction equation [301]:

$$-\nabla [k_m \nabla T(\mathbf{X}, t)] + \rho_m c_m \frac{\partial T(\mathbf{X}, t)}{\partial t} = q(\mathbf{X}, t) \quad (34)$$

where k_m , ρ_m and c_m represent the thermal conductivity, the mass density and the specific heat, respectively. In Eq. (34), $q(\mathbf{X}, t)$ is the heat generated by the photo-thermal effect per unit volume in the unit time. It can be evaluated as follows [301]:

$$q(\mathbf{X}, t) = A(\mathbf{X}, t) I(\mathbf{X}, t) \quad (35)$$

where $A(\mathbf{X}, t)$ is the absorbance of the material and $I(\mathbf{X}, t)$ is the light intensity field in the material domain. For sake of simplicity, in writing Eq. (34) we considered the generated heat to remain entirely in the medium where it can simply propagate by conduction, while other effects, such as thermal energy dispersions provided by thermal cooling, etc., are neglected [301].

The light diffusion in a 3D domain is governed by the Beer-Lambert law, equipped with the proper boundary conditions. Let's consider a region occupied by the material whose domain and boundary in the reference configuration are denoted with B_0 and ∂B_0 , respectively. The governing equations, written in the reference configuration, read [301, 414,426]:

$$\begin{aligned} \mathbf{l}(\mathbf{X}, t) \cdot \nabla_{\mathbf{X}} I(\mathbf{X}, t) &= -A(\mathbf{X}, t) I(\mathbf{X}, t) & \text{for } \mathbf{X} \in B_0 \\ I(\mathbf{X}, t) &= \bar{I}(\mathbf{X}, t) & \text{for } \mathbf{X} \in \partial B_0 \end{aligned} \quad (36)$$

where $\nabla_{\mathbf{X}}$ is the gradient operator evaluated in the reference configuration, $\mathbf{l}(\mathbf{X}, t)$ is the unit vector representing the direction of the incoming light (here assumed perpendicular to the irradiated boundary) and $\bar{I}(\mathbf{X}, t)$ is the (known) light intensity distribution over the irradiated domain at the time t . The incoming light intensity distribution is usually assumed to be Gaussian characterized by the maximum value I_m occurring at the point $\mathbf{X} = \bar{\mathbf{X}}$, and standard deviation c . The light source can eventually move along the irradiated domain with speed v . Under

these assumptions, the light intensity over the irradiated boundary can be described as [83,301,414]:

$$\bar{I}(\bar{\mathbf{X}}, t) = I_m \cdot g(\bar{\mathbf{X}}, v, t) = I_m \cdot \exp\left(-\frac{(|\bar{\mathbf{X}}| - vt)^2}{c}\right) \quad (37)$$

The absorbance of the material can be estimated by accounting for the absorbance of the various species present in the material and for the photopolymerization process (see Sect. 4.2 for more details); the absorbance of a LCE material with embedded photo-thermal particles can be evaluated as:

$$A(\mathbf{X}, t) = A_m(\mathbf{X}, t) + \theta C_n(\mathbf{X}, t) \quad (38)$$

where $A_m(\mathbf{X}, t)$ is the absorbance of the polymer network, while θ is the molar absorbance of the photo-thermal particles whose concentration is $C_n(\mathbf{X}, t)$. It is worth mentioning that $A_m(\mathbf{X}, t)$ is in general also related to the synthesis process of the material; it must be evaluated by taking into account for the degree of polymerization achieved by the material, see sect. 4.2. If no chemical reactions occur during the nematic-isotropic transition (i.e. the chemical composition and the concentrations of the material do not change), assuming incompressibility and taking the absorbance to be not dependent on the nematic-isotropic transition, we have $A = A_m + \theta C_n$, i.e. a constant value material property.

The described approach is suitable to analyze, simulate and design LCE-based devices by adopting a multi-physics-based systematic materials' programming approach [21,23,163,301], by exploiting the process-microstructure-responsiveness relationship. For instance, the possibility to precisely control the thermal-induced shape-morphing of architected LCE elements by patterning the nematic director distribution and controlling the nematic-isotropic transition temperature, has been explored in [163]. The effect of the cross-link density on the responsiveness of bi-layer LCE elements has been explored in [23]: it has been shown that different deformation patterns can be obtained by properly setting the cross-link density mismatch of the two layers. The photo-thermal response of LCE materials has been investigated in [301], where the role played by the absorbance of the material (related to the photo-thermal particles concentration) has been considered. Moreover, it has been also shown that the thermal conductivity of the material plays a crucial role in regulating the actuation of LCE materials [301]. The effect of a non-uniform Gaussian light intensity distribution has been also explored [301]: different shape-morphing have been obtained by tuning the speed of the light source or, alternatively, by adopting a light source at rest with a tailored Gaussian distribution. Based on such an approach, future studies may open new scenarios in understanding, optimizing and opening unexplored frontiers in the field of LCEs materials and devices.

4.2. Programmable mechanical response of photopolymerized materials

One of the crucial issues in the realm of AM is represented by the so-called process-related mechanical response of AM materials: the mechanical performance of the synthesized components is related not only to the characteristic properties of the bulk material but also to the process parameters (characteristic of each AM technique) used for the synthesis [84,87,427,428]. For this reason, despite to date the knowledge in this field is far from being exhaustive, the mechanical characterization of AM materials in relation to the synthesis (printing) process has to be known.

Whereas the process-related mechanical response is typically an issue in the realm of AM, it represents a new design perspective in obtaining materials with tailored properties and/or functionalities. Understanding how the process parameters affect the features of the synthesized material, opens new possibilities in the field of programmable materials.

Among the various AM techniques [429], photopolymerization is a well-known synthesis process which allows obtaining a solid polymeric

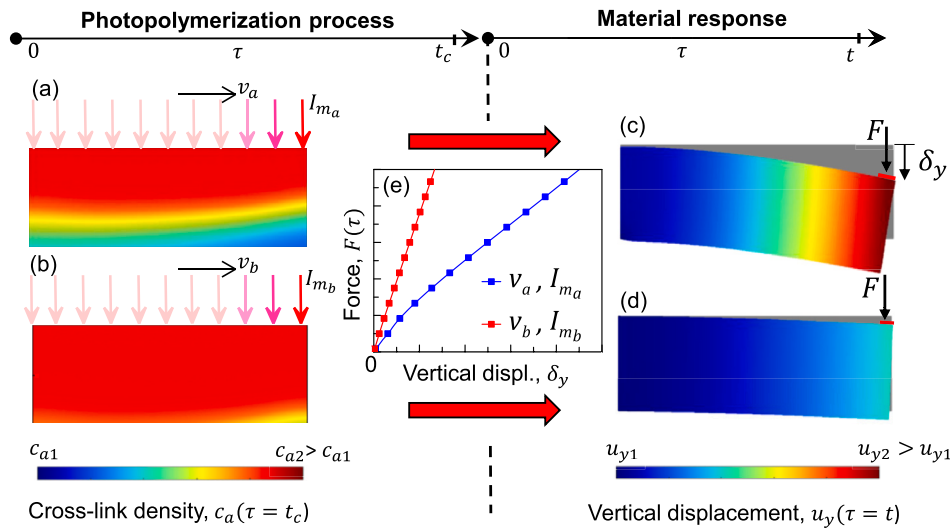


Fig. 8. Photopolymerization process, taking place in the time interval $0 \leq \tau \leq t_c$, (a,b) and mechanical response of the material occurring in time interval $0 \leq \tau \leq t$, (c-e): the mechanical response of the synthesized material depends on the mechanical properties encoded within the material during the synthesis. Schematic of the photopolymerization process obtained by adopting two different setups inducing different material's properties at the microscale, here illustrated by the cross-link density field (a,b); the first photopolymerization process is characterized by a laser speed $v = v_a$ ($t_c = t_{c_a}$) and a maximum light intensity $I_m = I_{m_a}$ (a), while the second one is characterized by $v_b < v_a$ ($t_{c_b} > t_{c_a}$) and $I_{m_b} > I_{m_a}$. Mechanical response of the beam element obtained from the two different photopolymerization setups (c,d). Corresponding load-displacement ($F - \delta_y$) curves (e).

material starting from a material initially in the liquid state (typically a polymeric resin); a light-induced polymerization chemical reaction [87] is used to solidify the material. This reaction triggers the evolution of chemical species initially present in the liquid resin, so inducing a liquid-solid transformation. During polymerization, the solid phase can exist in different states (corresponding to various degree of cure), each one characterized by distinct mechanical properties [83,85,430–433]. Recently, the principle of photopolymerization has been implemented in modern AM technologies, such as the stereolithography (STL) and the digital light processing (DLP), which enable the fabrication of objects of generic shapes by harnessing a selective and controlled exposure of the monomer resin to a moving light source (STL) or to a light coming from a projector (DLP), [87,429]. As recalled in the previous section, this technique is also exploited in the synthesis of LCEs made of a photosensitive ink, as occurs for instance in the DIW synthesis process.

From a functional perspective, different mechanical properties can be obtained through different photopolymerization setups. A proper physics-based process-microstructure-responsiveness relationship can be exploited to systematically encode the desired mechanical responses in polymers by harnessing the photopolymerization process. A multi-physics model for simulating the solidification (curing) of a liquid-resin material, coupled with a micromechanical-based description of the final polymer, is a promising tool to solve this challenge [83,87,414,415].

In order to study the mechanical response of photopolymerized materials, and to properly program their behavior, a two-folds approach must be followed: (1) simulation of the photopolymerization process and (2) mechanical process-related-description of the synthesized material, see Fig. 8. The simulation of the photopolymerization process taking place in the time interval $0 \leq \tau \leq t_c$, being t_c the curing time, Fig. 8(a,b), typically requires three ingredients: (a) evaluation of the light propagation within the medium, (b) assessment of the chemical species evolution through kinetics relations, and (c) computing of the corresponding mechanical properties evolution in the domain being photopolymerized. On the other hand, when stimulated by an external action, the description of the mechanical process-related-response of the synthesized material taking place in the time interval $0 \leq \tau \leq t$, Fig. 8(c,d), is aimed at assessing the mechanical response of the material by using a suitable model whose parameters depend on the material synthesis.

The chemical-physics phenomena involved in light-induced polymerization is usually described by a set of differential equations describing the evolution of the chemical species during synthesis [84,414,427]. The evolution of these species can be related to the mechanism of the polymer chains formation, here assumed to occur without any deformation of the domain ($F = 1$). The time-dependent description of such an evolution allows determining the degree of cure ρ (DoC, namely the degree of polymerization or degree of conversion), which can be related to the cross-link density c_a .

The material to be photopolymerized is typically formed by distinct chemical species. Some species (such as the liquid monomer M and the photo-initiators Ph_I) are initially mixed in the bulk material, while other species (such as free radicals/cross-link sites R and growing polymer chains, i.e. P or P_{end}) appear during the synthesis process.

When the light is spread into the material, photo-initiator molecules are converted into free radicals. The molar concentration of photo-initiators $C_I(\mathbf{X}, \tau)$, whose initial value is $C_I(\mathbf{X}, \tau = 0) = C_{I0}$, is gradually reduced in order to enable the production of free radicals, thus providing an increase of their concentration $C_R(\mathbf{X}, \tau)$. Free radicals react with monomer molecules inducing the polymer chains formation. Correspondingly, the monomer concentration $C_M(\mathbf{X}, \tau)$, whose initial value is $C_M(\mathbf{X}, \tau = 0) = C_{M0}$, is gradually reduced to form polymer chains. A polymer chain P stops propagating (termination, $P \rightarrow P_{end}$), when it encounters and binds to another chain or a cross-link site, [414]. The whole process is described by a set of chemical reactions [83,414] governed by differential equations whose solution provides $C_I(\mathbf{X}, \tau)$, $C_R(\mathbf{X}, \tau)$ and, finally, $C_M(\mathbf{X}, \tau)$, $\forall \tau \in 0 \leq \tau \leq t_c$. The knowledge of these concentrations allows us to determine the degree of cure as follows:

$$\rho(\mathbf{X}, \tau) = 1 - \frac{C_M(\mathbf{X}, \tau)}{C_{M0}(\mathbf{X})} \quad (39)$$

which physically represents the amount of monomer molecules converted into polymer chains [414]. Beyond the so-called gel point, which corresponds to $\rho = \rho_{gel}$ at $\tau = t_{gel}$, the mechanical stiffness of the material starts increasing [84]; the degree of cure can be related to the cross-link density of the polymer matrix as follows:

$$c_a(\mathbf{X}, \tau) = H[\rho(\mathbf{X}, \tau)] \cdot \frac{\bar{\mu}}{k_B T} \exp\{\gamma[\rho(\mathbf{X}, \tau) - 1]\} \quad (40)$$

where $\mathcal{H} = 0$ for $\rho(\mathbf{X}, \tau) \leq \rho_{gel}$ or $\mathcal{H} = 1$ for $\rho > \rho_{gel}$, and $c_a(\mathbf{X}, \tau = 0) = c_a(\mathbf{X}, \tau = t_{gel}) \cong 0$ have been assumed, [415]. $\bar{\mu}$ represents the shear modulus of the fully-cured polymer (i.e. the maximum achievable shear modulus characteristic of the resin being photopolymerized), while γ is a material-parameter regulating the rate of the mechanical stiffness increase, [83]. The mechanism of cross-link density evolution can be also conveniently expressed by adopting an integral form; at the end of the process, i.e. at $\tau = t_c$, we get:

$$c_a(\mathbf{X}, t_c) = c_a(\mathbf{X}, \tau = 0) + \int_{t_{gel}}^{t_c} \dot{c}_a(\mathbf{X}, \tau) d\tau = c_0 + \int_{t_{gel}}^{t_c} \gamma c_a(\mathbf{X}, \tau) \cdot \left(-\frac{\dot{C}_M(\mathbf{X}, \tau)}{C_{M0}} \right) d\tau \quad (41)$$

having used $\dot{c}_a(\mathbf{X}, \tau) = \gamma c_a(\mathbf{X}, \tau) \dot{\rho}(\mathbf{X}, \tau)$ from Eq. (40) and being $\dot{\rho}(\mathbf{X}, \tau) = -\dot{C}_M(\mathbf{X}, \tau)/C_{M0}$ from Eq. (39); it is worth mentioning that since $C_M(\mathbf{X}, \tau) \leq C_{M0} \forall \tau \in 0 \leq \tau \leq t_c$, $\dot{C}_M(\mathbf{X}, \tau) < 0$ and so the integral in Eq. (41) is a positive quantity because the chain concentration increases during the synthesis.

As recalled above, the mechanism of polymer chains formation is triggered by a light source which provides the photo-initiator decomposition. The light intensity within the domain must thus be determined; to this aim, the Beer-Lambert law described in the previous section, coupled with the known values of the incoming light intensity (Eqs. (36) and (37)), must be used. It is worth mentioning that during the light-induced polymerization, the material's absorbance, which has to be used in Eq. (36), results to be time-dependent; it can be related to the chemical species concentration as follows [84]:

$$A_m(\mathbf{X}, \tau) = A_I C_I(\mathbf{X}, \tau) + A_{pol} \rho(\mathbf{X}, \tau) + A_{mon} [1 - \rho(\mathbf{X}, \tau)] \quad (42)$$

which shows a further coupling in the multi-physics model. In Eq. (42), A_I is the molar absorbance of the photo-initiators while A_{pol} and A_{mon} represent the absorbance of the fully-cured polymer and of the un-cured monomer, respectively.

During the photopolymerization process the material is assumed to be in the stress-free state. At a given material point, identified by the vector \mathbf{X} , the statistical distribution of the polymer chains evolves according to the following expression:

$$\rho_0(\mathbf{r}, \tau) = \varphi_0(\mathbf{r}) \cdot c_a(\mathbf{X}, \tau) \quad \text{with} \quad 0 \leq \tau \leq t_c \quad (43)$$

φ_0 and c_a being the normalized Gaussian distribution function and the current cross-link density, see sect. 3. It is worth mentioning that, since the photopolymerization does not introduce any anisotropy at the microscale level, at each point of the continuum domain the distribution of polymer chains keep being isotropic in the chain configuration space. When the synthesis of the material has been completed, the statistical distribution of the polymer chains in the reference configuration is given by:

$$\rho_0(\mathbf{r}, t_c) = \varphi_0(\mathbf{r}) \cdot \left[c_a(\mathbf{X}, \tau = 0) + \int_{t_{gel}}^{t_c} \gamma c_a(\mathbf{X}, \tau) \cdot \left(-\frac{\dot{C}_M(\mathbf{X}, \tau)}{C_{M0}} \right) d\tau \right] = \varphi_0(\mathbf{r}) \cdot c_\mu \quad (44)$$

where Eq. (41) has been exploited in writing Eq. (44), and the equality $c_\mu = c_a(\mathbf{X}, \tau = 0) + \int_{t_{gel}}^{t_c} \dot{c}_a(\mathbf{X}, \tau) d\tau$, being c_μ the cross-link density at a given material point at the end of the synthesis, has been used.

Correspondingly, the strain energy density of the material (see Sect. 3) during synthesis changes because of the chain formation, [83]:

$$\Psi(\tau) = c_a(\mathbf{X}, \tau) \langle \varphi_0(\mathbf{r}) \psi(\mathbf{r}) \rangle \quad \text{with} \quad 0 \leq \tau \leq t_c \quad (45)$$

Once the synthesis has been completed, the component is subjected to external actions (e.g. forces, stretches, etc.) in the time interval $0 \leq \tau \leq t$ (mechanical problem). By neglecting the occurrence of any damage of

the material (chains rupture), viscoelastic effects, self-healing mechanisms etc., the cross-link density is constant, i.e. $c_a = c_\mu \forall \tau \in 0 \leq \tau \leq t$. Consequently, the strain energy density variation arising because of the external stimuli, written with respect to the reference state, is:

$$\Delta\Psi(\tau) = \Psi(\tau) - \Psi_0(\tau) = c_\mu \langle (\varphi(\mathbf{r}, \tau) - \varphi_0(\mathbf{r}, 0)) \psi_c(\mathbf{r}) \rangle \quad \text{with} \quad 0 \leq \tau \leq t \quad (46)$$

Correspondingly, the stress state in the material can be computed by taking into account for the synthesis process parameters as follows:

$$\boldsymbol{\sigma}(\tau) = J^{-1} \mathbf{P} \mathbf{F}^T = c_\mu \langle (\varphi(\mathbf{r}, \tau) - \varphi_0(\mathbf{r}, 0)) \left(\frac{\partial \psi}{\partial \mathbf{r}} \otimes \mathbf{r} \right) \rangle + \pi \mathbb{1} \quad (47)$$

It is worth mentioning that, if the free energy of an individual chain $\psi(\mathbf{r})$ is evaluated according to the Gaussian statistics (suitable for not too much stretched chains), the stress state can be evaluated through the chain distribution tensor by using Eq. (4) with $c_a = c_\mu$.

By exploiting the above described physics-based process-microstructure-responsiveness relationship, the model can be harnessed to encode a proper mechanical response into the material [83,414]. Programmable load-displacement curves, distinct shape-morphing induced by the same stimulus, or new unexplored functionalities, can be obtained from photopolymerized materials-based devices by properly setting and controlling the synthesis process [83,415], Fig. 8.

5. Conclusion and future perspectives

In the natural kingdom, biological matter exploit information encoded within the material structure to exhibit functional responses, or to display physical-chemical-mechanical property changes in response to a wide range of environmental stimuli. Similarly, the systematic programming of synthetic materials, achievable by an engineered design of their structure, aimed at responding to external signals, has the potentiality to revolutionize materials science [347]. Synthetic materials and devices capable of precisely morphing by displaying changes in their shape, color, surface roughness, etc., or exhibiting a tailored mechanical response under external stimuli are highly desirable for the development of advanced applications [347], Fig. 9.

In this review, we have considered some of the most compelling morphing and functional responses observable in nature, developed for different functional purposes (camouflage, locomotion, self-protection, etc.) and we have discussed the related underlying mechanism. A broad overview of the morphing strategies and programmed responses found in nature has been provided. In parallel, the most relevant functional polymer-based materials being developed in the last decades have been presented, and the mechanisms responsible for their functional responses have been compared with those of living systems; further, some basic concepts related to the mathematical modeling of this class of materials have been illustrated.

To date, the complex performances shown by natural systems cannot yet be fully replicated by using functional synthetic matters [434]. The functional responses of living organisms (fishes, animals, etc.), results from intricate material's architecture and properties, coupled with remarkable capabilities of stimuli detection and responsiveness through complex neural elaboration of signals; these features are still impossible to be obtained in the current synthetic functional materials. Beside the surprising capabilities of biological systems of exhibiting functional responses when triggered by external stimuli, the concept of adaptivity which characterizes the innate features of these systems, has been remarked throughout the present work. Biological systems are capable of self-tuning their characteristics in order to adapt to the surrounding environment. Despite being a trivial capability in nature, encoding adaptivity (or reconfigurability) in functional synthetic materials represents an extremely awkward task which opens fascinating challenges to be faced in future. As an example, a LCE-based component, thanks to a particular microstructure encoded in the material during synthesis, can

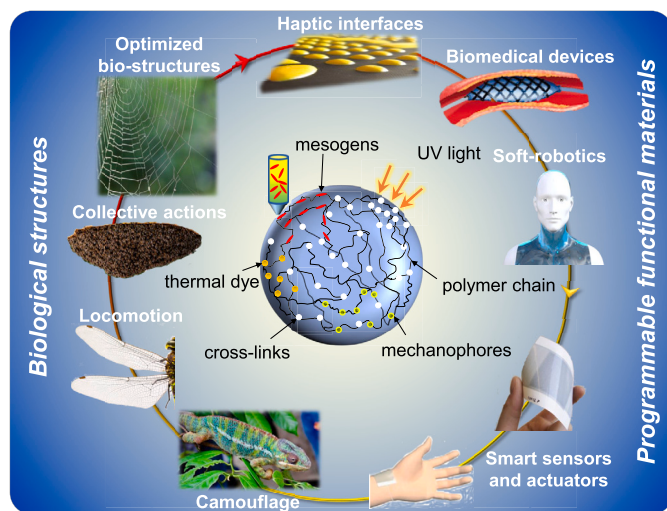


Fig. 9. From functional responses in nature to programmable functional materials exploited in advanced applications. Bio-encoded matter uses information encoded within the material's structure to display functional responses; optimized bio-structures (refuges and nests) characterized by programmable mechanical responses, collective actions taking place in cluster of insects, locomotion and camouflage of living organisms. Similarly, chemical-physical-mechanical programmed responses can be encoded in a functional polymer (schematic of a polymer network structures at the center of the figure) to obtain a precise tailored functional response. Some applications, which can benefit from the use of functional polymers, are illustrated: smart haptic interfaces, biomedical devices, soft-robots, smart sensors and actuators.

exhibit a well-desired shape-morphing under a thermal stimulus (see Sect. 4.1); however, in certain applications, different shape-morphing could be required in response to the same external stimulus applied at different time instants. How the response of a material can be adapted to different requirements or to the presence of multiple stimuli? Recent studies have shown the possibility of encoding adaptabilities in functional polymers (see Sect. 2), although the topic is still open to new discoveries. In the context of shape-morphing, the possibility of a material to morph its shape under a stimulus and to reversibly return back to the initial configuration by removing the applied stimulus is crucial to be achieved. A synthetic functional matter capable of displaying various types of morphing starting from an initial state to different ones (adaptivity), and to return to the initial state (reversibility) on demand, is one of the most outstanding and desired achievement in materials science.

Practically, all the natural matters are characterized by a multiscale structure. To date, the majority of the developed functional polymers typically exhibit a single functional response. The development of multi-stimuli and/or multi-functional smart polymers could noticeably improve the performances and thus the applications range of such materials [23,435]. As an example, materials capable of both shape-morphing and color-shifting have been recently proposed (see Sect. 2.2). Synthetic functional polymer-based robots, capable of multi-locomotion gaits in various environments, are highly desirable in soft-robotics (see Sect. 2.3); analogously, hydrogels capable of multi-stimuli (pH, temperature, etc.) controlled swelling responses could enable a step forward in the field of drug release. However, programming a multiple responsiveness in a synthetic material still represents an unsolved issue in materials science.

Another relevant aspect to be pointed out are the time scales involved in the synthesis processes and in material's response in biological matter and in synthetic functional materials. Typically, nature synthesizes matter in a relatively large time interval; for example, plants and bone tissues growth takes years. In contrast, new synthetic fabrication processes (such as AM) has been demonstrated to be able to synthesize matter in much smaller time intervals, in the order of minutes or days

[26]. From this viewpoint, concerning the synthesis process time scale the technological achievements overcome that of the natural kingdom. On the other hand, the time scale of the material's response is also quite different; a bio-material can display a functional response in an extreme short time interval, whereas the functional response exhibited by synthetic functional materials, often takes place in longer time periods. As an example, squids can quickly re-orient their arms upon external stimuli for camouflage to occur (see Sect. 2.2), whereas a swelling-driven or a LCE-based cantilever beam can exhibit a similar mechanical response in a time period ranging between seconds to days depending on material's properties, geometry and environmental conditions. Further, the speed of the functional response shown by living matters is often automatically controlled by the organisms; for instance, swimming locomotion of fishes in response to external stimuli can rapidly change from slow to extremely quick (see Sect. 2.4), whereas the actuation speed of functional polymers is far from being controllable, programmable, or adaptable. This represents an important issue when dealing with morphing inducing locomotion, actuation, etc. As far as hydrogels are concerned, being their response based on the fluid diffusion within the polymer network, their actuation capabilities are typically quite slow [436]. On the other hand, functional polymers such as LCEs are characterized by fast actuation that is eventually limited by the low thermal conductivity of the material. Further studies focusing on the quantitative comparison of the actuation speed obtained from different functional polymers are necessary to improve the understanding and the capabilities of existing and new functional polymers; a too low actuation speed and the difficulty to tune and adapt the actuation time rate to the application of interest, represent important drawbacks which can hinder the development of new technologies. Suitable multi-physics models (Sect. 4), coupled with experimentally-determined parameters, may help in assessing and tailoring the actuation velocity by tuning the material structure at the microscale.

Within the vast and complex outlined context, we believe that multi-physics-based models aimed at describing the chemical-physical-mechanical mechanisms inducing the functional response of smart materials, are essential for further improvements in this field. The mathematical description of the process-microstructure-responsiveness relationship, see Sect. 4, can be systematically exploited for materials programming (Sect. 3). Data-driven (D-D) approaches (such as those based on machine learning), if properly used to complement theoretical physics-based approaches, could further improve the development of new materials. D-D approaches could be exploited both for (1) learning from nature and (2) programming a synthetic functional material. On one hand, it may provide an effective route to mathematically assess the bio-encoded features of biological matter by providing a relationship between material's properties, structures, organization, and related functionalities. D-D approaches can be adopted to better understand the biological synthesis process, and thus to guide the nature-inspired design process for synthesizing new advanced materials or to guide the synthesis of new materials with outstanding properties [26]. However, due to the large database of input/output data typically required by data-driven approaches, D-D could be dramatically hard to be adopted. Thus, we believe that proper advanced mathematical models developed through a multi-disciplinary approach (involving material scientists, engineers, biologists, etc.) for describing the behavior of biological matter, can be directly used for obtaining large input/output databases to be used for D-D approaches. Similarly, D-D approaches could effectively assist in the design of synthetic functional materials: if coupled with proper mathematical multi-physics models (Sect. 4) used for generating an outputs starting from an input database, D-D approaches may reveal the best "algorithm" to design and guide the synthesis (process parameters) of programmable materials by exploiting the underlying process-microstructure-responsiveness relationship.

The knowledge of natural cunning can push forward the research in this field, offers new possibilities, and opens unexplored scenarios not yet considered in materials research. Several aspects have been

discussed in the present review which, far from being exhaustive, has focused on what we consider the most compelling mechanisms adopted in nature to obtain smart responses in biological materials and systems. Whenever possible, we have compared the response of bio-materials to those of synthetic functional materials, providing some inspiring hints for further advanced materials development. The parallelism between bio-encoded matters and programmable synthetic functional materials has been stressed throughout the manuscript: we believe that identifying the features shared among natural and synthetic functional matters could promote and inspire new developments in the smart materials field.

Funding

All The authors would like to thank the support from European Union's Horizon 2020 research and innovation program (H2020-WIDESPREAD-2018, SIRAMM) under grant agreement No 857124.

MPC would like to thank the support from the Project funded under the National Recovery and Resilience Plan (NRRP), Mission 4 Component 2 Investment 1.5 - Call for tender No. 3277, date 30/12/2021 of Italian Ministry of University and Research funded by the European Union – NextGenerationEU, Award Number: Project code ECS00000033, Concession Decree No. 1052 of 23/06/2022 adopted by the Italian Ministry of, CUP D93C22000460001, “Ecosystem for Sustainable Transition in Emilia-Romagna” (Ecosister), Spoke 4.

CRedit authorship contribution statement

Mattia Pancrazio Cosma: Conceptualization, Data curation, Investigation, Methodology, Writing – original draft. **Roberto Brighenti:** Funding acquisition, Investigation, Methodology, Supervision, Writing – review & editing.

Declaration of competing interest

The authors declare that they have no known competing financial interests or personal relationships that could have appeared to influence the work reported in this paper.

Data availability

Data will be made available on request.

References

- [1] J.M. McCracken, B.R. Donovan, T.J. White, Materials as machines, *Adv. Mater.* 32 (20) (2020) 1906564, <https://doi.org/10.1002/adma.201906564>.
- [2] K. Bhattacharya, R.D. James, The material is the machine, *Science* 307 (5706) (2005) 53–54, <https://doi.org/10.1126/science.1100892>.
- [3] K. Oliver, A. Seddon, R.S. Trask, Morphing in nature and beyond: a review of natural and synthetic shape-changing materials and mechanisms, *J. Mater. Sci.* 51 (24) (2016) 10663–10689, <https://doi.org/10.1007/s10853-016-0295-8>.
- [4] M.A. Meyers, P.-Y. Chen, A.Y.-M. Lin, Y. Seki, Biological materials: structure and mechanical properties, *Prog. Mater. Sci.* 53 (1) (2008) 1–206, <https://doi.org/10.1016/j.pmatsci.2007.05.002>.
- [5] P. Christen, K. Ito, R. Ellouz, S. Boutroy, E. Sornay-Rendu, R.D. Chapurlat, B. van Rietbergen, Bone remodeling in humans is load-driven but not lazy, *Nat. Commun.* 5 (1) (2014) 4855, <https://doi.org/10.1038/ncomms5855>.
- [6] T.B.H. Schroeder, J. Houghtaling, B.D. Wilts, M. Mayer, It's not a bug, it's a feature: functional materials in insects, *Adv. Mater.* 30 (19) (2018) 1705322, <https://doi.org/10.1002/adma.201705322>.
- [7] F.J. Vernerey, E. Benet, L. Blue, A.K. Fajrial, S.L. Sridhar, J.S. Lum, G. Shakya, K.H. Song, A.N. Thomas, M.A. Borden, Biological active matter aggregates: inspiration for smart colloidal materials, *Adv. Colloid Interface Sci.* 263 (2019) 38–51, <https://doi.org/10.1016/j.cis.2018.11.006>.
- [8] D. Hu, S. Phonekeo, E. Altschuler, F. Brochard-Wyart, Entangled active matter: from cells to ants, *Eur. Phys. J. Spec. Top.* 225 (4) (2016) 629–649, <https://doi.org/10.1140/epjst/e2015-50264-4>.
- [9] O. Peleg, J.M. Peters, M.K. Salcedo, L. Mahadevan, Collective mechanical adaptation of honeybee swarms, *Nat. Phys.* 14 (12) (2018) 1193–1198, <https://doi.org/10.1038/s41567-018-0262-1>.
- [10] T. Lefèvre, M. Auger, Spider silk inspired materials and sustainability: perspective, *Mater. Technol.* 31 (7) (2016) 384–399, <https://doi.org/10.1179/1753555715Y.0000000065>, publisher: Taylor & Francis.
- [11] H.R. Hepburn, S.P. Kurtstjens, The combs of honeybees as composite materials, *Apidologie* 19 (1) (1988) 25–36, <https://doi.org/10.1051/apido:19880102>.
- [12] S. Poppinga, C. Zollfrank, O. Prucker, J. Rühle, A. Menges, T. Cheng, T. Speck, Toward a new generation of smart biomimetic actuators for architecture, *Adv. Mater.* 30 (19) (2018) 1703653, <https://doi.org/10.1002/adma.201703653>.
- [13] S.A. Gladman, E.A. Matsumoto, R.G. Nuzzo, L. Mahadevan, J.A. Lewis, Biomimetic 4D printing, *Nat. Mater.* 15 (4) (2016) 413–418, <https://doi.org/10.1038/nmat4544>.
- [14] R. Brighenti, M.P. Cosma, Swelling mechanism in smart polymers responsive to mechano-chemical stimuli, *J. Mech. Phys. Solids* 143 (2020) 104011, <https://doi.org/10.1016/j.jmps.2020.104011>, publisher: Elsevier Ltd.
- [15] Y. Bar-Cohen, Electroactive polymers as artificial muscles: a review, *J. Spacecr. Rockets* 39 (6) (2002) 822–827, <https://doi.org/10.2514/2.3902>.
- [16] Y. Bar-Cohen, Electroactive polymers as an enabling materials technology, *Proc. Inst. Mech. Eng., Part G, J. Aeronaut. Eng.* 221 (4) (2007) 553–564, <https://doi.org/10.1243/095444100JAERO141>.
- [17] G.-Y. Gu, J. Zhu, L.-M. Zhu, X. Zhu, A survey on dielectric elastomer actuators for soft robots, *Bioinspir. Biomim.* 12 (1) (2017) 011003, <https://doi.org/10.1088/1748-3190/12/1/011003>, place: England.
- [18] T.J. White, D.J. Broer, Programmable and adaptive mechanics with liquid crystal polymer networks and elastomers, *Nat. Mater.* 14 (11) (2015) 1087–1098, <https://doi.org/10.1038/nmat4433>.
- [19] A. Kotikian, C. McMahan, E.C. Davidson, J.M. Muhammad, R.D. Weeks, C. Daraio, J.A. Lewis, Untethered soft robotic matter with passive control of shape morphing and propulsion, *Sci. Robot.* 4 (33) (2019), <https://doi.org/10.1126/scirobotics.aax7044>, publisher: Science Robotics.
- [20] Y.-Y. Xiao, Z.-C. Jiang, J.-B. Hou, Y. Zhao, Desynchronized liquid crystalline network actuators with deformation reversal capability, *Nat. Commun.* 12 (1) (2021) 624, <https://doi.org/10.1038/s41467-021-20938-6>.
- [21] R. Brighenti, C.G. McMahan, M.P. Cosma, A. Kotikian, J.A. Lewis, C. Daraio, A micromechanical-based model of stimulus responsive liquid crystal elastomers, *Int. J. Solids Struct.* 219–220 (2021) 92–105, <https://doi.org/10.1016/j.ijsolstr.2021.02.023>.
- [22] Y. Sun, J.S. Evans, T. Lee, B. Senyuk, P. Keller, S. He, I.I. Smalyukh, Optical manipulation of shape-morphing elastomeric liquid crystal microparticles doped with gold nanocrystals, *Appl. Phys. Lett.* 100 (24) (2012) 241901, <https://doi.org/10.1063/1.4729143>.
- [23] R. Brighenti, Y. Li, F.J. Vernerey, Smart polymers for advanced applications: a mechanical perspective review, *Front. Mater.* 7 (2020) 196, <https://doi.org/10.3389/fmats.2020.00196>.
- [24] L. Tan, A.C. Davis, D.J. Cappelleri, Smart polymers for microscale machines, *Adv. Funct. Mater.* 31 (9) (2021) 2007125, <https://doi.org/10.1002/adfm.202007125>.
- [25] S. Li, H. Bai, R.F. Shepherd, H. Zhao, Bio-inspired design and additive manufacturing of soft materials, machines, robots, and haptic interfaces, *Angew. Chem. Int. Ed.* 58 (33) (2019) 11182–11204, <https://doi.org/10.1002/anie.201813402>.
- [26] Y. Yang, X. Song, X. Li, Z. Chen, C. Zhou, Q. Zhou, Y. Chen, Recent progress in biomimetic additive manufacturing technology: from materials to functional structures, *Adv. Mater.* 30 (36) (2018) 1706539, <https://doi.org/10.1002/adma.201706539>.
- [27] E. Méhes, T. Vicsek, Collective motion of cells: from experiments to models, *Integr. Biol.* 9 (2014) 831–854, <https://doi.org/10.1039/c4ib00115j> place: England.
- [28] P.C. Foster, N.J. Mlot, A. Lin, D.L. Hu, Fire ants actively control spacing and orientation within self-assemblages, *J. Exp. Biol.* 217 (Pt 12) (2014) 2089–2100, <https://doi.org/10.1242/jeb.093021>, place: England.
- [29] M.G. Hinchey, R. Sterritt, C. Rouff, Swarms and swarm intelligence, *Computer* 40 (4) (2007) 111–113, <https://doi.org/10.1109/MC.2007.144>.
- [30] V. Mwaffo, F. Vernerey, Analysis of group of fish response to startle reaction, *J. Nonlinear Sci.* 32 (6) (2022) 96, <https://doi.org/10.1007/s00332-022-09855-0>.
- [31] F. Peruani, J. Starruß, V. Jakovljevic, L. Søgaard-Andersen, A. Deutsch, M. Bär, Collective motion and nonequilibrium cluster formation in colonies of gliding bacteria, *Phys. Rev. Lett.* 108 (9) (2012) 098102, <https://doi.org/10.1103/PhysRevLett.108.098102>, publisher: American Physical Society.
- [32] H.P. Zhang, A. Be'er, E.-L. Florin, H.L. Swinney, Collective motion and density fluctuations in bacterial colonies, *Proc. Natl. Acad. Sci.* 107 (31) (2010) 13626–13630, <https://doi.org/10.1073/pnas.1001651107>.
- [33] M. Nagy, A. Horicsányi, E. Kubinyi, I.D. Couzin, G. Vásárhelyi, A. Flack, T. Vicsek, Synergistic benefits of group search in rats, *Curr. Biol.* 30 (23) (2020) 4733–4738.e4, <https://doi.org/10.1016/j.cub.2020.08.079>.
- [34] I. Linsmeier, S. Banerjee, P.W. Oakes, W. Jung, T. Kim, M.P. Murrell, Disordered actomyosin networks are sufficient to produce cooperative and telescopic contractility, *Nat. Commun.* 7 (1) (2016) 12615, <https://doi.org/10.1038/ncomms12615>.
- [35] M. Schuppeler, F.C. Keber, M. Kröger, A.R. Bausch, Boundaries steer the contraction of active gels, *Nat. Commun.* 7 (1) (2016) 13120, <https://doi.org/10.1038/ncomms13120>.
- [36] T.D. Ross, H.J. Lee, Z. Qu, R.A. Banks, R. Phillips, M. Thomson, Controlling organization and forces in active matter through optically defined boundaries, *Nature* 572 (7768) (2019) 224–229, <https://doi.org/10.1038/s41586-019-1447-1>.

- [37] T. Nitta, Y. Wang, Z. Du, K. Morishima, Y. Hiratsuka, A printable active network actuator built from an engineered biomolecular motor, *Nat. Mater.* (Apr. 2021), <https://doi.org/10.1038/s41563-021-00969-6>.
- [38] W. Yang, M. Luo, Y. Gao, X. Feng, J. Chen, Mechanosensing model of fibroblast cells adhered on a substrate with varying stiffness and thickness, *J. Mech. Phys. Solids* (2022) 105137, <https://doi.org/10.1016/j.jmps.2022.105137>.
- [39] M. Serrpelli, M. Arricca, C. Bonanno, A. Salvadori, Modeling cells spreading, motility, and receptors dynamics: a general framework, *Acta Mech. Sin.* 37 (6) (2021) 1013–1030, <https://doi.org/10.1007/s10409-021-01088-w>.
- [40] V. Damioli, A. Salvadori, G.P. Beretta, C. Ravelli, S. Mitola, Multi-physics interactions drive VEGFR2 relocation on endothelial cells, *Sci. Rep.* 7 (1) (2017) 16700, <https://doi.org/10.1038/s41598-017-16786-4>.
- [41] C.G. Tusan, Y.-H. Man, H. Zarkoob, D.A. Johnston, O.G. Andriotis, P.J. Thurner, S. Yang, E.A. Sander, E. Gentleman, B.G. Sengers, et al., Collective cell behavior in mechanosensing of substrate thickness, *Biophys. J.* 114 (11) (2018) 2743–2755, publisher: Elsevier.
- [42] O. Shishkov, O. Peleg, Social insects and beyond: the physics of soft, dense invertebrate aggregations, <https://doi.org/10.48550/ARXIV.2206.11129>, <https://arxiv.org/abs/2206.11129>, 2022.
- [43] M. Tennenbaum, Z. Liu, D. Hu, A. Fernandez-Nieves, Mechanics of fire ant aggregations, *Nat. Mater.* 15 (1) (2016) 54–59, <https://doi.org/10.1038/nmat4450>.
- [44] N.J. Mlot, C.A. Tovey, D.L. Hu, Fire ants self-assemble into waterproof rafts to survive floods, *Proc. Natl. Acad. Sci. USA* 108 (19) (2011) 7669–7673, <https://doi.org/10.1073/pnas.1016658108>, place: United States.
- [45] J.M. Graham, A.B. Kao, D.A. Wilhelm, S. Garnier, Optimal construction of army ant living bridges, *J. Theor. Biol.* 435 (2017) 184–198, <https://doi.org/10.1016/j.jtbi.2017.09.017>.
- [46] S. Phonekeo, T. Dave, M. Kern, S.V. Franklin, D.L. Hu, Ant aggregations self-heal to compensate for the Ringelmann effect, *Soft Matter* 12 (18) (2016) 4214–4220, <https://doi.org/10.1039/C6SM00063K>, publisher: the Royal Society of Chemistry.
- [47] F.J. Vernerey, T. Shen, S.L. Sridhar, R.J. Wagner, How do fire ants control the rheology of their aggregations? A statistical mechanics approach, *J. R. Soc. Interface* 15 (147) (Oct. 2018), <https://doi.org/10.1098/rsif.2018.0642>, place: England.
- [48] M. Tennenbaum, A. Fernandez-Nieves, Activity-driven changes in the mechanical properties of fire ant aggregations, *Phys. Rev. E* 96 (5) (2017) 052601, <https://doi.org/10.1103/PhysRevE.96.052601>, publisher: American Physical Society.
- [49] B. Heinrich, Energetics of honeybee swarm thermoregulation, *Science* 212 (4494) (1981) 565–566, <https://doi.org/10.1126/science.212.4494.565>.
- [50] S.A. Ocko, L. Mahadevan, Collective thermoregulation in bee clusters, *J. R. Soc. Interface* 11 (91) (2014) 20131033, <https://doi.org/10.1098/rsif.2013.1033>.
- [51] R. Ni, N.T. Ouellette, On the tensile strength of insect swarms, *Phys. Biol.* 13 (4) (2016) 045002, <https://doi.org/10.1088/1478-3975/13/4/045002>, publisher: IOP Publishing.
- [52] A.M. Reynolds, On the origin of the tensile strength of insect swarms, *Phys. Biol.* 16 (4) (2019) 046002, <https://doi.org/10.1088/1478-3975/ab12b9>, publisher: IOP Publishing.
- [53] A.M. Reynolds, Understanding the thermodynamic properties of insect swarms, *Sci. Rep.* 11 (1) (2021) 14979, <https://doi.org/10.1038/s41598-021-94582-x>.
- [54] Z. Wang, J. Wang, J. Ayarza, T. Steeves, Z. Hu, S. Manna, A.P. Esser-Kahn, Bio-inspired mechanically adaptive materials through vibration-induced crosslinking, *Nat. Mater.* 20 (6) (2021) 869–874, <https://doi.org/10.1038/s41563-021-00932-5>.
- [55] C. Lazarus, A.N. Poulipoulos, M. Tinguely, V. Garbin, J.J. Choi, Clustering dynamics of microbubbles exposed to low-pressure 1-MHz ultrasound, *J. Acoust. Soc. Am.* 142 (5) (2017) 3135–3146, <https://doi.org/10.1121/1.5010170>.
- [56] H. Su, C.-A.H. Price, L. Jing, Q. Tian, J. Liu, K. Qian, Janus particles: design, preparation, and biomedical applications, *Mater. Today Bio* 4 (2019) 100033, <https://doi.org/10.1016/j.mtbio.2019.100033>.
- [57] Y. Lu, G. Allegri, J. Huskens, Vesicle-based artificial cells: materials, construction methods and applications, *Mater. Horiz.* 9 (3) (2022) 892–907, <https://doi.org/10.1039/D1MH01431E>, publisher: the Royal Society of Chemistry.
- [58] A. Morshed, B.I. Karawdeniya, Y.N.D. Bandara, M.J. Kim, P. Dutta, Mechanical characterization of vesicles and cells: a review, *Electrophoresis* 41 (7–8) (2020) 449–470, <https://doi.org/10.1002/elps.201900362>.
- [59] F.C. Keber, E. Loiseau, T. Sanchez, S.J. DeCamp, L. Giomi, M.J. Bowick, M.C. Marchetti, Z. Dogic, A.R. Bausch, Topology and dynamics of active nematic vesicles, *Science* 345 (6201) (2014) 1135–1139, <https://doi.org/10.1126/science.1254784>.
- [60] R.H. Azami, M. Aliabouzar, J. Osborn, K.N. Kumar, F. Forsberg, J.R. Eisenbrey, S. Mallik, K. Sarkar, Material properties, dissolution and time evolution of PEGylated lipid-shelled microbubbles: effects of the polyethylene glycol hydrophilic chain configurations, *Ultrasound Med. Biol.* 48 (9) (2022) 1720–1732, <https://doi.org/10.1016/j.ultrasmedbio.2022.04.216>.
- [61] D. Dubey, M.G. Christiansen, M. Vizovisek, S. Gebhardt, J. Feike, S. Schuerle, Engineering responsive ultrasound contrast agents through crosslinked networks on lipid-shelled microbubbles, *Small* 18 (12) (2022) 2107143, <https://doi.org/10.1002/smll.202107143>.
- [62] T.M. Estifeeva, R.A. Barmin, P.G. Rudakovskaya, A.M. Nechaeva, A.L. Luss, Y.O. Mezheuev, V.S. Chernyshev, E.G. Krivoborodov, O.A. Klimentko, O.A. Sindeeva, P.A. Demina, K.S. Petrov, R.N. Chuprov-Netochin, E.P. Fedotkina, O.E. Korotchenko, E.A. Sencha, A.N. Sencha, M.I. Shtilman, D.A. Gorin, Hybrid (bovine serum albumin)/poly(n-vinyl-2-pyrrolidone-co-acrylic acid)-shelled microbubbles as advanced ultrasound contrast agents, *ACS Appl. Bio Mater.* 5 (7) (2022) 3338–3348, <https://doi.org/10.1021/acsabm.2c00331>, publisher: American Chemical Society.
- [63] E.P. Stride, C.C. Coussios, Cavitation and contrast: the use of bubbles in ultrasound imaging and therapy, *Proc. Inst. Mech. Eng., Part H J. Eng. Med.* 224 (2) (2010) 171–191, <https://doi.org/10.1243/09544119JEIM622>.
- [64] M. Zhang, S. Zhang, J. Shi, Y. Hu, S. Wu, Z. Zan, P. Zhao, C. Gao, Y. Du, Y. Wang, F. Lin, X. Fu, D. Li, P. Qin, Z. Fan, Cell mechanical responses to subcellular perturbations generated by ultrasound and targeted microbubbles, *Acta Biomater.* (2022), <https://doi.org/10.1016/j.actbio.2022.11.017>.
- [65] Z. Fan, D. Chen, C.X. Deng, Characterization of the dynamic activities of a population of microbubbles driven by pulsed ultrasound exposure in sonoporation, *Ultrasound Med. Biol.* 40 (6) (2014) 1260–1272, <https://doi.org/10.1016/j.ultrasmedbio.2013.12.002>.
- [66] F.E. Shamout, A.N. Poulipoulos, P. Lee, S. Bonaccorsi, L. Towhidi, R. Krams, J.J. Choi, Enhancement of non-invasive trans-membrane drug delivery using ultrasound and microbubbles during physiologically relevant flow, *Ultrasound Med. Biol.* 41 (9) (2015) 2435–2448, <https://doi.org/10.1016/j.ultrasmedbio.2015.05.003>.
- [67] K.B. Bader, M.J. Gruber, C.K. Holland, Shaken and stirred: mechanisms of ultrasound-enhanced thrombolysis, *Ultrasound Med. Biol.* 41 (1) (2015) 187–196, <https://doi.org/10.1016/j.ultrasmedbio.2014.08.018>, place: England.
- [68] X. Zhang, Q. Fu, H. Duan, J. Song, H. Yang, Janus nanoparticles: from fabrication to (bio)applications, *ACS Nano* 15 (4) (2021) 6147–6191, <https://doi.org/10.1021/acsnano.1c01146>, publisher: American Chemical Society.
- [69] A. Walther, A.H.E. Müller, Janus particles: synthesis, self-assembly, physical properties, and applications, *Chem. Rev.* 113 (7) (2013) 5194–5261, <https://doi.org/10.1021/cr300089t>, publisher: American Chemical Society.
- [70] Y. Song, S. Chen, Janus nanoparticles: preparation, characterization, and applications, *chemistry, Asian J.* 9 (2) (2014) 418–430, <https://doi.org/10.1002/asia.201301398>.
- [71] X. Fan, J. Yang, X.J. Loh, Z. Li, Polymeric janus nanoparticles: recent advances in synthetic strategies, materials properties, and applications, *Macromol. Rapid Commun.* 40 (5) (2019) e1800203, <https://doi.org/10.1002/marc.201800203>, place: Germany.
- [72] F. Wurm, A.F.M. Kilbinger, Polymeric Janus particles, *Angew. Chem., Int. Ed.* 48 (45) (2009) 8412–8421, <https://doi.org/10.1002/anie.200901735>.
- [73] A. Alexeev, E.E. Uspal, A.C. Balazs, Harnessing Janus nanoparticles to create controllable pores in membranes, *ACS Nano* 2 (6) (2008) 1117–1122, <https://doi.org/10.1021/nl8000998>, publisher: American Chemical Society.
- [74] H. Xie, Z.-G. She, S. Wang, G. Sharma, J.W. Smith, One-step fabrication of polymeric janus nanoparticles for drug delivery, *Langmuir* 28 (9) (2012) 4459–4463, <https://doi.org/10.1021/la2042185>.
- [75] S. Khoei, A. Nouri, Chapter 4 - preparation of Janus nanoparticles and its application in drug delivery, in: A.M. Grumezescu (Ed.), *Design and Development of New Nanocarriers*, William Andrew Publishing, 2018, pp. 145–180.
- [76] Y. Song, J. Zhou, J.-B. Fan, W. Zhai, J. Meng, S. Wang, Hydrophilic/oleophilic magnetic Janus particles for the rapid and efficient oil–water separation, *Adv. Funct. Mater.* 28 (32) (2018) 1802493, <https://doi.org/10.1002/adfm.201802493>.
- [77] K.H. Ku, Y.J. Lee, G.-R. Yi, S.G. Jang, B.V.K.J. Schmidt, K. Liao, D. Klinger, C.J. Hawker, B.J. Kim, Shape-tunable biphasic Janus particles as pH-responsive switchable surfactants, *Macromolecules* 50 (23) (2017) 9276–9285, <https://doi.org/10.1021/acs.macromol.7b02365>, publisher: American Chemical Society.
- [78] H. Nie, C. Zhang, Y. Liu, A. He, Synthesis of Janus rubber hybrid particles and interfacial behavior, *Macromolecules* 49 (6) (2016) 2238–2244, <https://doi.org/10.1021/acs.macromol.6b00159>, publisher: American Chemical Society.
- [79] C. Marschelke, A. Fery, A. Synytska, Janus particles: from concepts to environmentally friendly materials and sustainable applications, *Colloid Polym. Sci.* 298 (7) (2020) 841–865, <https://doi.org/10.1007/s00396-020-04601-y>.
- [80] S.-H. Hu, X. Gao, Nanocomposites with spatially separated functionalities for combined imaging and magnetolytic therapy, *J. Am. Chem. Soc.* 132 (21) (2010) 7234–7237, <https://doi.org/10.1021/ja102489q>, publisher: American Chemical Society.
- [81] J. Wu, B. Wu, J. Xiong, S. Sun, P. Wu, Entropy-mediated polymer–cluster interactions enable dramatic thermal stiffening hydrogels for mechanoadaptive smart fabrics, *Angew. Chem., Int. Ed.* 61 (34) (2022) e202204960, <https://doi.org/10.1002/anie.202204960>.
- [82] L.K. Rivera-Tarazona, V.D. Bhat, H. Kim, Z.T. Campbell, T.H. Ware, Shape-morphing living composites, *Sci. Adv.* 6 (3) (2020), <https://doi.org/10.1126/sciadv.aax8582>, publisher: American Association for the Advancement of Science.
- [83] R. Brighenti, M.P. Cosma, Mechanical behavior of photopolymerized materials, *J. Mech. Phys. Solids* 153 (2021) 104456, <https://doi.org/10.1016/j.jmps.2021.104456>.
- [84] J. Wu, Z. Zhao, C.M. Hamel, X. Mu, X. Kuang, Z. Guo, H.J. Qi, Evolution of material properties during free radical photopolymerization, *J. Mech. Phys. Solids* 112 (2018) 25–49, <https://doi.org/10.1016/j.jmps.2017.11.018>, publisher: Elsevier Ltd.
- [85] C.N. Bowman, C.J. Kloxin, Toward an enhanced understanding and implementation of photopolymerization reactions, *AIChE J.* 54 (11) (2008) 2775–2795, <https://doi.org/10.1002/aic.11678>.

- [86] F. Zhang, L. Zhu, Z. Li, S. Wang, J. Shi, W. Tang, N. Li, J. Yang, The recent development of vat photopolymerization: a review, *Addit. Manuf.* 48 (2021) 102423, <https://doi.org/10.1016/j.addma.2021.102423>.
- [87] R. Brighenti, M.P. Cosma, L. Marsavina, A. Spagnoli, M. Terzano, Laser-based additively manufactured polymers: a review on processes and mechanical models, *J. Mater. Sci.* (2020), <https://doi.org/10.1007/s10853-020-05254-6>.
- [88] K. Yu, Z. Feng, H. Du, K.H. Lee, K. Li, Y. Zhang, S.F. Masri, Q. Wang, Constructive adaptation of 3D-printable polymers in response to typically destructive aquatic environments, *PNAS Nexus* 1 (3) (2022).
- [89] T. Matsuda, R. Kawakami, R. Namba, T. Nakajima, J.P. Gong, Mechanoresponsive self-growing hydrogels inspired by muscle training, *Science* 363 (6426) (2019) 504–508, <https://doi.org/10.1126/science.aau9533>.
- [90] A.L.B. Ramirez, Z.S. Kean, J.A. Orlicki, M. Champhekar, S.M. Elsagr, W.E. Krause, S.L. Craig, Mechanochemical strengthening of a synthetic polymer in response to typically destructive shear forces, *Nat. Chem.* 5 (9) (2013) 757–761, <https://doi.org/10.1038/nchem.1720>.
- [91] Z. Wang, X. Zheng, T. Ouchi, T.B. Kouznetsova, H.K. Beech, S. Av-Ron, T. Matsuda, B.H. Bowser, S. Wang, J.A. Johnson, J.A. Kalow, B.D. Olsen, J.P. Gong, M. Rubinstein, S.L. Craig, Toughening hydrogels through force-triggered chemical reactions that lengthen polymer strands, *Science* 374 (6564) (2021) 193–196, <https://doi.org/10.1126/science.abg2689>.
- [92] K.-A. Leslie, R. Doane-Solomon, S. Arora, S.J. Curley, C. Szczepanski, M.M. Driscoll, Gel rupture during dynamic swelling, *Soft Matter* 17 (6) (2021) 1513–1520, <https://doi.org/10.1039/D0SM01718C>, publisher: the Royal Society of Chemistry.
- [93] M. Zrinyi, F. Horkay, On the elastic modulus of swollen gels, *Polymer* 28 (7) (1987) 1139–1143, [https://doi.org/10.1016/0032-3861\(87\)90256-4](https://doi.org/10.1016/0032-3861(87)90256-4).
- [94] A. Boubakri, N. Haddar, K. Elleuch, Y. Bienvenu, Impact of aging conditions on mechanical properties of thermoplastic polyurethane, *Mater. Des.* 31 (9) (2010) 4194–4201, <https://doi.org/10.1016/j.matdes.2010.04.023>.
- [95] Y.-N. Zhou, J.-J. Li, T.-T. Wang, Y.-Y. Wu, Z.-H. Luo, Precision polymer synthesis by controlled radical polymerization: fusing the progress from polymer chemistry and reaction engineering, *Prog. Polym. Sci.* 130 (2022) 101555, <https://doi.org/10.1016/j.progpolymsci.2022.101555>.
- [96] M. Stevens, S. Merilaita, Animal camouflage: current issues and new perspectives, *Philos. Trans. R. Soc. B, Biol. Sci.* 364 (1516) (2009) 423–427, <https://doi.org/10.1098/rstb.2008.0217>.
- [97] J.J. Allen, L.M. Mähther, A. Barbosa, R.T. Hanlon, Cuttlefish use visual cues to control three-dimensional skin papillae for camouflage, *J. Comp. Physiol., A Sens. Neural Behav. Physiol.* 195 (6) (2009) 547–555, <https://doi.org/10.1007/s00359-009-0430-y>, place: Germany.
- [98] A.T. Pietrewicz, A.C. Kamil, Visual detection of cryptic prey by blue Jays (cyanocitta cristata), *Science* 195 (4278) (1977) 580–582, <https://doi.org/10.1126/science.195.4278.580>.
- [99] M.Q.R. Pembury Smith, G.D. Ruxton, Camouflage in predators, *Biol. Rev.* 95 (5) (2020) 1325–1340, <https://doi.org/10.1111/brv.12612>.
- [100] Y. Niu, H. Sun, M. Stevens, Plant camouflage: ecology, evolution, and implications, *Trends Ecol. Evol.* 33 (8) (2018) 608–618, <https://doi.org/10.1016/j.tree.2018.05.010>.
- [101] C.-C. Chiao, C. Chubb, R.T. Hanlon, A review of visual perception mechanisms that regulate rapid adaptive camouflage in cuttlefish, *J. Comp. Physiol.* 201 (9) (2015) 933–945, <https://doi.org/10.1007/s00359-015-0988-5>.
- [102] J. Teyssier, S.V. Saenko, D. van der Marel, M.C. Milinkovitch, Photonic crystals cause active colour change in chameleons, *Nat. Commun.* 6 (1) (2015) 6368, <https://doi.org/10.1038/ncomms7368>.
- [103] R. Hanlon, C.-C. Chiao, L. Mähther, A. Barbosa, K. Buresch, C. Chubb, Cephalopod dynamic camouflage: bridging the continuum between background matching and disruptive coloration, *Philos. Trans. R. Soc. B, Biol. Sci.* 364 (1516) (2009) 429–437, <https://doi.org/10.1098/rstb.2008.0270>.
- [104] L.M. Mähther, C.-C. Chiao, A. Barbosa, R.T. Hanlon, Color matching on natural substrates in cuttlefish, *Sepia officinalis*, *J. Comp. Physiol.* 194 (6) (2008) 577–585, <https://doi.org/10.1007/s00359-008-0332-4>.
- [105] J.M. Clough, A. Balan, R.P. Sijbesma, *Mechanochemical reactions reporting and repairing bond scission in polymers*, *Polym. Mech.* (2015) 209–238, Publisher: Springer.
- [106] Y. Chen, A.J.H. Spiering, S. Karthikeyan, G.W.M. Peters, E.W. Meijer, R.P. Sijbesma, Mechanically induced chemiluminescence from polymers incorporating a 1, 2-dioxetane unit in the main chain, *Nat. Chem.* 4 (7) (2012) 559–562, <https://doi.org/10.1038/nchem.1358>, place: England.
- [107] D.A. Davis, A. Hamilton, J. Yang, L.D. Cremar, D. Van Gough, S.L. Potisek, M.T. Ong, P.V. Braun, T.J. Martinez, S.R. White, J.S. Moore, N.R. Sottos, Force-induced activation of covalent bonds in mechanoresponsive polymeric materials, *Nature* 459 (7243) (2009) 68–72, <https://doi.org/10.1038/nature07970>, place: England.
- [108] R. Klajn, Spiropyran-based dynamic materials, *Chem. Soc. Rev.* 43 (1) (2014) 148–184, <https://doi.org/10.1039/C3CS60181A>, publisher: the Royal Society of Chemistry.
- [109] A. Black, J. Lenhardt, S. Craig, *From molecular mechanochemistry to stress-responsive materials*, *J. Mater. Chem.* 21 (6) (2011) 1655–1663, publisher: Royal Society of Chemistry.
- [110] A. Früh, F. Artoni, R. Brighenti, E. Dalcanale, *Strain field self-diagnostic poly(dimethylsiloxane) elastomers*, *Chem. Mater.* 29 (17) (2017) 7450–7457, publisher: ACS Publications.
- [111] Y. Sagara, T. Kato, Mechanically induced luminescence changes in molecular assemblies, *Nat. Chem.* 1 (8) (2009) 605–610, <https://doi.org/10.1038/nchem.411>.
- [112] X. Yan, F. Wang, B. Zheng, F. Huang, Stimuli-responsive supramolecular polymeric materials, *Chem. Soc. Rev.* 41 (18) (2012) 6042–6065, <https://doi.org/10.1039/C2CS35091B>, publisher: the Royal Society of Chemistry.
- [113] C.L. Brown, S.L. Craig, Molecular engineering of mechanophore activity for stress-responsive polymeric materials, *Chem. Sci.* 6 (4) (2015) 2158–2165, <https://doi.org/10.1039/C4SC01945H>, publisher: the Royal Society of Chemistry.
- [114] Z. Xia, V.D. Alphonse, D.B. Trigg, T.P. Harrigan, J.M. Paulson, Q.T. Luong, E.P. Lloyd, M.H. Barbee, S.L. Craig, 'Seeing' strain in soft materials, *Molecules (Basel, Switzerland)* 24 (3) (Feb. 2019), <https://doi.org/10.3390/molecules24030542>, place: Switzerland.
- [115] A.D. Das, G. Mannoni, A.E. Früh, D. Orsi, R. Pinalli, E. Dalcanale, Damage-reporting carbon fiber epoxy composites, *ACS Appl. Polym. Mater.* 1 (11) (2019) 2990–2997, <https://doi.org/10.1021/acscapm.9b00694>, publisher: American Chemical Society.
- [116] M. Silberstein, K. Min, L. Cremar, C. Degen, T. Martinez, N. Aluru, S. White, N. Sottos, Modeling mechanophore activation within a crosslinked glassy matrix, *J. Appl. Phys.* 114 (2) (2013) 023504, publisher: AIP.
- [117] R. Brighenti, F. Artoni, Mechanical modeling of self-diagnostic polymers, *Proc. Struct. Integrity* 13 (2018) 819–824, publisher: Elsevier.
- [118] R. Brighenti, F. Artoni, F. Vernerey, M. Torelli, A. Pedrini, I. Domenichelli, E. Dalcanale, Mechanics of responsive polymers via conformationally switchable molecules, *J. Mech. Phys. Solids* 113 (2018) 65–81, publisher: Elsevier.
- [119] R. Brighenti, F. Artoni, M.P. Cosma, *Mechanics of active mechano-chemical responsive polymers*, *IOP Conf. Ser., Mater. Sci. Eng.* 416 (1) (2018) 012080, IOP Publishing.
- [120] R. Brighenti, F. Artoni, M.P. Cosma, Mechanics of innovative responsive polymers, *Mech. Res. Commun.* 100 (2019) 103403, <https://doi.org/10.1016/j.mechrescom.2019.103403>.
- [121] X. Du, H. Cui, T. Xu, C. Huang, Y. Wang, Q. Zhao, Y. Xu, X. Wu, Reconfiguration, camouflage, and color-shifting for bioinspired adaptive hydrogel-based millirobots, *Adv. Funct. Mater.* 30 (10) (2020) 1909202, <https://doi.org/10.1002/adfm.201909202>.
- [122] R. Yu, L. Zhu, Y. Xia, J. Liu, J. Liang, J. Xu, B. Wang, S. Wang, Octopus inspired hydrogel actuator with synergistic structural color and shape change, *Adv. Mater. Interfaces* 9 (19) (2022) 2200401, <https://doi.org/10.1002/admi.202200401>.
- [123] R. Brighenti, M.P. Cosma, Mechanics of multi-stimuli temperature-responsive hydrogels, *J. Mech. Phys. Solids* 169 (2022) 105045, <https://doi.org/10.1016/j.jmps.2022.105045>.
- [124] H. Liu, L. Yu, B. Zhao, Y. Ni, P. Gu, H. Qiu, W. Zhang, K. Chen, Bio-inspired color-changing and self-healing hybrid hydrogels for wearable sensors and adaptive camouflage, *J. Mater. Chem. C* 11 (1) (2023) 285–298, <https://doi.org/10.1039/D2TC03102G>, publisher: the Royal Society of Chemistry.
- [125] C. Xu, M. Colorado Escobar, A.A. Gorodetsky, Stretchable cephalopod-inspired multimodal camouflage systems, *Adv. Mater.* 32 (16) (2020) 1905717, <https://doi.org/10.1002/adma.201905717>.
- [126] A. Barbosa, J.J. Allen, L.M. Mähther, R.T. Hanlon, Cuttlefish use visual cues to determine arm postures for camouflage, *proceedings, Biol. Sci.* 279 (1726) (2012) 84–90, <https://doi.org/10.1098/rspb.2011.0196>, edition: 2011/05/11, Publisher: the Royal Society.
- [127] R. Hu, W. Xi, Y. Liu, K. Tang, J. Song, X. Luo, J. Wu, C.-W. Qiu, Thermal camouflaging metamaterials, *Mater. Today* 45 (2021) 120–141, <https://doi.org/10.1016/j.mattod.2020.11.013>.
- [128] H. Godaba, Z.-Q. Zhang, U. Gupta, C. Chiang Foo, J. Zhu, Dynamic pattern of wrinkles in a dielectric elastomer, *Soft Matter* 13 (16) (2017) 2942–2951, <https://doi.org/10.1039/C7SM00198C>, publisher: the Royal Society of Chemistry.
- [129] X. Liu, B. Li, H. Chen, S. Jia, J. Zhou, Voltage-induced wrinkling behavior of dielectric elastomer, *J. Appl. Polym. Sci.* 133 (14) (2016).
- [130] A. Agrawal, P. Luchette, P. Palfy-Muhoray, S.L. Biswal, W.G. Chapman, R. Verduzco, Surface wrinkling in liquid crystal elastomers, *Soft Matter* 8 (27) (2012) 7138–7142, <https://doi.org/10.1039/C2SM25734C>, publisher: the Royal Society of Chemistry.
- [131] S. Zhao, F. Xu, C. Fu, Y. Huo, Controllable wrinkling patterns on liquid crystal polymer film/substrate systems by laser illumination, *Extrem. Mech. Lett.* 30 (2019) 100502, <https://doi.org/10.1016/j.eml.2019.100502>.
- [132] R. Alberini, A. Spagnoli, M. Terzano, Numerical modeling of wrinkled hyperelastic membranes with topologically complex internal boundary conditions, *Int. J. Mech. Sci.* 212 (2021) 106816, <https://doi.org/10.1016/j.ijmeosci.2021.106816>.
- [133] C. Zhang, B. Li, J.-Y. Tang, X.-L. Wang, Z. Qin, X.-Q. Feng, Experimental and theoretical studies on the morphogenesis of bacterial biofilms, *Soft Matter* 13 (40) (2017) 7389–7397, <https://doi.org/10.1039/C7SM01593C>, publisher: the Royal Society of Chemistry.
- [134] Y. Zhao, W. Guo, H. Zhu, Y. He, C. Jiang, Y. Cao, Pattern selection on axial-compressed bilayer systems with a non-zero Gauss curvature, *J. Mech. Phys. Solids* 154 (2021) 104516, <https://doi.org/10.1016/j.jmps.2021.104516>.
- [135] Y. Liu, Z. Feng, C. Xu, A. Chatterjee, A.A. Gorodetsky, Reconfigurable micro- and nano-structured camouflage surfaces inspired by cephalopods, *ACS Nano* 15 (11) (2021) 17299–17309, <https://doi.org/10.1021/acsnano.0c09990>, publisher: American Chemical Society.

- [136] T. Wang, Y. Yang, F. Xu, Mechanics of tension-induced film wrinkling and restabilization: a review, *Proc. R. Soc. A, Math. Phys. Eng. Sci.* 478 (2263) (2022) 20220149, <https://doi.org/10.1098/rspa.2022.0149>.
- [137] J.H. Pikul, S. Li, H. Bai, R.T. Hanlon, I. Cohen, R.F. Shepherd, Stretchable surfaces with programmable 3D texture morphing for synthetic camouflaging skins, *Science (N. Y.)* 358 (6360) (2017) 210–214, <https://doi.org/10.1126/science.aan5627>, place: United States.
- [138] L. Jin, M. Yeager, Y.-J. Lee, D.J. O'Brien, S. Yang, Shape-morphing into 3D curved surfaces with nacre-like composite architectures, *Sci. Adv.* 8 (41) (2022) eabq3248, <https://doi.org/10.1126/sciadv.abq3248>.
- [139] B. Aksoy, H. Shea, Multistable shape programming of variable-stiffness electromagnetic devices, *Sci. Adv.* 8 (21) (2022) eabk0543, <https://doi.org/10.1126/sciadv.abk0543>.
- [140] R. Chellattoan, G. Lubineau, A stretchable fiber with tunable stiffness for programmable shape change of soft robots, *Soft Robot.* 9 (6) (2022) 1052–1061, <https://doi.org/10.1089/soro.2021.0032>.
- [141] X. Xia, C.M. Spadaccini, J.R. Greer, Responsive materials architected in space and time, *Nat. Rev. Mater.* 7 (9) (2022) 683–701, <https://doi.org/10.1038/s41578-022-00450-z>.
- [142] N. Sholl, A. Moss, M. Krieg, K. Mohseni, Controlling the deformation space of soft membranes using fiber reinforcement, *Int. J. Robot. Res.* 40 (1) (2021) 178–196, <https://doi.org/10.1177/0278364919897134>.
- [143] J.W. Boley, W.M. v. Rees, C. Lissandrello, M.N. Horenstein, R.L. Truby, A. Kotikian, J.A. Lewis, L. Mahadevan, Shape-shifting structured lattices via multimaterial 4D printing, *Proc. Natl. Acad. Sci.* 116 (42) (2019) 20856–20862, <https://doi.org/10.1073/pnas.1908806116>.
- [144] M. Badaoui, G. Kresge, C. Ushay, J. Marthelot, P.-T. Brun, Formation of pixelated elastic films via capillary suction of curable elastomers in templated Hele-Shaw cells, *Adv. Mater.* 34 (27) (2022) 2109682, <https://doi.org/10.1002/adma.202109682>.
- [145] Ankit, T.Y.K. Ho, A. Nirmal, M.R. Kulkarni, D. Accoto, N. Mathews, Soft actuator materials for electrically driven haptic interfaces, *Adv. Intell. Syst.* 4 (2) (2022) 2100061, <https://doi.org/10.1002/aisy.202100061>.
- [146] Y. Zhai, Z. Wang, K.-S. Kwon, S. Cai, D.J. Lipomi, T.N. Ng, Printing multi-material organic haptic actuators, *Adv. Mater.* 33 (19) (2021) 2002541, <https://doi.org/10.1002/adma.202002541>.
- [147] R.S. Dahiya, G. Metta, M. Valle, G. Sandini, Tactile sensing—from humans to humanoid, *IEEE Trans. Robot.* 26 (1) (2010) 1–20, <https://doi.org/10.1109/TRO.2009.2033627>.
- [148] C. Basdogan, F. Giraud, V. Levesque, S. Choi, A review of surface haptics: enabling tactile effects on touch surfaces, *IEEE Trans. Haptics* 13 (3) (2020) 450–470, <https://doi.org/10.1109/TOH.2020.2990712>.
- [149] T.-H. Yang, J.R. Kim, H. Jin, H. Gil, J.-H. Koo, H.J. Kim, Recent advances and opportunities of active materials for haptic technologies in virtual and augmented reality, *Adv. Funct. Mater.* 31 (39) (2021) 2008831, <https://doi.org/10.1002/adfm.202008831>.
- [150] C. Pacchierotti, S. Scheggi, D. Prattichizzo, S. Misra, Haptic feedback for micro-robotics applications: a review, *Front. Robot. AI* 3 (2016), <https://doi.org/10.3389/frobt.2016.00053>, <https://www.frontiersin.org/articles/10.3389/frobt.2016.00053>.
- [151] W. Guo, Y. Hu, Z. Yin, H. Wu, On-skin stimulation devices for haptic feedback and human-machine interfaces, *Adv. Mater. Technol.* 7 (2) (2022) 2100452, <https://doi.org/10.1002/admt.202100452>.
- [152] K.K. Kim, Y. Suh, S.H. Ko, Smart stretchable electronics for advanced human-machine interface, *Adv. Intell. Syst.* 3 (2) (2021) 2000157, <https://doi.org/10.1002/aisy.202000157>.
- [153] S. Mun, S. Yun, S. Nam, S.K. Park, S. Park, B.J. Park, J.M. Lim, K.-U. Kyung, Electro-active polymer based soft tactile interface for wearable devices, *IEEE Trans. Haptics* 11 (1) (2018) 15–21, <https://doi.org/10.1109/TOH.2018.2805901>.
- [154] T. Wang, M. Farajollahi, Y.S. Choi, I.-T. Lin, J.E. Marshall, N.M. Thompson, S. Kar-Narayan, J.D.W. Madden, S.K. Smoukov, Electroactive polymers for sensing, *Interface Focus* 6 (4) (2016) 20160026, <https://doi.org/10.1098/rsfs.2016.0026>.
- [155] J. Gao, Y. He, X. Cong, H. Yi, J. Guo, Reconfigurable fluorescent liquid crystal elastomers for integrated visual and haptic information storage, *ACS Appl. Mater. Interfaces* 14 (47) (2022) 53348–53358, <https://doi.org/10.1021/acami.2c17494>, publisher: American Chemical Society.
- [156] N. Torras, K.E. Zinoviev, C.J. Camargo, E.M. Campo, H. Campanella, J. Esteve, J.E. Marshall, E.M. Terentjev, M. Omastová, I. Krupa, P. Teplický, B. Mamojka, P. Bruns, B. Roeder, M. Vallribera, R. Malet, S. Zuffanelli, V. Soler, J. Roig, N. Walker, D. Wenn, F. Vossen, F.M.H. Cropvoets, Tactile device based on optomechanical actuation of liquid crystal elastomers, *Sens. Actuators A, Phys.* 208 (2014) 104–112, <https://doi.org/10.1016/j.sna.2014.01.012>.
- [157] E.D. Brodie, Salamander antipredator postures, *Copeia* 1977 (3) (1977) 523–535, <https://doi.org/10.2307/1443271>, publisher: [American Society of Ichthyologists and Herpetologists (ASIH), Allen Press] <http://www.jstor.org/stable/1443271>.
- [158] A. Hughes, E. Liggins, M. Stevens, Imperfect camouflage: how to hide in a variable world?, *Proc. R. Soc. B, Biol. Sci.* 286 (1902) (2019) 20190646, <https://doi.org/10.1098/rspb.2019.0646>.
- [159] L. Hines, K. Petersen, G.Z. Lum, M. Sitti, Soft actuators for small-scale robotics, *Adv. Mater.* 29 (13) (2017) 1603483, <https://doi.org/10.1002/adma.201603483>.
- [160] H. Cui, Q. Zhao, Y. Wang, X. Du, Bioinspired actuators based on stimuli-responsive polymers, *chemistry, Asian J.* 14 (14) (2019) 2369–2387, <https://doi.org/10.1002/asia.201900292>.
- [161] Y. Chen, J. Yang, X. Zhang, Y. Feng, H. Zeng, L. Wang, W. Feng, Light-driven bi-morph soft actuators: design, fabrication, and properties, *Mater. Horiz.* 8 (3) (2021) 728–757, <https://doi.org/10.1039/D0MH01406K>, publisher: the Royal Society of Chemistry.
- [162] R. Brighenti, M.P. Cosma, Smart actuation of liquid crystal elastomer elements: cross-link density-controlled response, *Smart Mater. Struct.* 31 (1) (2021) 015012, <https://doi.org/10.1088/1361-665x/ac34bf>, publisher: IOP Publishing.
- [163] M.P. Cosma, R. Brighenti, Controlled morphing of architected liquid crystal elastomer elements: modeling and simulations, *Mech. Res. Commun.* 121 (2022) 103858, <https://doi.org/10.1016/j.mechrescom.2022.103858>.
- [164] Z. Li, P. Liu, X. Ji, J. Gong, Y. Hu, W. Wu, X. Wang, H.-Q. Peng, R.T.K. Kwok, J.W.Y. Lam, J. Lu, B.Z. Tang, Bioinspired simultaneous changes in fluorescence color, brightness, and shape of hydrogels enabled by AIEgens, *Adv. Mater.* 32 (11) (2020) 1906493, <https://doi.org/10.1002/adma.201906493>.
- [165] C.-M. Tu, C.-H. Chao, S.-C. Hung, S.-Y. Ou, C.-H. Zhuang, C.-Y. Liu, Bio-inspired thermal responsive liquid crystal actuators showing shape and color variations simultaneously, *J. Taiwan Inst. Chem. Eng.* 140 (2022) 104536, <https://doi.org/10.1016/j.jtice.2022.104536>.
- [166] S. Sponberg, The emergent physics of animal locomotion, *Phys. Today* 70 (9) (2017) 34–40, <https://doi.org/10.1063/PT.3.3691>, publisher: American Institute of Physics.
- [167] S.A. Combes, R. Dudley, Turbulence-driven instabilities limit insect flight performance, *Proc. Natl. Acad. Sci.* 106 (22) (2009) 9105–9108, publisher: National Academy of Sciences.
- [168] A. Bernadou, V. Fourcassié, Does substrate coarseness matter for foraging ants? An experiment with *Lasius Niger* (hymenoptera; formicidae), *J. Insect Physiol.* 54 (3) (2008) 534–542, <https://doi.org/10.1016/j.jinsphys.2007.12.001>, place: England.
- [169] H.C. Astley, B.C. Jayne, Effects of perch diameter and incline on the kinematics, performance and modes of arboreal locomotion of corn snakes (*Elaphe guttata*), *J. Exp. Biol.* 210 (Pt 21) (2007) 3862–3872, <https://doi.org/10.1242/jeb.009050>, place: England.
- [170] T. Kohlsdorf, C.A. Navas, Evolution of jumping capacity in Tropicidurinae lizards: does habitat complexity influence obstacle-crossing ability?, *Biol. J. Linn. Soc.* 91 (3) (2007) 393–402, <https://doi.org/10.1111/j.1095-8312.2007.00804.x>.
- [171] B. Vanhooydonck, A. Andronescu, A. Herrel, D.J. Irschick, Effects of substrate structure on speed and acceleration capacity in climbing geckos, *Biol. J. Linn. Soc.* 85 (3) (2005) 385–393, <https://doi.org/10.1111/j.1095-8312.2005.00495.x>.
- [172] L. Mahadevan, S. Daniel, M.K. Chaudhury, Biomimetic ratcheting motion of a soft, slender, sessile gel, *Proc. Natl. Acad. Sci.* 101 (1) (2004) 23–26, <https://doi.org/10.1073/pnas.2637051100>.
- [173] R.M. Alexander, *Principles of Animal Locomotion*, Princeton University Press, 2003.
- [174] X.-Q. Wang, G.W. Ho, Design of untethered soft material micromachine for life-like locomotion, *Mater. Today* 53 (2022) 197–216, <https://doi.org/10.1016/j.mattod.2022.01.014>.
- [175] H. Shahsavan, S.M. Salili, A. Jákli, B. Zhao, Thermally active liquid crystal network gripper mimicking the self-peeling of gecko toe pads, *Adv. Mater.* 29 (3) (2017) 1604021, <https://doi.org/10.1002/adma.201604021>.
- [176] J.C. Liao, D.N. Beal, G.V. Lauder, M.S. Triantafyllou, Fish exploiting vortices decrease muscle activity, *Science* 302 (5650) (2003) 1566–1569, <https://doi.org/10.1126/science.1088295>.
- [177] M.A.R. Koehl, M.A. Reidenbach, Swimming by microscopic organisms in ambient water flow, *Exp. Fluids* 43 (5) (2007) 755–768, <https://doi.org/10.1007/s00348-007-0371-6>.
- [178] J. Johansen, D. Bellwood, C. Fulton, Coral reef fishes exploit flow refuges in high-flow habitats, *Mar. Ecol. Prog. Ser.* 360 (2008) 219–226.
- [179] M. Sfakiotakis, D. Lane, J. Davies, Review of fish swimming modes for aquatic locomotion, *IEEE J. Ocean. Eng.* 24 (2) (1999) 237–252, <https://doi.org/10.1109/48.757275>.
- [180] H. Shahsavan, A. Aghakhani, H. Zeng, Y. Guo, Z.S. Davidson, A. Priimagi, M. Sitti, Bioinspired underwater locomotion of light-driven liquid crystal gels, *Proc. Natl. Acad. Sci.* 117 (10) (2020) 5125–5133, <https://doi.org/10.1073/pnas.1917952117>.
- [181] J.W. Bush, D.L. Hu, WALKING ON WATER: biolocomotion at the interface, *Annu. Rev. Fluid Mech.* 38 (1) (2006) 339–369, <https://doi.org/10.1146/annurev.fluid.38.050304.092157>.
- [182] X. Yang, Y. Chen, X. Zhang, P. Xue, P. Lv, Y. Yang, L. Wang, W. Feng, Bioinspired light-fueled water-walking soft robots based on liquid crystal network actuators with polymerizable miniaturized gold nanorods, *Nano Today* 43 (2022) 101419, <https://doi.org/10.1016/j.nantod.2022.101419>.
- [183] X. Zhang, J. Zhao, Q. Zhu, N. Chen, M. Zhang, Q. Pan, Bioinspired aquatic microbot capable of walking on water surface like a water strider, *ACS Appl. Mater. Interfaces* 3 (7) (2011) 2630–2636, <https://doi.org/10.1021/am200382g>, publisher: American Chemical Society.
- [184] J. Yan, K. Yang, G. Liu, J. Zhao, Flexible driving mechanism inspired water strider robot walking on water surface, *IEEE Access* 8 (2020) 89643–89654, <https://doi.org/10.1109/ACCESS.2020.2993078>.

- [185] T. Engels, D. Kolomenskiy, K. Schneider, M. Farge, F.-O. Lehmann, J. Sesterhenn, Impact of turbulence on flying insects in tethered and free flight: high-resolution numerical experiments, *Phys. Rev. Fluids* 4 (1) (2019) 013103, <https://doi.org/10.1103/PhysRevFluids.4.013103>, publisher: American Physical Society.
- [186] F.-O. Lehmann, S. Gorb, N. Nasir, P. Schützner, Elastic deformation and energy loss of flapping fly wings, *J. Exp. Biol.* 214 (17) (2011) 2949–2961, <https://doi.org/10.1242/jeb.045351>.
- [187] R. Dudley, *The Biomechanics of Insect Flight: Form, Function, Evolution*, Princeton University Press, 2002.
- [188] C.S.X. Ng, M.W.M. Tan, C. Xu, Z. Yang, P.S. Lee, G.Z. Lum, Locomotion of miniature soft robots, *Adv. Mater.* 33 (19) (2021) 2003558, <https://doi.org/10.1002/adma.202003558>.
- [189] M. Pilz da Cunha, M.G. Debije, A.P.H.J. Schenning, Bioinspired light-driven soft robots based on liquid crystal polymers, *Chem. Soc. Rev.* 49 (18) (2020) 6568–6578, <https://doi.org/10.1039/D0CS00363H>, publisher: the Royal Society of Chemistry.
- [190] M. Camacho-Lopez, H. Finkelmann, P. Palffy-Muhoray, M. Shelley, Fast liquid-crystal elastomer swims into the dark, *Nat. Mater.* 3 (5) (2004) 307–310, <https://doi.org/10.1038/nmat1118>.
- [191] C. Huang, J.-a. Lv, X. Tian, Y. Wang, Y. Yu, J. Liu, Miniaturized swimming soft robot with complex movement actuated and controlled by remote light signals, *Sci. Rep.* 5 (1) (2015) 17414, <https://doi.org/10.1038/srep17414>.
- [192] K. Hou, D. Guan, H. Li, Y. Sun, Y. Long, K. Song, Programmable light-driven swimming actuators via wavelength signal switching, *Sci. Adv.* 7 (37) (2021) eabh3051, <https://doi.org/10.1126/sciadv.abb3051>.
- [193] H. Zhu, B. Xu, Y. Wang, X. Pan, Z. Qu, Y. Mei, Self-powered locomotion of a hydrogel water strider, *Sci. Robot.* 6 (53) (2021) eabe7925, <https://doi.org/10.1126/scirobotics.abe7925>.
- [194] G. Li, X. Chen, F. Zhou, Y. Liang, Y. Xiao, X. Cao, Z. Zhang, M. Zhang, B. Wu, S. Yin, Y. Xu, H. Fan, Z. Chen, W. Song, W. Yang, B. Pan, J. Hou, W. Zou, S. He, X. Yang, G. Mao, Z. Jia, H. Zhou, T. Li, S. Qu, Z. Xu, Z. Huang, Y. Luo, T. Xie, J. Gu, S. Zhu, W. Yang, Self-powered soft robot in the Mariana Trench, *Nature* 591 (7848) (2021) 66–71, <https://doi.org/10.1038/s41586-020-03153-z>.
- [195] C. Li, G.C. Lau, H. Yuan, A. Aggarwal, V.L. Dominguez, S. Liu, H. Sai, L.C. Palmer, N.A. Sather, T.J. Pearson, D.E. Freedman, P.K. Amiri, M.O. d. l. Cruz, S.I. Stupp, Fast and programmable locomotion of hydrogel-metal hybrids under light and magnetic fields, *Sci. Robot.* 5 (49) (2020) eabb9822, <https://doi.org/10.1126/scirobotics.abb9822>.
- [196] W. Hu, G.Z. Lum, M. Mastrangeli, M. Sitti, Small-scale soft-bodied robot with multimodal locomotion, *Nature* 554 (7690) (2018) 81–85, <https://doi.org/10.1038/nature25443>.
- [197] Y. Zhao, C. Xuan, X. Qian, Y. Alsaid, M. Hua, L. Jin, X. He, Soft phototactic swimmer based on self-sustained hydrogel oscillator, *Sci. Robot.* 4 (33) (2019) eaax7112, <https://doi.org/10.1126/scirobotics.aax7112>.
- [198] Z. Ren, W. Hu, X. Dong, M. Sitti, Multi-functional soft-bodied jellyfish-like swimming, *Nat. Commun.* 10 (1) (2019) 2703, <https://doi.org/10.1038/s41467-019-10549-7>.
- [199] Y. Yu, M. Nakano, T. Ikeda, Directed bending of a polymer film by light, in: *A New Opto-Mechanical Effect in Solids*, *Nature* 425 (6954) (2003) 145, <https://doi.org/10.1038/425145a>.
- [200] H. Finkelmann, E. Nishikawa, G.G. Pereira, M. Warner, A new opto-mechanical effect in solids, *Phys. Rev. Lett.* 87 (1) (2001) 015501, <https://doi.org/10.1103/PhysRevLett.87.015501>, publisher: American Physical Society.
- [201] T. Cheng, G. Li, Y. Liang, M. Zhang, B. Liu, T.-W. Wong, J. Forman, M. Chen, G. Wang, Y. Tao, T. Li, Untethered soft robotic jellyfish, *Smart Mater. Struct.* 28 (1) (2018) 015019, <https://doi.org/10.1088/1361-665X/aaed4f>, publisher: IOP Publishing.
- [202] D. Okawa, S.J. Pastine, A. Zettl, J.M.J. Fréchet, Surface tension mediated conversion of light to work, *J. Am. Chem. Soc.* 131 (15) (2009) 5396–5398, <https://doi.org/10.1021/ja900130n>, publisher: American Chemical Society.
- [203] B. Shin, J. Ha, M. Lee, K. Park, G.H. Park, T.H. Choi, K.-J. Cho, H.-Y. Kim, Hygrobot: a self-locomotive ratcheted actuator powered by environmental humidity, *Sci. Robot.* 3 (14) (2018), <https://doi.org/10.1126/scirobotics.aar2629> eaar2629.
- [204] M. Rogó, H. Zeng, C. Xuan, D.S. Wiersma, P. Wasylyczyk, Light-driven soft robot mimics caterpillar locomotion in natural scale, *Adv. Opt. Mater.* 4 (11) (2016) 1689–1694, <https://doi.org/10.1002/adom.201600503>.
- [205] Y. Tanaka, K. Ito, T. Nakagaki, R. Kobayashi, Mechanics of peristaltic locomotion and role of anchoring, *J. R. Soc. Interface* 9 (67) (2012) 222–233, <https://doi.org/10.1098/rsif.2011.0339>.
- [206] M. Wang, X.-B. Hu, B. Zuo, S. Huang, X.-M. Chen, H. Yang, Liquid crystal elastomer actuator with serpentine locomotion, *Chem. Commun.* 56 (55) (2020) 7597–7600, <https://doi.org/10.1039/D0CC02823A>, publisher: the Royal Society of Chemistry.
- [207] X. Liu, S.-K. Kim, X. Wang, Thermomechanical liquid crystalline elastomer capillaries with biomimetic peristaltic crawling function, *J. Mater. Chem. B* 4 (45) (2016) 7293–7302, <https://doi.org/10.1039/C6TB02372J>, publisher: the Royal Society of Chemistry.
- [208] Z. Sun, Y. Yamauchi, F. Araoka, Y.S. Kim, J. Bergueiro, Y. Ishida, Y. Ebina, T. Sasaki, T. Hikima, T. Aida, An anisotropic hydrogel actuator enabling earthworm-like directed peristaltic crawling, *Angew. Chem., Int. Ed.* 57 (48) (2018) 15772–15776, <https://doi.org/10.1002/anie.201810052>.
- [209] K. Saito, H. Nagai, K. Suto, N. Ogawa, Y.a. Seong, T. Tachi, R. Niiyama, Y. Kawahara, Insect wing 3D printing, *Sci. Rep.* 11 (1) (2021) 18631, <https://doi.org/10.1038/s41598-021-98242-y>.
- [210] J.K. Shang, S.A. Combes, B.M. Finio, R.J. Wood, Artificial insect wings of diverse morphology for flapping-wing micro air vehicles, *Bioinspir. Biomim.* 4 (3) (2009) 036002, <https://doi.org/10.1088/1748-3182/4/3/036002>.
- [211] R.J. Wootton, Functional morphology of insect wings, *Annu. Rev. Entomol.* 37 (1) (1992) 113–140, <https://doi.org/10.1146/annurev.en.37.010192.000553>.
- [212] R.J. Wootton, Geometry and mechanics of insect hindwing fans: a modeling approach, *Proc. R. Soc. Lond. B, Biol. Sci.* 262 (1364) (1995) 181–187, <https://doi.org/10.1098/rspb.1995.0194>.
- [213] R. Wootton, The geometry and mechanics of insect wing deformations in flight: a modeling approach, *Insects* 11 (7) (2020), <https://doi.org/10.3390/insects11070446>, <https://www.mdpi.com/2075-4450/11/7/446>.
- [214] S.A. Combes, Materials, structure, and dynamics of insect wings as bioinspiration for MAVs, in: *Encyclopedia of Aerospace Engineering*, John Wiley & Sons, Ltd, 2010, section: 3.
- [215] F. Wang, H. Gong, X. Chen, C.Q. Chen, Folding to curved surfaces: a generalized design method and mechanics of origami-based cylindrical structures, *Sci. Rep.* 6 (1) (2016) 33312, <https://doi.org/10.1038/srep33312>.
- [216] H. Zeng, P. Wasylyczyk, D.S. Wiersma, A. Priimagi, Light robots: bridging the gap between microrobotics and photomechanics in soft materials, *Adv. Mater.* 30 (24) (2018) 1703554, <https://doi.org/10.1002/adma.201703554>.
- [217] S. Tanaka, A. Asignacion, T. Nakata, S. Suzuki, H. Liu, Review of biomimetic approaches for drones, *Drones* 6 (11) (2022), <https://doi.org/10.3390/drones6110320>, <https://www.mdpi.com/2504-446X/6/11/320>.
- [218] Y. Guo, J. Guo, L. Liu, Y. Liu, J. Leng, Bioinspired multimodal soft robot driven by a single dielectric elastomer actuator and two flexible electroadhesive feet, *Extrem. Mech. Lett.* 53 (2022) 101720, <https://doi.org/10.1016/j.eml.2022.101720>.
- [219] S. Mintchev, D. Floreano, Adaptive morphology: a design principle for multimodal and multifunctional robots, *IEEE Robot. Autom. Mag.* 23 (3) (2016) 42–54, <https://doi.org/10.1109/MRA.2016.2580593>.
- [220] P. Gullan, P. Cranston, *The Insects An Outline of Entomology* Blackwell Publishing, 2005.
- [221] Z. Emberts, I. Escalante, P.W. Bateman, The ecology and evolution of autotomy, *Biol. Rev.* 94 (6) (2019) 1881–1896, <https://doi.org/10.1111/brv.12539>.
- [222] T.P. Lozito, R.S. Tuan, Lizard tail regeneration as an instructive model of enhanced healing capabilities in an adult amniote, *Connect. Tissue Res.* 58 (2) (2017) 145–154, <https://doi.org/10.1080/03080207.2016.1215444>, place: England.
- [223] J. Zhang, W. Qu, X. Li, Z. Wang, Surface engineering of filter membranes with hydrogels for oil-in-water emulsion separation, *Sep. Purif. Technol.* 304 (2023) 122340, <https://doi.org/10.1016/j.seppur.2022.122340>.
- [224] B. Wang, W. Liang, Z. Guo, W. Liu, Biomimetic super-lyophobic and super-lyophilic materials applied for oil/water separation: a new strategy beyond nature, *Chem. Soc. Rev.* 44 (1) (2015) 336–361, <https://doi.org/10.1039/c4cs00220b>, place: England.
- [225] G. Ju, M. Cheng, F. Shi, A pH-responsive smart surface for the continuous separation of oil/water/oil ternary mixtures, *NPG Asia Mater.* 6 (7) (2014) e111, <https://doi.org/10.1038/am.2014.44>.
- [226] D. Dong, Y. Zhu, W. Fang, M. Ji, A. Wang, S. Gao, H. Lin, R. Huang, J. Jin, Double-defense design of super-anti-fouling membranes for oil/water emulsion separation, *Adv. Funct. Mater.* 32 (24) (2022) 2113247, <https://doi.org/10.1002/adfm.202113247>.
- [227] H. Qiu, K. Feng, A. Gapeeva, K. Meurisch, S. Kaps, X. Li, L. Yu, Y.K. Mishra, R. Adelung, M. Baum, Functional polymer materials for modern marine bio-fouling control, *Prog. Polym. Sci.* 127 (2022) 101516, <https://doi.org/10.1016/j.progpolymsci.2022.101516>.
- [228] R.F. Brady, A fracture mechanical analysis of fouling release from nontoxic antifouling coatings, *Prog. Org. Coat.* 43 (1) (2001) 188–192, [https://doi.org/10.1016/S0300-9440\(01\)00180-1](https://doi.org/10.1016/S0300-9440(01)00180-1).
- [229] R.F. Brady, I.L. Singer, Mechanical factors favoring release from fouling release coatings, *Biofouling* 15 (1–3) (2000) 73–81, <https://doi.org/10.1080/08927010009386299>, place: England.
- [230] L. Pociavsek, J. Pugar, R. O’Dea, S.-H. Ye, W. Wagner, E. Tzeng, S. Velankar, E. Cerda, Topography-driven surface renewal, *Nat. Phys.* 14 (9) (2018) 948–953, <https://doi.org/10.1038/s41567-018-0193-x>.
- [231] A.K. Bajpai, S.K. Shukla, S. Bhanu, S. Kankane, Responsive polymers in controlled drug delivery, *Prog. Polym. Sci.* 33 (11) (2008) 1088–1118, <https://doi.org/10.1016/j.progpolymsci.2008.07.005>.
- [232] Y.K. Sung, S.W. Kim, Recent advances in polymeric drug delivery systems, *Biomater. Res.* 24 (1) (2020) 12, <https://doi.org/10.1186/s40824-020-00190-7>.
- [233] Y. Wang, G. Chen, H. Zhang, C. Zhao, L. Sun, Y. Zhao, Emerging functional biomaterials as medical patches, *ACS Nano* 15 (4) (2021) 5977–6007, <https://doi.org/10.1021/acsnano.0c10724>, publisher: American Chemical Society.
- [234] G. Suarato, R. Bertorelli, A. Athanassiou, Borrowing from nature: biopolymers and biocomposites as smart wound care materials, *Bioeng. Biotechnol.* 6 (2018) 137, publisher: Frontiers Media SA.
- [235] Y. Zhang, W. Zhao, S. Ma, H. Liu, X. Wang, X. Zhao, B. Yu, M. Cai, F. Zhou, Modulus adaptive lubricating prototype inspired by instant muscle hardening mechanism of catfish skin, *Nat. Commun.* 13 (1) (2022) 377, <https://doi.org/10.1038/s41467-022-28038-9>.

- [236] J. Shim, C. Perdigué, E.R. Chen, K. Bertoldi, P.M. Reis, Buckling-induced encapsulation of structured elastic shells under pressure, *Proc. Natl. Acad. Sci. USA* 109 (16) (2012) 5978–5983, <https://doi.org/10.1073/pnas.1115674109>, <https://europepmc.org/articles/PMC3341048>.
- [237] N. Hu, R. Burguéño, Buckling-induced smart applications: recent advances and trends, *Smart Mater. Struct.* 24 (6) (2015) 063001, <https://doi.org/10.1088/0964-1726/24/6/063001>, publisher: IOP Publishing.
- [238] P. Wang, F. Casadei, S. Shan, J.C. Weaver, K. Bertoldi, Harnessing buckling to design tunable locally resonant acoustic metamaterials, *Phys. Rev. Lett.* 113 (1) (2014) 014301, <https://doi.org/10.1103/PhysRevLett.113.014301>, publisher: American Physical Society.
- [239] J. Liu, T. Gu, S. Shan, S.H. Kang, J.C. Weaver, K. Bertoldi, Harnessing buckling to design architected materials that exhibit effective negative swelling, *Adv. Mater.* 28 (31) (2016) 6619–6624, <https://doi.org/10.1002/adma.201600812>.
- [240] A. Rafsanjani, K. Bertoldi, Buckling-induced Kirigami, *Phys. Rev. Lett.* 118 (8) (2017) 084301, <https://doi.org/10.1103/PhysRevLett.118.084301>, publisher: American Physical Society.
- [241] M.C. Fernandes, S. Mhatre, A.E. Forte, B. Zhao, O. Mesa, J.C. Weaver, M. Bechtold, K. Bertoldi, Surface texture modulation via buckling in porous inclined mechanical metamaterials, *Extrem. Mech. Lett.* 51 (2022) 101549, <https://doi.org/10.1016/j.eml.2021.101549>.
- [242] J. Shim, S. Shan, A. Košmrlj, S.H. Kang, E.R. Chen, J.C. Weaver, K. Bertoldi, Harnessing instabilities for design of soft reconfigurable auxetic/chiral materials, *Soft Matter* 9 (34) (2013) 8198–8202, <https://doi.org/10.1039/C3SM51148K>, publisher: The Royal Society of Chemistry.
- [243] K. Bertoldi, P.M. Reis, S. Willshaw, T. Mullin, Negative Poisson's ratio behavior induced by an elastic instability, *Adv. Mater.* 22 (3) (2010) 361–366, <https://doi.org/10.1002/adma.200901956>.
- [244] Z. Xu, Y. Zhou, B. Zhang, C. Zhang, J. Wang, Z. Wang, Recent progress on plant-inspired soft robotics with hydrogel building blocks: fabrication, actuation and application, *Micromachines* 12 (6) (May 2021), <https://doi.org/10.3390/mi12060608>, <https://europepmc.org/articles/PMC8225014>.
- [245] J.Z. Kiss, Up, down, and all around: how plants sense and respond to environmental stimuli, *Proc. Natl. Acad. Sci. USA* 103 (4) (2006) 829–830, <https://doi.org/10.1073/pnas.0510471102>, edition: 2006/01/17 Publisher: National Academy of Sciences, <https://pubmed.ncbi.nlm.nih.gov/16418288>.
- [246] J.M. Skotheim, L. Mahadevan, Physical limits and design principles for plant and fungal movements, *Science* 308 (5726) (2005) 1308–1310, <https://doi.org/10.1126/science.1107976>.
- [247] Y. Forterre, Slow, fast and furious: understanding the physics of plant movements, *J. Exp. Bot.* 64 (15) (2013) 4745–4760, <https://doi.org/10.1093/jxb/ert230>.
- [248] J. Edwards, D. Whitaker, S. Klionsky, M.J. Laskowski, Botany: a record-breaking pollen catapult, *Nature* 435 (7039) (2005) 164, <https://doi.org/10.1038/435164a>, place: England.
- [249] O. Vincent, C. Weiskopf, S. Poppinga, T. Masselter, T. Speck, M. Joyeux, C. Quiliet, P. Marmottant, Ultra-fast underwater suction traps, *Proc. R. Soc. B, Biol. Sci.* 278 (1720) (2011) 2909–2914, <https://doi.org/10.1098/rspb.2010.2292>.
- [250] N.C. Carpita, D.M. Gibeau, Structural models of primary cell walls in flowering plants: consistency of molecular structure with the physical properties of the walls during growth, *Plant J.* 1 (1993) 1–30, <https://doi.org/10.1111/j.1365-313x.1993.tb00007.x>, for cell and molecular biology 3, place: England.
- [251] D.J. Cosgrove, Growth of the plant cell wall, *Nat. Rev. Mol. Cell Biol.* 6 (11) (2005) 850–861, <https://doi.org/10.1038/nrm1746>.
- [252] S.L. Sridhar, J.K.E. Ortega, F.J. Vernerey, A statistical model of expansive growth in plant and fungal cells: the case of phycomyces, *Biophys. J.* 115 (12) (2018) 2428–2442, <https://doi.org/10.1016/j.bpj.2018.11.014>.
- [253] J. Huang, S. Xia, Z. Li, X. Wu, J. Ren, Applications of four-dimensional printing in emerging directions: review and prospects, *J. Mater. Sci. Technol.* 91 (2021) 105–120, <https://doi.org/10.1016/j.jmst.2021.02.040>.
- [254] H. Lee, C. Xia, N.X. Fang, First jump of microgel; actuation speed enhancement by elastic instability, *Soft Matter* 6 (18) (2010) 4342–4345, <https://doi.org/10.1039/C0SM00092B>, publisher: the Royal Society of Chemistry.
- [255] Y. Forterre, J.M. Skotheim, J. Dumais, L. Mahadevan, How the Venus flytrap snaps, *Nature* 433 (7024) (2005) 421–425, <https://doi.org/10.1038/nature03185>.
- [256] D.P. Holmes, A.J. Crosby, Snapping surfaces, *Adv. Mater.* 19 (21) (2007) 3589–3593, <https://doi.org/10.1002/adma.200700584>.
- [257] N. San Ha, G. Lu, A review of recent research on bio-inspired structures and materials for energy absorption applications, *Composites, Part B, Eng.* 181 (2020) 107496, publisher: Elsevier.
- [258] O.M. Wani, H. Zeng, A. Primagi, A light-driven artificial flytrap, *Nat. Commun.* 8 (1) (2017) 15546, <https://doi.org/10.1038/ncomms15546>.
- [259] G. Tedeschi, J.J. Benitez, L. Ceseracciu, K. Dastmalchi, B. Itin, R.E. Stark, A. Heredia, A. Athanassiou, J.A. Heredia-Guerrero, Sustainable fabrication of plant cuticle-like packaging films from tomato pomace agro-waste, beeswax, and alginate, *ACS Sustain. Chem. Eng.* 6 (11) (2018) 14955–14966, <https://doi.org/10.1021/acssuschemeng.8b03450>.
- [260] M. Haneef, L. Ceseracciu, C. Canale, I.S. Bayer, J.A. Heredia-Guerrero, A. Athanassiou, Advanced materials from fungal mycelium: fabrication and tuning of physical properties, *Sci. Rep.* 7 (2017) 41292, <https://doi.org/10.1038/srep41292>, place: England.
- [261] D. Merino, U.C. Paul, A. Athanassiou, Bio-based plastic films prepared from potato peels using mild acid hydrolysis followed by plasticization with a polyglycerol, *Food Pack. Shelf Life* 29 (2021) 100707, publisher: Elsevier.
- [262] D. Merino, L. Bertolacci, U.C. Paul, R. Simonutti, A. Athanassiou, Avocado peels and seeds: processing strategies for the development of highly antioxidant bioplastic films, *ACS Appl. Mater. Interfaces* 13 (32) (2021) 38688–38699, publisher: ACS Publications.
- [263] M.E. Antinori, M. Contardi, G. Suarato, A. Armirotti, R. Bertorelli, G. Mancini, D. Debellis, A. Athanassiou, Advanced mycelium materials as potential self-growing biomedical scaffolds, *Sci. Rep.* 11 (1) (2021) 1–14, publisher: Springer.
- [264] M.E. Antinori, L. Ceseracciu, G. Mancini, J.A. Heredia-Guerrero, A. Athanassiou, Fine-tuning of physicochemical properties and growth dynamics of mycelium-based materials, *ACS Appl. Bio Mater.* 3 (2) (2020) 1044–1051, publisher: ACS Publications.
- [265] F. Vollrath, Strength and structure of spiders' silks, *Rev. Mol. Biotechnol.* 74 (2) (2000) 67–83, [https://doi.org/10.1016/S1389-0352\(00\)00006-4](https://doi.org/10.1016/S1389-0352(00)00006-4).
- [266] W. Li, F. Wang, O. Sigmund, X.S. Zhang, Design of composite structures with programmable elastic responses under finite deformations, *J. Mech. Phys. Solids* 151 (2021) 104356, <https://doi.org/10.1016/j.jmps.2021.104356>.
- [267] J. Pérez-Rigueiro, M. Elices, G.R. Plaza, G.V. Guinea, Basic principles in the design of spider silk fibers, *Molecules* 26 (6) (2021), <https://doi.org/10.3390/molecules26061794>, <https://www.mdpi.com/1420-3049/26/6/1794>.
- [268] J.L. Yarger, B.R. Cherry, A. van der Vaart, Uncovering the structure–function relationship in spider silk, *Nat. Rev. Mater.* 3 (3) (2018) 18008, <https://doi.org/10.1038/natrevmats.2018.8>.
- [269] O. Tokareva, M. Jacobsen, M. Buehler, J. Wong, D.L. Kaplan, Structure–function–property–design interplay in biopolymers: spider silk, *Acta Biomater.* 10 (4) (2014) 1612–1626, <https://doi.org/10.1016/j.actbio.2013.08.020>.
- [270] J. Gosline, P. Guerette, C. Ortlepp, K. Savage, The mechanical design of spider silks: from fibroin sequence to mechanical function, *J. Exp. Biol.* 202 (23) (1999) 3295–3303, <https://doi.org/10.1242/jeb.202.23.3295>.
- [271] N. Du, Z. Yang, X.Y. Liu, Y. Li, H.Y. Xu, Structural origin of the strain-hardening of spider silk, *Adv. Funct. Mater.* 21 (4) (2011) 772–778, <https://doi.org/10.1002/adfm.201001397>.
- [272] H. Venkatesan, J. Chen, H. Liu, W. Liu, J. Hu, A spider-capture-silk-like fiber with extremely high-volume directional water collection, *Adv. Funct. Mater.* 30 (30) (2020) 2002437, <https://doi.org/10.1002/adfm.202002437>.
- [273] K. Zhang, H. Duan, B.L. Karihaloo, J. Wang, Hierarchical, multilayered cell walls reinforced by recycled silk cocoons enhance the structural integrity of honeybee combs, *Proc. Natl. Acad. Sci.* 107 (21) (2010) 9502–9506, <https://doi.org/10.1073/pnas.0912066107>, publisher: National Academy of Sciences.
- [274] A.P. Kiseleva, P.V. Krivoschapkin, E.F. Krivoschapkina, Recent Advances in Development of Functional Spider Silk-Based Hybrid Materials, *Frontiers in Chemistry*, vol. 8, 2020.
- [275] Q. Zhang, X. Yang, P. Li, G. Huang, S. Feng, C. Shen, B. Han, X. Zhang, F. Jin, F. Xu, T.J. Lu, Bioinspired engineering of honeycomb structure – using nature to inspire human innovation, *Prog. Mater. Sci.* 74 (2015) 332–400, <https://doi.org/10.1016/j.pmatsci.2015.05.001>.
- [276] K. Song, D. Li, C. Zhang, T. Liu, Y. Tang, Y.M. Xie, W. Liao, Bio-inspired hierarchical honeycomb metastructures with superior mechanical properties, *Compos. Struct.* 304 (2023) 116452, <https://doi.org/10.1016/j.compstruct.2022.116452>.
- [277] C. Qi, F. Jiang, S. Yang, Advanced honeycomb designs for improving mechanical properties: a review, *Composites, Part B, Eng.* 227 (2021) 109393, <https://doi.org/10.1016/j.compositesb.2021.109393>.
- [278] F. Wang, Systematic design of 3D auxetic lattice materials with programmable Poisson's ratio for finite strains, *J. Mech. Phys. Solids* 114 (2018) 303–318, <https://doi.org/10.1016/j.jmps.2018.01.013>.
- [279] F. Wang, O. Sigmund, J.S. Jensen, Design of materials with prescribed nonlinear properties, *J. Mech. Phys. Solids* 69 (2014) 156–174, <https://doi.org/10.1016/j.jmps.2014.05.003>.
- [280] S. Shan, S.H. Kang, J.R. Raney, P. Wang, L. Fang, F. Candido, J.A. Lewis, K. Bertoldi, Multistable architected materials for trapping elastic strain energy, *Adv. Mater.* 27 (29) (2015) 4296–4301, <https://doi.org/10.1002/adma.201501708>.
- [281] O. Sigmund, Tailoring materials with prescribed elastic properties, *Mech. Mater.* 20 (4) (1995) 351–368, [https://doi.org/10.1016/0167-6636\(94\)00069-7](https://doi.org/10.1016/0167-6636(94)00069-7).
- [282] L.H. Dudte, E. Vouga, T. Tachi, L. Mahadevan, Programming curvature using origami tessellations, *Nat. Mater.* 15 (5) (2016) 583–588, <https://doi.org/10.1038/nmat4540>, place: England.
- [283] A.R. Studart, Additive manufacturing of biologically-inspired materials, *Chem. Soc. Rev.* 45 (2) (2016) 359–376, <https://doi.org/10.1039/C5CS00836K>, publisher: the Royal Society of Chemistry.
- [284] D. Roy, J.N. Cambre, B.S. Sumerlin, Future perspectives and recent advances in stimuli-responsive materials, *Prog. Polym. Sci.* 35 (1) (2010) 278–301, <https://doi.org/10.1016/j.progpolymsci.2009.10.008>.
- [285] M. Wei, Y. Gao, X. Li, M.J. Serpe, Stimuli-responsive polymers and their applications, *Polym. Chem.* 8 (1) (2017) 127–143, <https://doi.org/10.1039/C6PY01585A>.
- [286] J.A. Jackson, M.C. Messner, N.A. Dudukovic, W.L. Smith, L. Bekker, B. Moran, A.M. Golobic, A.J. Pascall, E.B. Duoss, K.J. Loh, C.M. Spadaccini, Field responsive mechanical metamaterials, *Sci. Adv.* 4 (12) (2018) eaau6419, <https://doi.org/10.1126/sciadv.aau6419>.

- [287] F.J. Vernerey, R. Long, R. Brighenti, A statistically-based continuum theory for polymers with transient networks, *J. Mech. Phys. Solids* 107 (2017) 1–20, <https://doi.org/10.1016/j.jmps.2017.05.016>.
- [288] M. Doi, *Introduction to Polymer Physics*, Oxford University Press, 1996.
- [289] R. Brighenti, F. Artoni, M.P. Cosma, Viscous and failure mechanisms in polymer networks: a theoretical micromechanical approach, *Materials* 12 (10) (2019) 1576, <https://doi.org/10.3390/ma12101576>.
- [290] M. Doi, *Soft Matter Physics*, Oxford University Press, 2013.
- [291] M. Warner, E. Terentjev, *Liquid Crystal Elastomers*, vol. 120, Oxford University Press, 2007.
- [292] M. Warner, K.P. Gelling, T.A. Vilgis, Theory of nematic networks, *J. Chem. Phys.* 88 (6) (1988) 4008–4013, <https://doi.org/10.1063/1.453852>.
- [293] M. Warner, E.M. Terentjev, Nematic elastomers—a new state of matter?, *Prog. Polym. Sci.* 21 (5) (1996) 853–891, [https://doi.org/10.1016/S0079-6700\(96\)00013-5](https://doi.org/10.1016/S0079-6700(96)00013-5).
- [294] P.-G. De Gennes, J. Prost, *The Physics of Liquid Crystals*, vol. 83, Oxford University Press, 1993.
- [295] D. Mistry, N.A. Traugott, B. Sanborn, R.H. Volpe, L.S. Chatham, R. Zhou, B. Song, K. Yu, K.N. Long, C.M. Yakacki, Soft elasticity optimises dissipation in 3D-printed liquid crystal elastomers, *Nat. Commun.* 12 (1) (2021) 6677, <https://doi.org/10.1038/s41467-021-27013-0>.
- [296] Z. Wang, Z. Wang, Y. Zheng, Q. He, Y. Wang, S. Cai, Three-dimensional printing of functionally graded liquid crystal elastomer, *Sci. Adv.* 6 (39) (2020), <https://doi.org/10.1126/sciadv.abc0034>, publisher: American Association for the Advancement of Science.
- [297] C.P. Ambulo, J.J. Burroughs, J.M. Boothby, H. Kim, M.R. Shankar, T.H. Ware, Four-dimensional printing of liquid crystal elastomers, *ACS Appl. Mater. Interfaces* 9 (42) (2017) 37332–37339, <https://doi.org/10.1021/acsami.7b11851>, publisher: American Chemical Society.
- [298] A. Kotikian, R.L. Truby, J.W. Boley, T.J. White, J.A. Lewis, 3D printing of liquid crystal elastomeric actuators with spatially programmed nematic order, *Adv. Mater.* 30 (10) (2018) 1706164, <https://doi.org/10.1002/adma.201706164>.
- [299] Y. Guo, J. Zhang, W. Hu, M.T.A. Khan, M. Sitti, Shape-programmable liquid crystal elastomer structures with arbitrary three-dimensional director fields and geometries, *Nat. Commun.* 12 (1) (2021) 5936, <https://doi.org/10.1038/s41467-021-26136-8>.
- [300] M. Warner, E. Terentjev, *Liquid Crystal Elastomers*, Oxford Science Publications, 2003.
- [301] R. Brighenti, M.P. Cosma, Multiphysics modeling of light-actuated liquid crystal elastomers, *Proc. R. Soc. A, Math. Phys. Eng. Sci.* 479 (2269) (2023) 20220417, <https://doi.org/10.1098/rspa.2022.0417>.
- [302] Z. Yang, J. Li, X. Chen, Y. Fan, J. Huang, H. Yu, S. Yang, E.-Q. Chen, Precisely controllable artificial muscle with continuous morphing based on “breathing” of supramolecular columns, *Adv. Mater.* 35 (14) (2023) 2211648, <https://doi.org/10.1002/adma.202211648>.
- [303] J. Chen, F.K.-C. Leung, M.C.A. Stuart, T. Kajitani, T. Fukushima, E. van der Giessen, B.L. Feringa, Artificial muscle-like function from hierarchical supramolecular assembly of photoresponsive molecular motors, *Nat. Chem.* 10 (2) (2018) 132–138, <https://doi.org/10.1038/nchem.2887>.
- [304] M.L. Huggins, Solutions of long chain compounds, *J. Chem. Phys.* 9 (5) (1941) 440, <https://doi.org/10.1063/1.1750930>.
- [305] P.J. Flory, Statistical mechanics of swelling of network structures, *J. Chem. Phys.* 18 (1) (1950) 108–111, <https://doi.org/10.1063/1.1747424>.
- [306] M.L. Huggins, A revised theory of high polymer solutions, *J. Am. Chem. Soc.* 86 (17) (1964) 3535–3540, <https://doi.org/10.1021/ja01071a028>, publisher: American Chemical Society.
- [307] T. Tanaka, D. Fillmore, Kinetics of swelling of gels, *J. Chem. Phys.* 70 (3) (1979) 1214–1218, publisher: AIP.
- [308] M. Doi, *Gel dynamics*, *J. Phys. Soc. Jpn.* 78 (5) (2009) 052001–052001, publisher: the Physical Society of Japan.
- [309] Y. Wu, X. Hao, R. Xiao, J. Lin, Z.L. Wu, J. Yin, J. Qian, Controllable bending of bi-hydrogel strips with differential swelling, *Acta Mech. Solida Sin.* 32 (5) (2019) 652–662, <https://doi.org/10.1007/s10338-019-00106-6>.
- [310] Y. Zhang, K. Liu, T. Liu, C. Ni, D. Chen, J. Guo, C. Liu, J. Zhou, Z. Jia, Q. Zhao, P. Pan, T. Xie, Differential diffusion driven far-from-equilibrium shape-shifting of hydrogels, *Nat. Commun.* 12 (1) (2021) 6155, <https://doi.org/10.1038/s41467-021-26464-9>.
- [311] M.A. Haq, Y. Su, D. Wang, Mechanical properties of PNIPAM based hydrogels: a review, *Mater. Sci. Eng. C* 70 (2017) 842–855, <https://doi.org/10.1016/j.msec.2016.09.081>.
- [312] M.P.H. Pedigo, T.-A. Asoh, Y.-I. Hsu, H. Uyama, Stimuli-responsive composite hydrogels with three-dimensional stability prepared using oxidized cellulose nanofibers and chitosan, *Carbohydr. Polym.* 278 (2022) 118907, <https://doi.org/10.1016/j.carbpol.2021.118907>.
- [313] J. Li, D.J. Mooney, Designing hydrogels for controlled drug delivery, *Nat. Rev. Mater.* 1 (12) (2016) 16071, <https://doi.org/10.1038/natrevmats.2016.71>.
- [314] J. Gong, W. Hong, Mechanics and physics of hydrogels, *Soft Matter* 8 (31) (2012) 8006–8007, <https://doi.org/10.1039/C2SM90083A>, publisher: the Royal Society of Chemistry.
- [315] K. Ishida, T. Uno, T. Itoh, M. Kubo, Synthesis and property of temperature-responsive hydrogel with movable cross-linking points, *Macromolecules* 45 (15) (2012) 6136–6142, <https://doi.org/10.1021/ma301065j>, publisher: American Chemical Society.
- [316] H. Cheng, L. Shen, C. Wu, LLS and FTIR studies on the hysteresis in association and dissociation of poly(N-isopropylacrylamide) chains in water, *Macromolecules* 39 (6) (2006) 2325–2329, <https://doi.org/10.1021/ma052561m>.
- [317] P.J. Flory, J. Rehner, Statistical mechanics of cross-linked polymer networks I. Rubberlike elasticity, *J. Chem. Phys.* 11 (11) (1943) 512–520, <https://doi.org/10.1063/1.1723791>, publisher: American Institute of Physics.
- [318] W. Hong, X. Zhao, J. Zhou, Z. Suo, A theory of coupled diffusion and large deformation in polymeric gels, *J. Mech. Phys. Solids* 56 (5) (2008) 1779–1793, publisher: Elsevier.
- [319] S. Cai, Z. Suo, Mechanics and chemical thermodynamics of phase transition in temperature-sensitive hydrogels, *J. Mech. Phys. Solids* 59 (11) (2011) 2259–2278, <https://doi.org/10.1016/j.jmps.2011.08.008>.
- [320] M. Terzano, A. Spagnoli, D. Dini, A.E. Forte, Fluid–solid interaction in the rate-dependent failure of brain tissue and biomimicking gels, *J. Mech. Behav. Biomed. Mater.* 119 (2021) 104530, <https://doi.org/10.1016/j.jmbm.2021.104530>.
- [321] A.E. Forte, S.M. Gentleman, D. Dini, On the characterization of the heterogeneous mechanical response of human brain tissue, *Biomech. Model. Mechanobiol.* 16 (3) (2017) 907–920, <https://doi.org/10.1007/s10237-016-0860-8>.
- [322] C. Nicholson, Diffusion and related transport mechanisms in brain tissue, *Rep. Prog. Phys.* 64 (7) (2001) 815, publisher: IOP Publishing.
- [323] A.E. Forte, S. Galvan, D. Dini, Models and tissue mimics for brain shift simulations, *Biomech. Model. Mechanobiol.* 17 (2018) 249–261, publisher: Springer.
- [324] A. Dorfmann, R.W. Ogden, Nonlinear electroelasticity, *Acta Mech.* 174 (3) (2005) 167–183, <https://doi.org/10.1007/s00707-004-0202-2>.
- [325] R. Bustamante, A. Dorfmann, R.W. Ogden, Nonlinear electroelastostatics: a variational framework, *Z. Angew. Math. Phys.* 60 (1) (2009) 154–177, <https://doi.org/10.1007/s00033-007-7145-0>.
- [326] L. Dorfmann, R.W. Ogden, *Nonlinear Theory of Electroelastic and Magnetoelastic Interactions*, vol. 1, Springer, 2014.
- [327] M.G. Broadhurst, G.T. Davis, Physical basis for piezoelectricity in PVDF, *Ferroelectrics* 60 (1) (1984) 3–13, <https://doi.org/10.1080/00150198408017504>, publisher: Taylor & Francis.
- [328] S. Sukumaran, S. Chatbouri, D. Rouxel, E. Tisserand, F. Thiebaud, T.B. Zineb, Recent advances in flexible PVDF based piezoelectric polymer devices for energy harvesting applications, *J. Intell. Mater. Syst. Struct.* 32 (7) (2021) 746–780, <https://doi.org/10.1177/1045389X20966058>.
- [329] F. Carpi, D. De Rossi, R. Kornbluh, R.E. Pelrine, P. Sommer-Larsen, *Dielectric Elastomers as Electromechanical Transducers: Fundamentals, Materials, Devices, Models and Applications of an Emerging Electroactive Polymer Technology*, Elsevier, 2011.
- [330] Y. Cha, M. Porfiri, Mechanics and electrochemistry of ionic polymer metal composites, *J. Mech. Phys. Solids* 71 (2014) 156–178, <https://doi.org/10.1016/j.jmps.2014.07.006>.
- [331] A. Lerondi, L. Bardella, Modeling actuation and sensing in ionic polymer metal composites by electrochemo-poromechanics, *J. Mech. Phys. Solids* 148 (2021) 104292, <https://doi.org/10.1016/j.jmps.2021.104292>.
- [332] R.E. Pelrine, R.D. Kornbluh, J.P. Joseph, Electrostriction of polymer dielectrics with compliant electrodes as a means of actuation, *Sens. Actuators A, Phys.* 64 (1) (1998) 77–85, [https://doi.org/10.1016/S0924-4247\(97\)01657-9](https://doi.org/10.1016/S0924-4247(97)01657-9).
- [333] R. Bustamante, A. Dorfmann, R.W. Ogden, On variational formulations in nonlinear magnetoelastostatics, *Math. Mech. Solids* 13 (8) (2008) 725–745, <https://doi.org/10.1177/1081286507079832>.
- [334] R.A. Toupin, The elastic dielectric, *J. Ration. Mech. Anal.* 5 (6) (1956) 849–915, publisher: JSTOR.
- [335] R. Brighenti, A. Menzel, F.J. Vernerey, A physics-based micromechanical model for electroactive viscoelastic polymers, *J. Intell. Mater. Syst. Struct.* 29 (14) (2018) 2902–2918, <https://doi.org/10.1177/1045389X18781036>.
- [336] M. Milosevic, C. Marquez-Chin, K. Masani, M. Hirata, T. Nomura, M.R. Popovic, K. Nakazawa, Why brain-controlled neuroprosthetics matter: mechanisms underlying electrical stimulation of muscles and nerves in rehabilitation, *Biomed. Eng. Online* 19 (1) (2020) 1–30, publisher: BioMed Central.
- [337] M. Behl, A. Lendlein, Shape-memory polymers, *Mater. Today* 10 (4) (2007) 20–28, [https://doi.org/10.1016/S1369-7021\(07\)70047-0](https://doi.org/10.1016/S1369-7021(07)70047-0).
- [338] C. Liu, H. Qin, P.T. Mather, Review of progress in shape-memory polymers, *J. Mater. Chem.* 17 (16) (2007) 1543–1558, <https://doi.org/10.1039/B615954K>, publisher: the Royal Society of Chemistry.
- [339] A. Lendlein, H. Jiang, O. Jünger, R. Langer, Light-induced shape-memory polymers, *Nature* 434 (7035) (2005) 879–882, <https://doi.org/10.1038/nature03496>, place: England.
- [340] M. Behl, M.Y. Razzaq, A. Lendlein, Multifunctional shape-memory polymers, *Adv. Mater.* 22 (31) (2010) 3388–3410, <https://doi.org/10.1002/adma.200904447>.
- [341] M.D. Hager, S. Bode, C. Weber, U.S. Schubert, Shape memory polymers: past, present and future developments, *Prog. Polym. Sci.* 49–50 (2015) 3–33, <https://doi.org/10.1016/j.progpolymsci.2015.04.002>.
- [342] A. Lendlein, O.E.C. Gould, Reprogrammable recovery and actuation behaviour of shape-memory polymers, *Nat. Rev. Mater.* 4 (2) (2019) 116–133, <https://doi.org/10.1038/s41578-018-0078-8>.

- [343] H. Tobushi, K. Okumura, S. Hayashi, N. Ito, Thermomechanical constitutive model of shape memory polymer, *Mech. Mater.* 33 (10) (2001) 545–554, [https://doi.org/10.1016/S0167-6636\(01\)00075-8](https://doi.org/10.1016/S0167-6636(01)00075-8).
- [344] Y. Li, Z. Liu, A novel constitutive model of shape memory polymers combining phase transition and viscoelasticity, *Polymer* 143 (2018) 298–308, <https://doi.org/10.1016/j.polymer.2018.04.026>.
- [345] A. Shojaei, W. Xu, C. Yan, Q. Yang, G. Li, Insight in thermomechanical constitutive modeling of shape memory polymers, *Front. Mech. Eng.* 8 (2022), <https://doi.org/10.3389/fmech.2022.956129>.
- [346] Y. Liu, K. Gall, M.L. Dunn, A.R. Greenberg, J. Diani, Thermomechanics of shape memory polymers: uniaxial experiments and constitutive modeling, *Int. J. Plast.* 22 (2) (2006) 279–313, <https://doi.org/10.1016/j.ijplas.2005.03.004>.
- [347] A. Lendlein, M. Balk, N.A. Tarazona, O.E. Gould, Bioprospectives for shape-memory polymers as shape programmable, active materials, *Biomacromolecules* 20 (10) (2019) 3627–3640, publisher: ACS Publications.
- [348] Z. Liu, D. Jiao, Z. Zhang, Remarkable shape memory effect of a natural biopolymer in aqueous environment, *Biomaterials* 65 (2015) 13–21, publisher: Elsevier.
- [349] X. Xiao, J. Hu, Animal hairs as water-stimulated shape memory materials: mechanism and structural networks in molecular assemblies, *Sci. Rep.* 6 (1) (2016) 26393, publisher: Nature Publishing Group UK London.
- [350] M. Manrique-Juarez, S. Rat, L. Salmon, G. Molnár, C. Quintero, L. Nicu, H. Shepherd, A. Bousseksou, Switchable molecule-based materials for micro- and nanoscale actuating applications: achievements and prospects, *Coord. Chem. Rev.* 308 (2016) 395–408, publisher: Elsevier.
- [351] A. Pucci, F. Di Cuia, F. Signori, G. Ruggeri, Bis(benzoxazoly)stilbene excimers as temperature and deformation sensors for biodegradable poly(1, 4-butylene succinate) films, *J. Mater. Chem.* 17 (8) (2007) 783–790, <https://doi.org/10.1039/B612033D>, publisher: the Royal Society of Chemistry.
- [352] S. Dai, P. Ravi, K. Tam, pH-responsive polymers: synthesis, properties and applications, *Soft Matter* 4 (3) (2008) 435–449, publisher: Royal Society of Chemistry.
- [353] J. Li, C. Nagamani, J. Moore, Polymer mechanochemistry: from destructive to productive, *Acc. Chem. Res.* 48 (8) (2015) 2181–2190, publisher: ACS Publications.
- [354] T. Manouras, M. Vamvakaki, Field responsive materials: photo-, electro-, magnetic- and ultrasound-sensitive polymers, *Polym. Chem.* 8 (1) (2017) 74–96, publisher: Royal Society of Chemistry.
- [355] F. Jochum, P. Theato, Temperature- and light-responsive smart polymer materials, *Chem. Soc. Rev.* 42 (17) (2013) 7468–7483, publisher: Royal Society of Chemistry.
- [356] M.A. Ghanem, A. Basu, R. Behrou, N. Boechler, A.J. Boydston, S.L. Craig, Y. Lin, B.E. Lynde, A. Nelson, H. Shen, D.W. Storti, The role of polymer mechanochemistry in responsive materials and additive manufacturing, *Nat. Rev. Mater.* 6 (1) (2021) 84–98, <https://doi.org/10.1038/s41578-020-00249-w>.
- [357] D. Schütze, K. Holz, J. Müller, M.K. Beyer, U. Lüning, B. Hartke, Pinpointing mechanochemical bond rupture by embedding the mechanophore into a macrocycle, *Angew. Chem., Int. Ed.* 54 (8) (2015) 2556–2559, <https://doi.org/10.1002/anie.201409691>.
- [358] J. Lenhardt, M. Ong, R. Choe, C. Evenhuis, T. Martinez, S. Craig, Trapping a diradical transition state by mechanochemical polymer extension, *Science* 329 (5995) (2010) 1057–1060, publisher: American Association for the Advancement of Science.
- [359] M. Larsen, A. Boydston, “Flex-activated” mechanophores: using polymer mechanochemistry to direct bond bending activation, *J. Am. Chem. Soc.* 135 (22) (2013) 8189–8192, publisher: ACS Publications.
- [360] A. Piermattei, S. Karthikeyan, R. Sijbesma, Activating catalysts with mechanical force, *Nat. Chem.* 1 (2) (2009) 133–137, publisher: Nature Publishing Group.
- [361] P. Hänggi, P. Talkner, M. Borkovec, Reaction-rate theory: fifty years after Kramers, *Rev. Mod. Phys.* 62 (2) (1990) 251, publisher: APS.
- [362] D.E. Makarov, Perspective: mechanochemistry of biological and synthetic molecules, *J. Chem. Phys.* 144 (3) (2016) 030901, publisher: AIP Publishing LLC.
- [363] T. Chidanguro, W. Weng, Y.C. Simon, Mechanochemistry: Inspiration from Biology, publisher: Royal Society of Chemistry, 2017.
- [364] A. Kaminski, G.R. Fedorchak, J. Lammerding, The cellular mastermind (?)—mechano-transduction and the nucleus, *Progr. Mol. Biol. Trans. Sci.* 126 (2014) 157–203, publisher: Elsevier.
- [365] G.E. Fantner, E. Oroudjev, G. Schitter, L.S. Golde, P. Thurner, M.M. Finch, P. Turner, T. Gutschmann, D.E. Morse, H. Hansma others, Sacrificial bonds and hidden length: unraveling molecular mesostructures in tough materials, *Biophys. J.* 90 (4) (2006) 1411–1418, publisher: Elsevier.
- [366] B.L. Smith, T.E. Schäffer, M. Viani, J.B. Thompson, N.A. Frederick, J. Kindt, A. Belcher, G.D. Stucky, D.E. Morse, P.K. Hansma, Molecular mechanistic origin of the toughness of natural adhesives, fibres and composites, *Nature* 399 (6738) (1999), publisher: Nature Publishing Group UK London.
- [367] M. Kadic, G.W. Milton, M. van Hecke, M. Wegener, 3D metamaterials, *Nat. Rev. Phys.* 1 (3) (2019) 198–210, <https://doi.org/10.1038/s42254-018-0018-y>.
- [368] J.U. Surjadi, L. Gao, H. Du, X. Li, X. Xiong, N.X. Fang, Y. Lu, Mechanical metamaterials and their engineering applications, *Adv. Eng. Mater.* 21 (3) (2019) 1800864, <https://doi.org/10.1002/adem.201800864>.
- [369] K. Bertoldi, V. Vitelli, J. Christensen, M. van Hecke, Flexible mechanical metamaterials, *Nat. Rev. Mater.* 2 (11) (2017) 17066, <https://doi.org/10.1038/natrevmats.2017.66>.
- [370] S. Waitukaitis, R. Menaut, B.G.-g. Chen, M. van Hecke, Origami multistability: from single vertices to metasheets, *Phys. Rev. Lett.* 114 (5) (2015) 055503, <https://doi.org/10.1103/PhysRevLett.114.055503>, publisher: American Physical Society.
- [371] T. Takata, D. Aoki, Topology-transformable polymers: linear-branched polymer structural transformation via the mechanical linking of polymer chains, *Polym. J.* 50 (1) (2018) 127–147, publisher: Nature Publishing Group.
- [372] Y. Tezuka, H. Oike, Topological polymer chemistry: systematic classification of nonlinear polymer topologies, *J. Am. Chem. Soc.* 123 (47) (2001) 11570–11576, publisher: ACS Publications.
- [373] Y. Noda, Y. Hayashi, K. Ito, From topological gels to slide-ring materials, *J. Appl. Polym. Sci.* 131 (15) (2014), publisher: Wiley Online Library.
- [374] A. Bele, M. Dascalu, C. Tugui, A. Farcas, Silicone elastomers with improved electro-mechanical performance using slide-ring polymers, *J. Polym. Res.* 29 (5) (2022) 202, publisher: Springer.
- [375] S. Wang, Y. Chen, Y. Sun, Y. Qin, H. Zhang, X. Yu, Y. Liu, Stretchable sliding supramolecular hydrogel for flexible electronic devices, *Commun. Mat.* 3 (1) (2022) 2, publisher: Nature Publishing Group UK London.
- [376] Y. Miyamoto, W. Kaysser, B. Rabin, A. Kawasaki, R.G. Ford, *Functionally Graded Materials: Design, Processing and Applications*, vol. 5, Springer Science & Business Media, 2013.
- [377] A.A. Bauhofer, S. Krödel, J. Rys, O.R. Bilal, A. Constantinescu, C. Daraio, Harnessing photochemical shrinkage in direct laser writing for shape morphing of polymer sheets, *Adv. Mater.* 29 (42) (2017) 1703024, <https://doi.org/10.1002/adma.201703024>.
- [378] M. Miniaci, A. Krushynska, A.S. Gliozzi, N. Kherraz, F. Bosia, N.M. Pugno, Design and fabrication of bioinspired hierarchical dissipative elastic metamaterials, *Phys. Rev. Appl.* 10 (2) (2018) 024012, <https://doi.org/10.1103/PhysRevApplied.10.024012>, publisher: American Physical Society.
- [379] S. Yin, W. Guo, H. Wang, Y. Huang, R. Yang, Z. Hu, D. Chen, J. Xu, R.O. Ritchie, Strong and tough bioinspired additive-manufactured dual-phase mechanical material composites, *J. Mech. Phys. Solids* 149 (2021) 104341, publisher: Elsevier.
- [380] M. Xu, Z. Zhao, P. Wang, S. Duan, H. Lei, D. Fang, Mechanical performance of bio-inspired hierarchical honeycomb metamaterials, *Int. J. Solids Struct.* 254 (2022) 111866, publisher: Elsevier.
- [381] E. Munch, M.E. Launey, D.H. Alsem, E. Saiz, A.P. Tomsia, R.O. Ritchie, Tough, bio-inspired hybrid materials, *Science* 322 (5907) (2008) 1516–1520, publisher: American Association for the Advancement of Science.
- [382] Y. Gao, M. Wei, X. Li, W. Xu, A. Ahiabun, J. Perdiz, Z. Liu, M.J. Serpe, Stimuli-responsive polymers: fundamental considerations and applications, *Macromol. Rev.* 25 (6) (2017) 513–527, <https://doi.org/10.1007/s13233-017-5088-7>.
- [383] M.B. Yatvin, J.N. Weinstein, W.H. Dennis, R. Blumenthal, Design of liposomes for enhanced local release of drugs by hyperthermia, *Science (N. Y.)* 202 (4374) (1978) 1290–1293, <https://doi.org/10.1126/science.364652>, place: United States.
- [384] N.N. Ferreira, L.M.B. Ferreira, V.M.O. Cardoso, F.I. Boni, A.L.R. Souza, M.P.D. Gremião, Recent advances in smart hydrogels for biomedical applications: from self-assembly to functional approaches, *Eur. Polym. J.* 99 (2018) 117–133, <https://doi.org/10.1016/j.eurpolymj.2017.12.004>.
- [385] T.R. Hoare, D.S. Kohane, Hydrogels in drug delivery: progress and challenges, *Polymer* 49 (8) (2008) 1993–2007, <https://doi.org/10.1016/j.polymer.2008.01.027>.
- [386] P. Bawa, V. Pillay, Y.E. Choonara, L.C.d. Toit, Stimuli-responsive polymers and their applications in drug delivery, *Biomed. Mater.* 4 (2) (2009) 022001, <https://doi.org/10.1088/1748-6041/4/2/022001>.
- [387] S. Chatterjee, P. Chi-leung Hui, Review of stimuli-responsive polymers in drug delivery and textile application, *Molecules* 24 (14) (2019), <https://doi.org/10.3390/molecules24142547>.
- [388] P. Rothmund, Y. Kim, R.H. Heisser, X. Zhao, R.F. Shepherd, C. Keplinger, Shaping the future of robotics through materials innovation, *Nat. Mater.* 20 (12) (2021) 1582–1587, <https://doi.org/10.1038/s41563-021-01158-1>.
- [389] J. Lei, H. Ju, Signal amplification using functional nanomaterials for biosensing, *Chem. Soc. Rev.* 41 (6) (2012) 2122–2134, <https://doi.org/10.1039/C1CS15274B>, publisher: the Royal Society of Chemistry.
- [390] K. Kraus, Z. Šika, P. Beneš, J. Krivošej, T. Vyhlídal, Mechatronic robot arm with active vibration absorbers, *J. Vib. Control* 26 (13–14) (2020) 1145–1156, <https://doi.org/10.1177/1077546320918488>.
- [391] X. Lin, H. Yan, L. Zhao, N. Duan, Z. Wang, S. Wu, Hydrogel-integrated sensors for food safety and quality monitoring: fabrication strategies and emerging applications, *Crit. Rev. Food Sci. Nutr.* (2023) 1–20, <https://doi.org/10.1080/10408398.2023.2168619>, publisher: Taylor & Francis.
- [392] R. De Fazio, V.M. Mastronardi, M. Petrucci, M. De Vittorio, P. Visconti, Human-machine interaction through advanced haptic sensors: a piezoelectric sensory glove with edge machine learning for gesture and object recognition, *Future Internet* 15 (1) (2023), <https://doi.org/10.3390/fi15010014>, <https://www.mdpi.com/1999-5903/15/1/14>.
- [393] T.M. Lutz, C. Kimna, A. Casini, O. Lieleg, Bio-based and bio-inspired adhesives from animals and plants for biomedical applications, *Mater. Today Bio* 13 (2022) 100203, <https://doi.org/10.1016/j.mtbio.2022.100203>.
- [394] X. Mao, H. Yuk, X. Zhao, Hydration and swelling of dry polymers for wet adhesion, *J. Mech. Phys. Solids* 137 (2020) 103863, <https://doi.org/10.1016/j.jmps.2020.103863>.

- [395] H. Yuk, C.E. Varela, C.S. Nabzdyk, X. Mao, R.F. Padera, E.T. Roche, X. Zhao, Dry double-sided tape for adhesion of wet tissues and devices, *Nature* 575 (7781) (2019) 169–174, <https://doi.org/10.1038/s41586-019-1710-5>.
- [396] D. Wang, S. Maharjan, X. Kuang, Z. Wang, L.S. Mille, M. Tao, P. Yu, X. Cao, L. Lian, L. Lv, J.J. He, G. Tang, H. Yuk, C.K. Ozaki, X. Zhao, Y.S. Zhang, Microfluidic bioprinting of tough hydrogel-based vascular conduits for functional blood vessels, *Sci. Adv.* 8 (43) (2022) eabq6900, <https://doi.org/10.1126/sciadv.abq6900>.
- [397] S. Derakhshanfar, R. Mbeleck, K. Xu, X. Zhang, W. Zhong, M. Xing, 3D bioprinting for biomedical devices and tissue engineering: a review of recent trends and advances, *Bioact. Mater.* 3 (2) (2018) 144–156, <https://doi.org/10.1016/j.bioactmat.2017.11.008>, publisher: Elsevier Ltd.
- [398] J. Li, C. Wu, P.K. Chu, M. Gelinsky, 3D printing of hydrogels: rational design strategies and emerging biomedical applications, *Mater. Sci. Eng., R Rep.* 140 (2020) 100543, <https://doi.org/10.1016/j.mser.2020.100543>.
- [399] K. Liu, J. Wu, G.H. Paulino, H.J. Qi, Programmable deployment of tensegrity structures by stimulus-responsive polymers, *Sci. Rep.* 7 (1) (2017) 3511, <https://doi.org/10.1038/s41598-017-03412-6>.
- [400] S. Nastysyn, Y. Stetsyshyn, J. Raczowska, Y. Nastishin, Y. Melnyk, Y. Panchenko, A. Budkowski, Temperature-responsive polymer brush coatings for advanced biomedical applications, *Polymers* 14 (19) (2022), <https://doi.org/10.3390/polym14194245>, <https://www.mdpi.com/2073-4360/14/19/4245>.
- [401] T. Yang, S. Wang, H. Yang, H. Gui, Y. Du, F. Liang, Temperature-triggered dynamic Janus fabrics for smart directional water transport, *Adv. Funct. Mater.* 33 (18) (2023) 2214183, <https://doi.org/10.1002/adfm.202214183>.
- [402] K. Auepattana-Aumrung, D. Crespy, Self-healing and anticorrosion coatings based on responsive polymers with metal coordination bonds, *Chem. Eng. J.* 452 (2023) 139055, <https://doi.org/10.1016/j.cej.2022.139055>.
- [403] C.B. Goy, R.E. Chaile, R.E. Madrid, Microfluidics and hydrogel: a powerful combination, *React. Funct. Polym.* 145 (2019) 104314, <https://doi.org/10.1016/j.reactfunctpolym.2019.104314>.
- [404] W. Hilber, Stimulus-active polymer actuators for next-generation microfluidic devices, *Appl. Phys. A* 122 (8) (2016) 751, <https://doi.org/10.1007/s00339-016-0258-6>.
- [405] J. ter Schiphorst, J. Saez, D. Diamond, F. Benito-Lopez, A.P.H.J. Schenning, Light-responsive polymers for microfluidic applications, *Lab Chip* 18 (5) (2018) 699–709, <https://doi.org/10.1039/C7LC01297G>, publisher: the Royal Society of Chemistry.
- [406] F. Lamberti, C. Mazzariol, F. Spolaore, R. Ceccato, L. Salmaso, S. Gross, Design of experiment: a rational and still unexplored approach to inorganic materials synthesis, *Sustain. Chem.* 3 (1) (2022) 114–130, <https://doi.org/10.3390/suschem3010009>, <https://www.mdpi.com/2673-4079/3/1/9>.
- [407] A. Talapatra, S. Boluki, P. Honarmandi, A. Solomou, G. Zhao, S.F. Ghoreishi, A. Molkeri, D. Allaire, A. Srivastava, X. Qian, E.R. Dougherty, D.C. Lagoudas, R. Arróyave, Experiment design frameworks for accelerated discovery of targeted materials across scales, *Front. Mater.* 6 (2019), <https://doi.org/10.3389/fmats.2019.00082>, <https://www.frontiersin.org/articles/10.3389/fmats.2019.00082>.
- [408] X. Xin, L. Liu, Y. Liu, J. Leng, 4D printing auxetic metamaterials with tunable, programmable, and reconfigurable mechanical properties, *Adv. Funct. Mater.* 30 (43) (2020) 2004226, <https://doi.org/10.1002/adfm.202004226>.
- [409] A.R. Studart, Biological and bioinspired composites with spatially tunable heterogeneous architectures, *Adv. Funct. Mater.* 23 (36) (2013) 4423–4436, <https://doi.org/10.1002/adfm.201300340>.
- [410] C. Zhang, X. Lu, G. Fei, Z. Wang, H. Xia, Y. Zhao, 4D printing of a liquid crystal elastomer with a controllable orientation gradient, *ACS Appl. Mater. Interfaces* 11 (47) (2019) 44774–44782, <https://doi.org/10.1021/acsami.9b18037>, publisher: American Chemical Society.
- [411] M.O. Saed, C.P. Ambulo, H. Kim, R. De, V. Raval, K. Searles, D.A. Siddiqui, J.M.O. Cue, M.C. Stefan, M.R. Shankar, T.H. Ware, Molecularly-engineered, 4D-printed liquid crystal elastomer actuators, *Adv. Funct. Mater.* 29 (3) (2019) 1806412, <https://doi.org/10.1002/adfm.201806412>.
- [412] L. Ren, B. Li, Y. He, Z. Song, X. Zhou, Q. Liu, L. Ren, Programming shape-morphing behavior of liquid crystal elastomers via parameter-encoded 4D printing, *ACS Appl. Mater. Interfaces* 12 (13) (2020) 15562–15572, <https://doi.org/10.1021/acsami.0c00027>, publisher: American Chemical Society.
- [413] R.M. Erb, J.S. Sander, R. Grisch, A.R. Studart, Self-shaping composites with programmable bioinspired microstructures, *Nat. Commun.* 4 (1) (2013) 1712, <https://doi.org/10.1038/ncomms2666>.
- [414] R. Brighenti, M.P. Cosma, L. Marsavina, A. Spagnoli, M. Terzano, Multiphysics modeling of the mechanical properties in polymers obtained via photo-induced polymerization, *Int. J. Adv. Manuf. Technol.* (Jul. 2021), <https://doi.org/10.1007/s00170-021-07273-2>.
- [415] M.P. Cosma, R. Brighenti, Photopolymerized additive manufacturing materials: modeling of the printing process, mechanical behavior, and sensitivity analysis, *Mater. Des. Process. Commun.* 3 (6) (2021) e225, <https://doi.org/10.1002/mdp2.225>.
- [416] R. Brighenti, L. Marsavina, M.P. Marghitas, M.P. Cosma, M. Montanari, Mechanical characterization of additively manufactured photopolymerized polymers, *Mech. Adv. Mat. Struct.* (2022) 1–12, Publisher: Taylor & Francis.
- [417] Y. Zhang, C. Xuan, Y. Jiang, Y. Huo, Continuum mechanical modeling of liquid crystal elastomers as dissipative ordered solids, *J. Mech. Phys. Solids* 126 (2019) 285–303, <https://doi.org/10.1016/j.jmps.2019.02.018>.
- [418] T.S. Hebrner, R.G. Bowman, D. Duffy, C. Mostajeran, I. Griniasty, I. Cohen, M. Warner, C.N. Bowman, T.J. White, Discontinuous metric programming in liquid crystalline elastomers, *arXiv preprint*, arXiv:2212.13273, 2022.
- [419] Z.-C. Jiang, Y.-Y. Xiao, X. Tong, Y. Zhao, Selective decrosslinking in liquid crystal polymer actuators for optical reconfiguration of origami and light-fueled locomotion, *Angew. Chem., Int. Ed.* 58 (16) (2019) 5332–5337, <https://doi.org/10.1002/anie.201900470>.
- [420] R. Yang, Y. Zhao, Non-uniform optical inscription of actuation domains in a liquid crystal polymer of uniaxial orientation: an approach to complex and programmable shape changes, *Angew. Chem., Int. Ed.* 56 (45) (2017) 14202–14206, <https://doi.org/10.1002/anie.201709528>.
- [421] K.A. Burke, I.A. Rousseau, P.T. Mather, Reversible actuation in main-chain liquid crystalline elastomers with varying crosslink densities, *Polymer* 55 (23) (2014) 5897–5907, <https://doi.org/10.1016/j.polymer.2014.06.088>.
- [422] J. Küpfer, E. Nishikawa, H. Finkelmann, Densely crosslinked liquid single-crystal elastomers, *Polym. Adv. Technol.* 5 (2) (1994) 110–115, <https://doi.org/10.1002/pat.1994.2200520205>.
- [423] J.S. Biggins, M. Warner, K. Bhattacharya, Elasticity of polydomain liquid crystal elastomers, *J. Mech. Phys. Solids* 60 (4) (2012) 573–590, <https://doi.org/10.1016/j.jmps.2012.01.008>.
- [424] E. Lee, D. Kim, H. Kim, J. Yoon, Photothermally driven fast responding photoactuators fabricated with comb-type hydrogels and magnetite nanoparticles, *Sci. Rep.* 5 (1) (2015) 15124, <https://doi.org/10.1038/srep15124>.
- [425] C. Ou, C.-S. Wang, S. Giasson, Enhanced swelling using photothermal responsive surface-immobilized microgels, *J. Appl. Polym. Sci.* 138 (38) (2021) 50973, <https://doi.org/10.1002/app.50973>.
- [426] A.B. Davis, A. Marshak, Photon propagation in heterogeneous optical media with spatial correlations: enhanced mean-free-paths and wider-than-exponential free-path distributions, *J. Quant. Spectrosc. Radiat. Transf.* 84 (1) (2004) 3–34, [https://doi.org/10.1016/S0022-4073\(03\)00114-6](https://doi.org/10.1016/S0022-4073(03)00114-6).
- [427] R. Anastasio, W. Peerbooms, R. Cardinaels, L.C. Van Breemen, Characterization of ultraviolet-cured methacrylate networks: from photopolymerization to ultimate mechanical properties, *Macromolecules* 52 (23) (2019) 9220–9231, <https://doi.org/10.1021/acs.macromol.9b01439>.
- [428] Y. Yang, L. Li, J. Zhao, Mechanical property modeling of photosensitive liquid resin in stereolithography additive manufacturing: bridging degree of cure with tensile strength and hardness, *Mater. Des.* 162 (2019) 418–428, <https://doi.org/10.1016/j.matdes.2018.12.009>.
- [429] H. Bikas, P. Stavropoulos, G. Chryssoulouris, Additive manufacturing methods and modeling approaches: a critical review, *Int. J. Adv. Manuf. Technol.* 83 (1) (2016) 389–405, <https://doi.org/10.1007/s00170-015-7576-2>.
- [430] J.H. Lee, R.K. Prud'homme, I.A. Aksay, Cure depth in photopolymerization: experiments and theory, *J. Mater. Res.* 16 (12) (2001) 3536–3544, <https://doi.org/10.1557/JMR.2001.0485>.
- [431] Y. Tang, C. Henderson, J. Muzzy, D.W. Rosen, Stereolithography cure modeling and simulation, *Int. J. Mater. Prod. Technol.* 21 (4) (2004) 255, <https://doi.org/10.1504/IJMPT.2004.004941>.
- [432] M.F. Perry, G.W. Young, A mathematical model for photopolymerization from a stationary laser light source, *Macromol. Theory Simul.* 14 (1) (2005) 26–39, <https://doi.org/10.1002/mats.200400056>.
- [433] P.J.d.S. Bartolo, Photo-curing modeling: direct irradiation, *Int. J. Adv. Manuf. Technol.* 32 (5–6) (2007) 480–491, <https://doi.org/10.1007/s00170-005-0374-5>.
- [434] M. Li, A. Pal, A. Aghakhani, A. Pena-Francesch, M. Sitti, Soft actuators for real-world applications, *Nat. Rev. Mater.* 7 (3) (2022) 235–249, <https://doi.org/10.1038/s41578-021-00389-7>.
- [435] J. Zhuang, M.R. Gordon, J. Ventura, L. Li, S. Thayumanavan, Multi-stimuli responsive macromolecules and their assemblies, *Chem. Soc. Rev.* 42 (17) (2013) 7421–7435, publisher: Royal Society of Chemistry.
- [436] H. Yuk, S. Lin, C. Ma, M. Takaffoli, N.X. Fang, X. Zhao, Hydraulic hydrogel actuators and robots optically and sonically camouflaged in water, *Nat. Commun.* 8 (1) (2017) 14230, <https://doi.org/10.1038/ncomms14230>.